Doctoral Dissertation

Fabrication of Porphyrin-based Polyurea Thin Film by Solution-based Molecular Layer Deposition (MLD) Technique

溶液を用いた分子層堆積(MLD)法によるポルフィリン含有ポリ尿素薄膜の作成

S. M. NIZAM UDDIN

Supervisor: Associate Professor Yuki Nagao

School of Materials Science

Japan Advanced Institute of Science and Technology

December, 2017

Referee-in-chief: Associate Professor Dr. Yuki Nagao
Japan Advanced Institute of Science and Technology

Referee: Professor Dr. Noriyoshi Matsumi
Japan Advanced Institute of Science and Technology

Professor Dr. Donglin Jiang
Japan Advanced Institute of Science and Technology

Associate Professor Dr. Toshiaki Taniike
Japan Advanced Institute of Science and Technology

Associate Professor Dr. Tatsuya Nishimura
Kanazawa University

Table of Contents

Chapter 2

Investigation of Self-assembled Monolayers (SAMs) 25

List of Figures

List of Tables

List of Schemes

List of Abbreviation

LbL	Layer-by-Layer
LB	Langmuir-Blodgett
PVD	Physical Vapor Deposition
CVD	Chemical Vapor Deposition
ALD	Atomic Layer Deposition
MLD	Molecular Layer Deposition
SAMs	Self-Assembled Monolayers
APTMS	3-Aminopropyltrimethoxysilane
APDMES	3-aminopropyldimethylethoxysilane
DMF	N, N-dimethylformamide
RT	Room Temperature
XPS	X-ray photoelectron spectroscopy
AFM	Atomic Force Microscope
CA	Contact Angle
RMS	Root Mean Square
1,4-PDI	1,4-phenylene diisocyanate
H_2TAPP	5,10,15,20-tetrakis-(4-aminophenyl)porphyrin
RH	Relative Humidity
$CHCl_3$	Chloroform
THF	Tetrahydrofuran
FTIR	Fourier-transform infrared
MCT	Mercury Cadmium Telluride

Abstract

Synthesis of organic thin film materials on solid surfaces is important for prospective applications in many research fields today. One of the simple and versatile techniques to prepare nanometer scale multilayer thin films is solution based molecular layer deposition (MLD). Organic thin film growth depends on several factors such as solid surface properties, self-assembled monolayer, as well as optimized reaction condition.

First part of this research was focused on the study of aminnosilane self-assembled monolayer formation on Si/SiO_2 surfaces. A major problem of aminosilane-modified surface is their chemical stability. To examine the issue of losing surface functionality, I prepared the self-assembled monolayer of one and three alkoxy group containing 3-aminopropyldimethyl ethoxysilane (APDMES) and 3-aminopropyl trimethoxysilane (APTMS) on SiO_2 substrates respectively. Silanization condition of APDMES was investigated in four different solvents under various reaction conditions. APDMES layer prepared in ethanol at 70 ºC for 3 hr shows the highest N-at. % along with highest free amine %. In contrast, APTMS-modified SiO_2 substrate was prepared in ethanol at RT for 1, 2, 3hr of silanization and found that 1 hr silanization is enough for APTMS-modification on SiO_2. The chemical stability of APDMES and APTMS-modified SiO_2 substrates were also investigated after 7 hr immersion into H_2O and 0.1 M $HClO_4$ solution at 40 ºC and RT respectively. Contact angle and XPS analysis showed that 22.4 % APDMES and 6.7 % APTMS were removed from the surface when the modified substrates were immersed into H_2O at 40 ºC for 7 hr. On the other hand, 38.7 % APDMES and 14.9 % APTMS were removed from the surface when the modified substrates were immersed into 0.1 M $HClO_4$ (aq) solution at RT for 7 hr. Thus Indicating, three alkoxy groups containing APTMS is more chemically stable (in hot H_2O and $HClO_4$) than one alkoxy group containing APDMES.

In the second part of this article, I demonstrated a solution-based molecular layer deposition (MLD) approach to prepare porphyrin-based covalent molecular networks on APTMS modified substrate surface using the urea coupling reaction between 1,4-phenylene diisocyanate (1,4-PDI) and 5,10,15,20-tetrakis-(4-aminophenyl)porphyrin (H_2TAPP) at room temperature. Multilayer growth was investigated under different relative humidity (RH) conditions. Sequential molecular growth at low relative humidity (≤10% RH) was observed using UV-vis absorption spectroscopy and atomic force microscopy (AFM). The high-RH condition shows limited film growth. Infrared spectroscopy (IR) and X-ray photoelectron spectroscopy (XPS) revealed the polyurea bond formation in sequential multilayer thin films, demonstrating that stepwise multilayer film growth was achieved using the urea coupling reaction.

Keywords: Self-assembled monolayer, Molecular layer deposition, Porphyrin, Polyurea, Covalent linkage, Thin film.

Chapter-01

General Introduction

1.1 Thin Films

Thin film is a progressing research field has been used to create and development of device performance. Thin film technology controls the synthesis of a layer of materials ranging from fractions of a nanometer to several micrometers in thickness. It opens a wide range of application windows in physics, chemistry, biology and medical science. Based on the particular application demands, thin films deposition has been carried out on different types of substrates including conducting, semiconductors, non-conducting and porous materials. The thin film growth depends on the surface-interface interaction among the substrate and reacting materials which can enhance functional properties compare to the corresponding bulk materials. Thus the physical and chemical properties of the thin film can be monitored and improved by choosing the appropriate set of reacting materials to anchor with the substrate surfaces. As in thin film technology, it is possible to optimize the specific film growth along with the control over the film thickness. It has become very attractive in various research fields such as functional film and materials, battery research, organic electronic, optics and process technology.[1-4] **Figure 1.1** shows some of the attractive research fields in thin film technology.

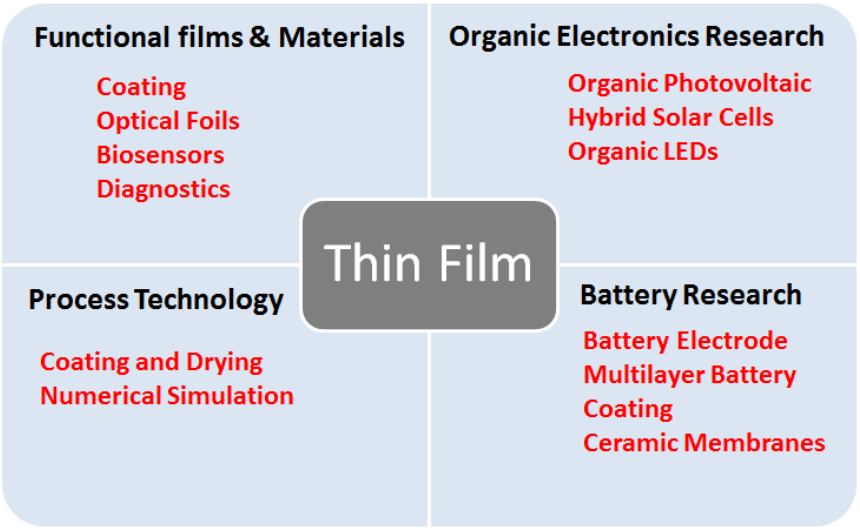

Figure 1.1 Highlights of thin film research fields.

1.2 Thin Films Fabrication

Thin film growth is an important part of the consideration in the present research world as it is required for many devices in the modern technology. The control of thin film growth at the molecular level is required for device miniaturization as the morphology plays a vital role for most of the device performances.[5] Two major synthetic approaches are well known for thin film fabrication such as top-down and bottom-up approach (**Figure 1.2**). Top-down is an approach where the nanostructures are synthesized by etching out the film which are already exist on the substrate surface using beam lithography.[6] Thus, top-down approach is used to remove the building block from the substrate to form the nanostructure for device applications. On the other hand, bottom-up

approach are used to synthesized the nanostructure on the substrate surface by stacking the atoms and/or molecules on each other.[7] Thus, bottom-up is an approach where the building blocks are combined onto the substrate surface to form nanostructures. The bottom-up approaches are more advantageous than top-up approach because of the better chance of producing nanostructures with less defects and more homogenous chemical composition. Bottom-up approach includes the various thin film fabrication techniques such as Layer-by-layer (LbL),[8] Langmuir-Blodgett (LB),[9-12] microwave,[13] colloidal,[14] electrochemical deposition,[15] inkjet,[16] spray coating[17] and spin coating.[18] Among all of these techniques, LbL is an easy and cost-effective technique to fabricate multilayer thin films.[4,19]

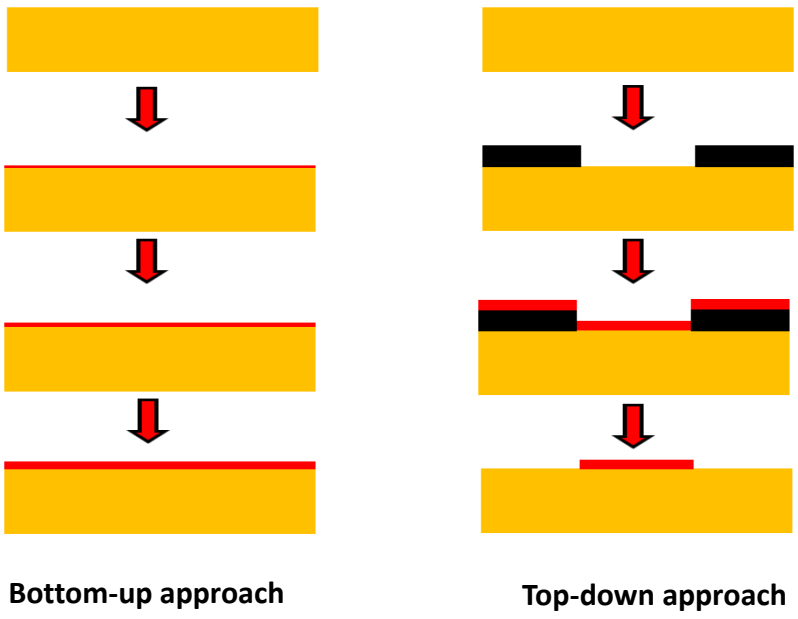

Figure 1.2 Top-down and bottom-up approach for thin film fabrication.

1.2.1 Layer-by-layer (LbL)

LbL is a thin film fabrication technique where films are formed by depositing alternative layers of materials. Various types of intermolecular interactions are used in LbL techniques such as electrostatic[20-25] and non-electrostatic interactions,[26-27] hydrogen, covalent and coordination bonding[28-34] and others.[35-37] **Figure 1.3** shows the schematic drawing of conventional LbL process for polyelectrolyte multilayer thin film growth. LbL is an efficient technique to fabricate multilayer thin film with control over the film thickness and reproducibility. The polyelectrolyte multilayer thin films are synthesized by the electrostatic interaction of polycation and polyanion between the polymers chains. By

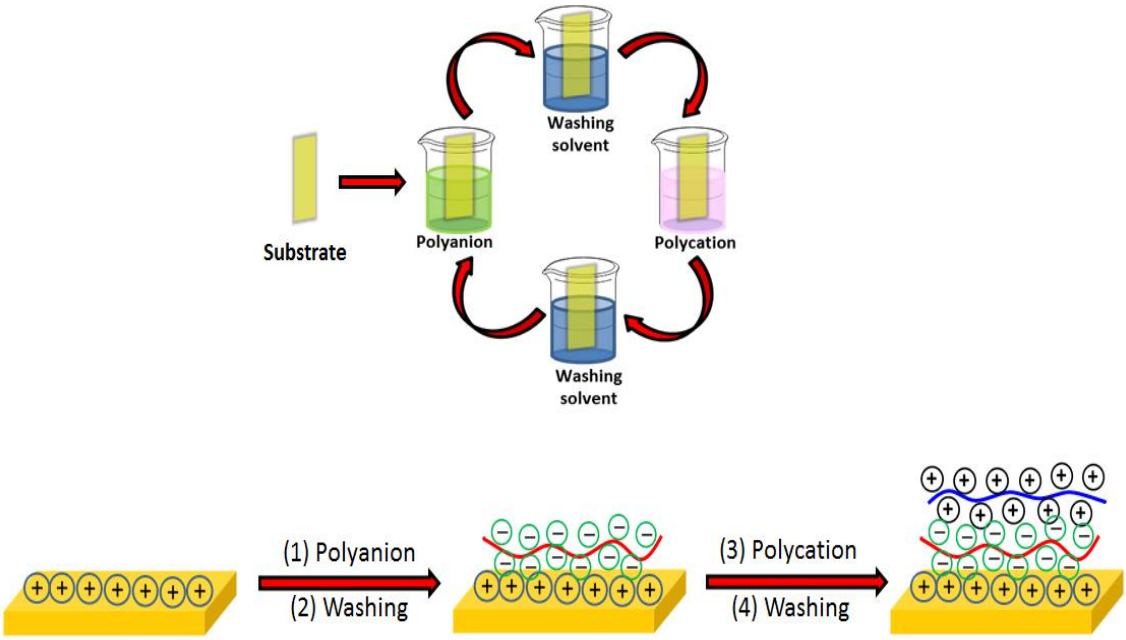

Figure 1.3 Schematic drawing of polyelectrolyte multilayer thin film growth using LbL technique.

using the advantage of charge-charge interaction, LbL technique has gained a great attention in biological science as many proteins, nucleic acids and enzymes bear charged groups that are able to interact with each other to form multilayer thin films.[30]

1.2.1.1 Vapor Deposition Technique

Vapor deposition is a technique in which materials in a vapor state are condensed through condensation, chemical reaction, or conversion to form a solid material. It is an emerging technique to achieve the well-controlled films composition, conformation, structure and smooth film morphology. Usually vapor-based deposition techniques are two types- (i) physical vapor deposition (PVD) and (ii) chemical vapor deposition (CVD). Among them chemical vapor deposition techniques, specially atomic layer deposition (ALD)[38-43] and molecular layer deposition (MLD)[44-49] have gained much attention because of having control over film thickness at atomic or molecular scale (angstrom to nanoscale level). ALD is a special type of CVD technique to fabricate the ultra-thin films of inorganic materials using metal, metal oxide and metal nitrile in sequential self-limiting reaction steps.[42-43] The substrate surface has a finite number of reactive sites, therefore only a finite number of reactant species can deposit on the surface. The self-limiting nature of the ALD process removes the randomness of reactant flux which helps to fabricate an extremely smooth and conformal thin film on the substrate. **Figure 1.4** shows a schematic

representation of vapor-based ALD technique for multilayer film formation.

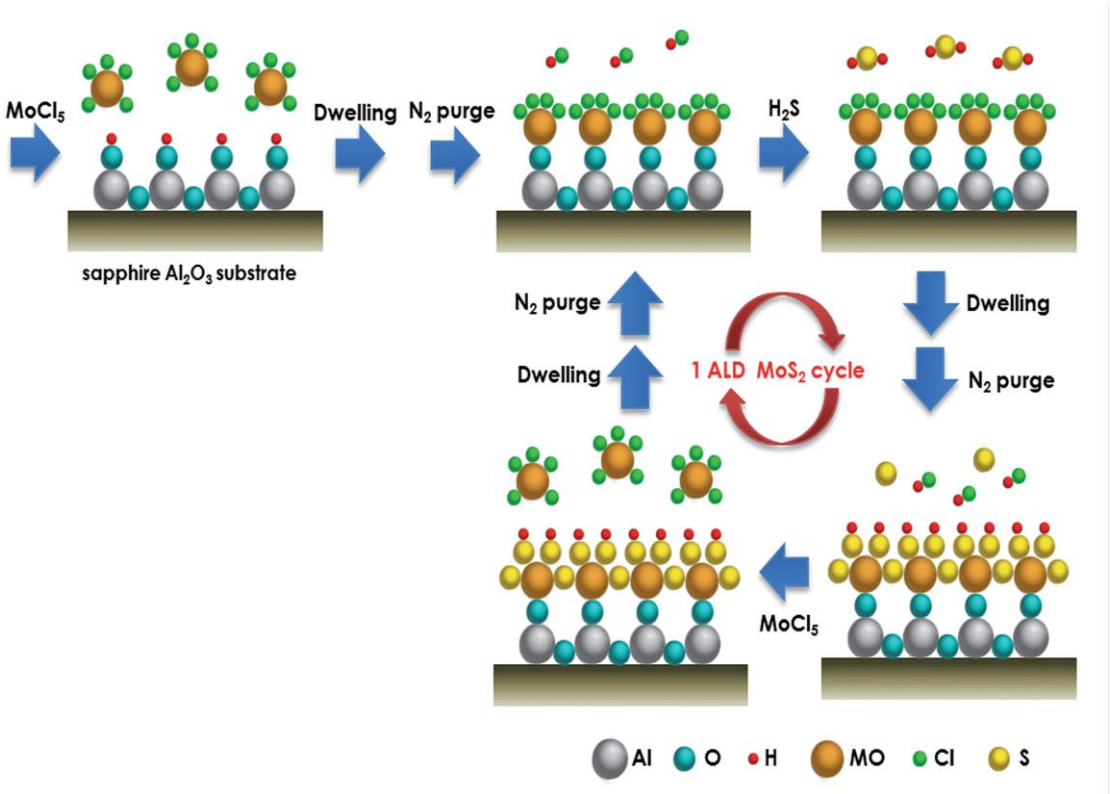

Figure 1.4 Schematic representation of vapor-based ALD process.[50]

In contrast to ALD, MLD process has been used for organic and organic-inorganic hybrid thin film growth on substrate surface by limiting the deposition rate to no more than one molecular layer per deposition step.[51] The self-assembled monolayers of the desired functionality should be fabricated first to initiate the film growth. Then the terminus of the film can be varied by substituting a desired functionality into the final molecule of the MLD sequence. Due to the stepwise film growth, it is anticipated that the orientation and

arrangement of the organic precursors should have less random compare to bulk polymeric materials. The vast numbers of organic molecules are available to select for the film growth, based on the corresponding polymerization chemistry. Typically, bifunctional organic molecules are used in vapor-based MLD techniques. A Schematic illustration of vapor-based MLD process is shown in **Figure 1.5**.

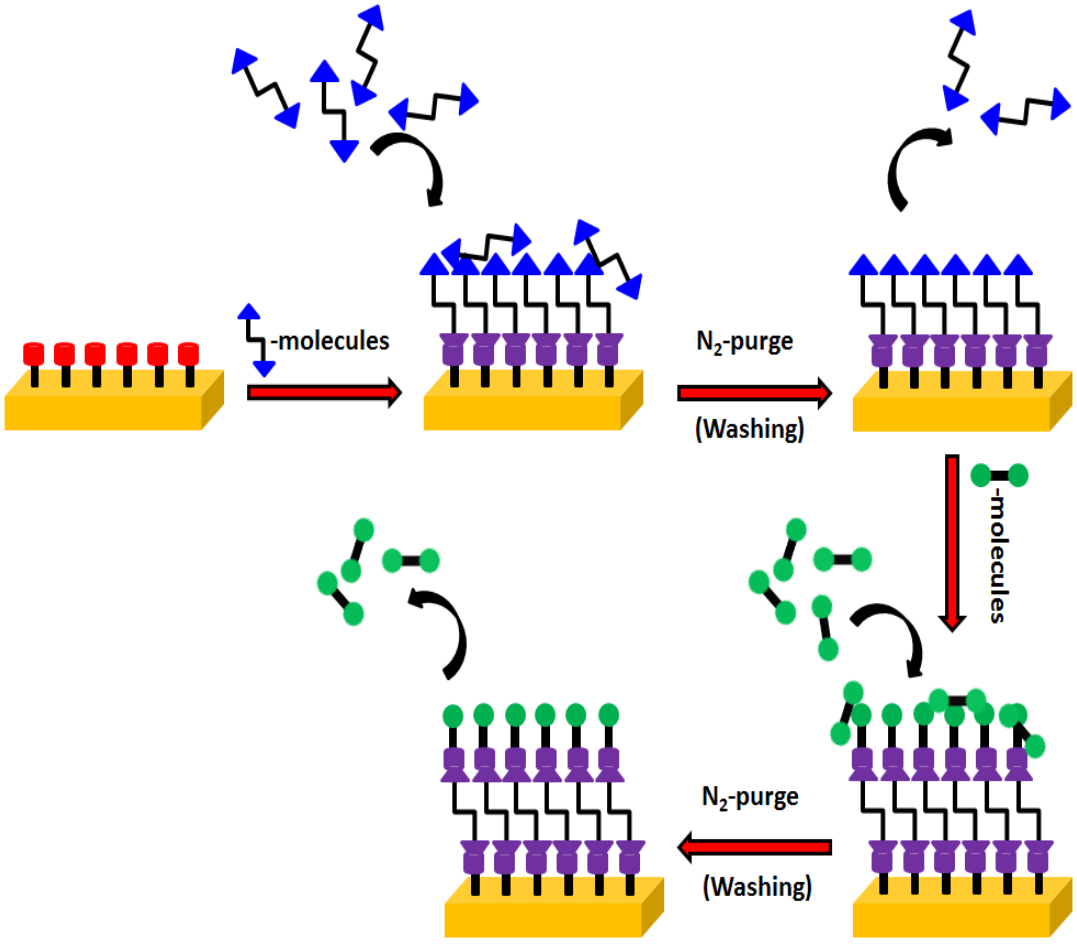

Figure 1.5 Conceptual representation of the vapor-based MLD process.

1.2.1.2 Solution-based Molecular Layer Deposition (MLD)

To date, most MLD processes have been conducted through polymerization of volatile bifunctional monomers under vacuum conditions to prepare polyamide,[45,52-53] polyimide,[48,54] polyurethane,[55] and polyurea[56-58] based nanostructures. However, vapor-based MLD technique is not applicable for macromolecules because of their high molar mass and boiling points.[59] In addition, the major difficulty is to remove physio-absorb monomers by using inert carrier gas in the time of deposition steps, the pH can't be varied and a catalyst can't be easily used.[49]

Recently, solution-based MLD process has taken much attention because of its simplicity and advantage over the vapor-based MLD techniques.[59-60] In this process, the multilayer thin films are fabricated by immersing the substrate into a series of solvents, containing selected multifunctional reacting monomers based on the target application. During the film growth, the unreacted physio-absorb monomers can be easily removed from the film surface by rinsing with a suitable set of solvents. As this process is based on solution-phase, it offers an opportunity to use catalyst or pH change according to the reaction requirements. In addition, the most attracting point of this technique is that it provides an opportunity to use macromolecular precursors for fabricating multilayer thin films.[61-62] Compared to conventional MLD film fabrication based on non-covalent interactions such as coulombic interactions[63-64] and hydrogen bonding,[65] covalently bonded

films possess much higher chemical and thermal stability because of their chemical characteristics.[66-67] **Figure 1.6** Schematic representation of organic multilayer thin film growth on solid surface using tetrafunctional precursors.

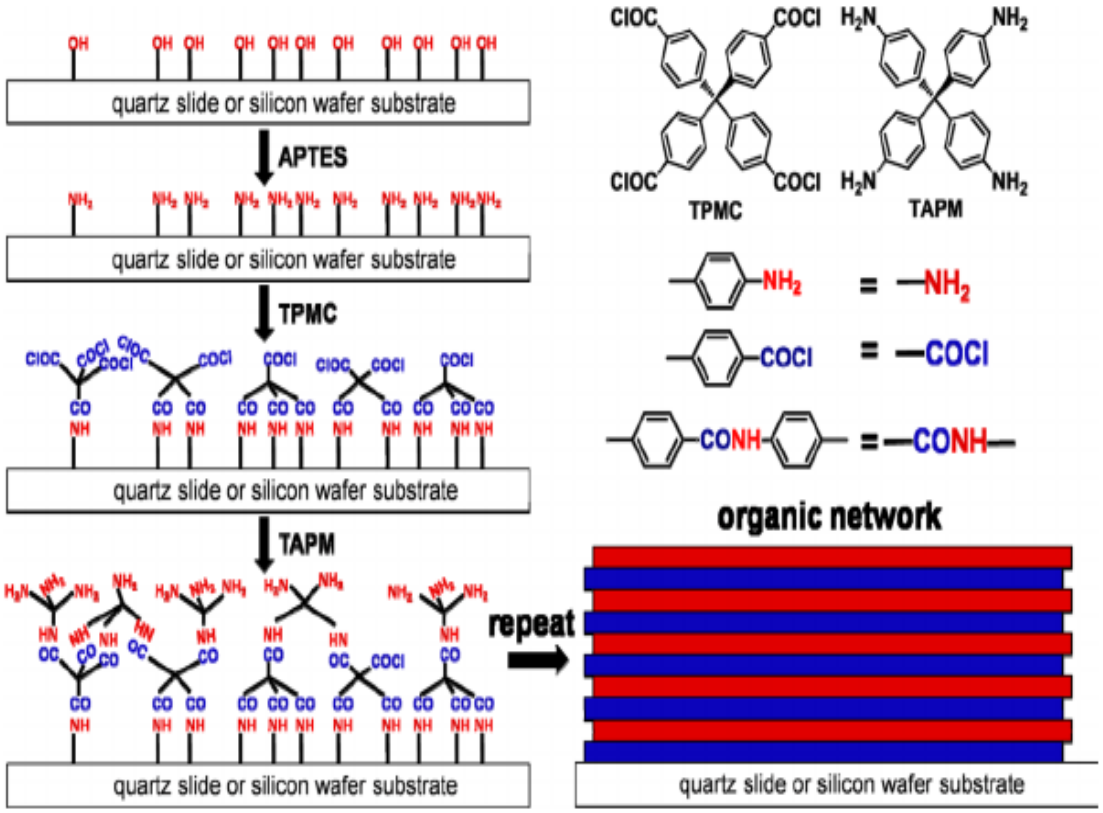

'igure 1.6 Schematic representation of organic multilayer thin film growth n solid surface using tetrafunctional precursors.[59]

1.3 Comparison of Bulk and Thin Film Materials

Thin film materials have a significant advantage over bulk materials. Bulk materials have a wide range of applications in chemistry, physics and biology but the main obstacle of bulk materials is the process ability for devices applications. In contrast, thin film materials are regarded as a suitable choice that allows the fabrication of devices with smaller volume and weight, low-cost and good performances for its higher flexibility, structural diversity, orientation, and control over the film thickness.[68-70] Control of thin film growth at the molecular level is necessary for device miniaturization because morphology plays a crucially important role in the performance of many devices,[5,71] but it is very challenging in the case of bulk materials. In addition, the immobilization property of the nanoscale molecular assembly on solid surface has taken a great attention for the improvement in utilization with long time durability.[72-73] **Figure 1.7** represents the comparison between bulk and surface-induce thin film synthesis. As we know that it is possible to synthesize crystalline as well as the non-crystalline materials by using bulk processes. But thin film offers an opportunity to control over the molecular orientation (**Figure 1.7a)** that can help to enhance their application performances.[74] Another most important benefits of this process is to control over the sequential molecular growth (**Figure 1.7b**). Suppose, precursor X contains a specific functional group which can react with two different precursors Y and Z (having same functional group). Then it is difficult

or impossible to control the molecular sequence in bulk reaction process whether substrate-induce thin film growth can control it easily.

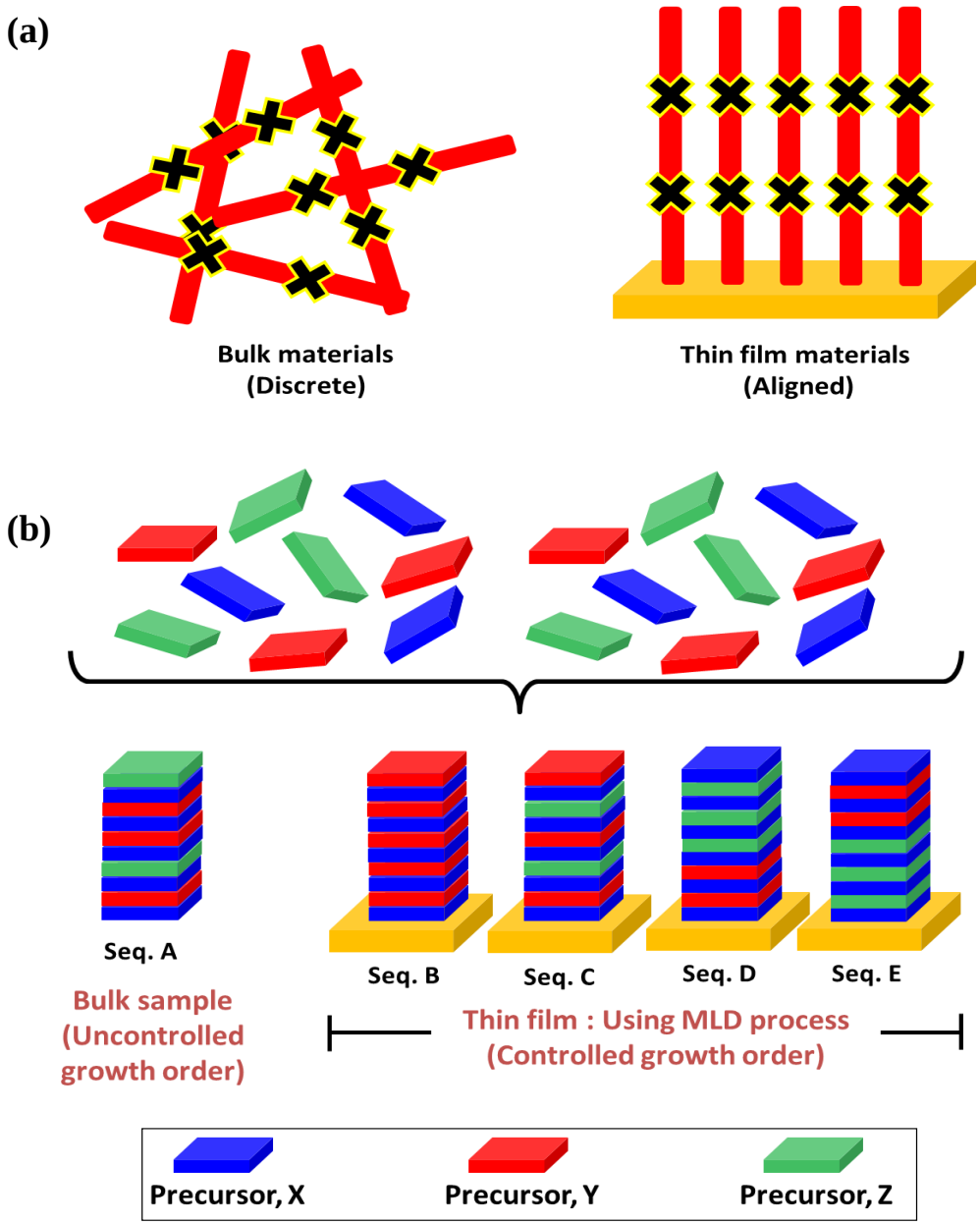

Figure 1.7 Comparison between bulk and surface-induce thin film fabrication: (a) molecular orientation and (b) molecular growth sequence.

1.4 Research Objectives

The main objective of this research is to use the solution-based molecular layer deposition method to fabricate porphyrin-based covalent molecular networks on a amine-functionalized substrate surface using the urea coupling reaction. This research was mainly addressed in two parts as following:

(a) Investigation of the chemical stability of one and three alkoxy group containing 3-aminopropyldimethylethoxysilane (APDMES) and 3-aminopropyltrimethoxysilane (APTMS) on Si/SiO_2 substrates respectively.

(b) The study of thin film synthesis of porphyrin-based covalent molecular networks on a amine-functionalized substrate surface using the urea coupling reaction, especially in these aspects:

- Investigation of RH effect on multilayer thin film growth using urea coupling reaction.
- Growth phenomena, chemical bonding and surface morphology.

1.5 Thesis Outline

In chapter 1, the general introduction of this thesis was mentioned about the thin film technology and there scope modern science.

In chapter 2, the chemical stability of the self-assembled monolayer of one and three alkoxy group containing 3-aminopropyldimethyl ethoxysilane (APDMES) and 3-aminopropyl trimethoxysilane (APTMS) on SiO_2 substrates were investigated by considering there appropriate preparation conditions. The finding in this chapter motivated to the use of APTMS in the study of thin film preparation in chapter 3.

In chapter 3, I have demonstrated the solution-based MLD thin film growth of porphyrin-based covalent molecular networks on a APTMS-modified substrate surface using the urea coupling reaction between 1,4-PDI and H_2TAPP at room temperature. The growth phenomena and thin film properties were examined. Stepwise multilayer film growth was observed at ≤14% RH, whereas the high RH conditions showed film growth-limiting behavior. Presumably, numerous 1,4-PDI self-polymerization took place at high RH conditions. This suggests about the effect of RH on polyure-based multilayer film growth.

In chapter 4, general conclusion and future prospects of this research were presented.

References

(1) Castner, D. G.; Ratner, B. D. Biomedical Surface Science: Foundations to Frontiers. *Surf. Sci.* **2002**, *500*, 28-60.

(2) Lord, M. S.; Foss , M.; Besenbacher, F. Influence of Nanoscale Surface Topography on Protein Adsorption and Cellular Response, *Nano Today* **2010**, *5*, 66-78.

(3) Koegler, P.; Clayton, A.; Thisen, H.; Santos, G. N. C.; Kingshott, P. The Influence of Nanostructured Materials on Biointerfacial Interactions. *Adv. Drug Delivery rev.* **2012**, *64*, 1820-1939.

(4) Xiao, F.-X.; Pagliaro, M.; Xu, Y.-J.; Liu, B. Layer-by-Layer Assembly of Versatile Nanoarchitectures with Diverse Dimensionality: a new Perspective for Rational Construction of Multilayer Assemblies. *Chem. Soc. Rev.* **2016**, *45*, 3088-3121.

(5) Huang, W.; Gann, E.; Cheng, Y-B.; McNeill, C. R. In-Depth Understanding of the Morphology−Performance Relationship in Polymer Solar Cells. *ACS Appl. Mater. Interfaces* **2015**, *7*, 14026−14034.

(6) Doherty, C. M.; Grenci, G.; Riccò, R.; Mardel, J. I.; Reboul, J.; Furukawa, F.; Kitagawa, S.; Hill, A. J.; Falcaro, P. Combining UV Lithography and an Imprinting Technique for Patterning Metal-Organic Frameworks. *Adv. Mater.* **2013**, *25*, 4701-4705.

(7) Teo, B. K.; Sun, X. H. From Top-Down to Bottom-Up to Hybrid Nanotechnologies: Road to Nanodevices. *J. Cluster Sci.* **2006**, *17*, 529-540.

(8) Zacher, D.; Yusenko, K.; Bétard, A.; Henke, S.; Molon, M.; Ladnorg, T.; Shekhah, O.; Schüpbach, B.; de los Arcos, T.; Krasnopolski, M.; Meilikhov, M.; Winter, J.; Terfort, A.; Wöll, C.; Fischer, R. A. Liquid-Phase Epitaxy of Multicomponent Layer-Based Porous Coordination Polymer Thin Films of [M(L)(P)0.5] Type: Importance of Deposition Sequence on the Oriented Growth. *Chem. Eur. J.* **2011**, *17*, 1448–1455.

(9) Blodgett. K. B. Films Built by Depositing Successive Monomolecular Layers on a Solid Surface. *J. Am. Chem. Soc.* **1935**, *57*, 1007-1022.

(10) Langmuir, I.; Schaefer, V. J. Monolayers and Multilayers of Chlorophyll. *J. Am. Chem. Soc.* **1937**, *59*, 2075-2076.

(11) Talham, D. R. Conducting and Magnetic Langmuir−Blodgett Films. *Chem. Rev.* **2004**, *104*, 5479-5502.

(12) Ariga, K.; Yamauchi, Y. Mori, T.; Hill, J. P. 25th Anniversary Article: What Can Be Done with the Langmuir-Blodgett Method? Recent Developments and its Critical Role in Materials Science. *Adv. Mater.* **2013**, *25*, 6477-6512.

(13) Li, Z.-Q.; Zhang, M.; Liu, B.; Guo, C.-Y.; Zhou, M. Rapid Fabrication of Metal-Organic Framework Thin Film Using in situ Microwave Irradiation and Its Photocatalytic Property. *Inorg. Chem. Commun.* **2013**, *36*, 241-244.

(14) Horcajada, P.; Serre, C.; Grosso, D.; Boissière, C.; Perruchas, S.; Sanchez, C.; Férey, G. Colloidal Route for Preparing Optical Thin Films of Nanoporous Metal-Organic

Frameworks. *Adv. Mater.* **2009**, *21*, 1931-1935.

(15) Wade, C. R.; Li, M.; Dincá, M. Facile Deposition of Multicolored Electrochromic Metal-Organic Framework Thin Films. *Angew. Chem. Int. Ed.* **2013**, *52*, 13377-13381.

(16) Zhuang, J.-L.; Ar, Z.; Yu, X.-J.; Liu, J.-X.; Terfort, A. Patterned Deposition of Metal-Organic Frameworks onto Plastic, Paper, and Textile Substrates by Inkjet Printing of a Precursor Solution. *Adv. Mater.* **2013**, *25*, 4631-4635.

(17) Arslan, H. K.; Shekhah, O.; Wohlgemuth, J.; Franzreb, M. High-Throughput Fabrication of Uniform and Homogenous MOF Coatings. *Adv. Funct. Mater.* **2011**, *21*, 4228-4231.

(18) Zhuang, J.-L.; Ceglarek, D.; Pethuraj, S.; Terfort, A. Rapid Room-Temperature Synthesis of Metal-Organic Framework HKUST-1 Crystals in Bulk and as Oriented and Patterned Thin Films. *Adv. Funct. Mater.* **2011**, *21*, 1442–1447.

(19) Borges, J.; Mano, J. F. Molecular Interactions Driving the Layer-by-Layer Assembly of Multilayers. *Chem. Rev.* 2014, *114*, 8883-8942.

(20) Dubas, S. T.; Schlenoff, J. B. Factors Controlling the Growth of Polyelectrolyte Multilayers. *Macromolecules* **1999**, *32*, 8153-8160.

(21) Dubas, S. T.; Schlenoff, J. B. Swelling and Smoothing of Polyelectrolyte Multilayers by Salt. *Langmuir* **2001**, *17*, 7725-7727.

(22) Hammond, P. T. Form and Function in Multilayer Assembly: New Applications at the Nanoscale. *Adv. Mater.* **2004**, *16*, 1271-1293.

(23) Hammond, P. T. Recent Explorations in Electrostatic Multilayer Thin Film Assembly. *Curr. Opin. Colloid Interface Sci.* **2000**, *4*, 430-442.

(24) Hammond, P. T. Engineering Materials Layer-by-Layer: Challenges and Opportunities in Multilayer Assembly. *AIChE J*. **2011**, *57*, 2928-2940.

(25) Schoeler, B.; Kumaraswamy, G.; Caruso, F. Investigation of the Influence of Polyelectrolyte Charge Density on the Growth of Multilayer Thin Films Prepared by the Layer-by-Layer Technique. *Macromolecules* **2002**, *35*, 889-897.

(26) Shimazaki, Y.; Mitsuishi, M.; Ito, S.; Yamamoto, M.; Inaki, Y. Preparation of the Nucleoside-containing Nanolayered Film by the Layer-by-Layer Deposition Technique. *Thin Solid Films* **1998**, *333*, 5-8.

(27) Serizawa, T.; Yamamoto, K.; Akashi, M. A Novel Fabrication of Ultrathin Poly(vinylamine) Films with a Molecularly Smooth Surface. *Langmuir* **1999**, *15*, 4682-4684.

(28) Zelikin, A. N.; Li, Q.; Caruso, F. Disulfide-Stabilized Poly(methacrylic acid) Capsules: Formation, Cross-Linking, and Degradation Behavior. *Chem. Mater.* **2008**, *20*, 2655-2661.

(29) Stockton, W. B.; Rubner, M. F. Molecular-Level Processing of Conjugated Polymers. 4. Layer-by-Layer Manipulation of Polyaniline via Hydrogen-Bonding Interactions. *Macromolecules* **1997**, *30*, 2717-2725.

(30) Wang, X.; Jiang, Z.; Shi, J.; Liang, Y.; Zhang, C.; Wu, H. Metal Organic Coordination-Enabled Layer-by-Layer Self-Assembly to Prepare Hybrid Microcapsules for Efficient Enzyme Immobilization. *ACS Appl. Mater. Interfaces* **2012**, *4*, 3476-3483.

(31) Lee, H.; Kepley, L. J.; Hong, H.-G.; Mallouk, T. E. Adsorption of Ordered Zirconium Phosphonate Multilayer films on silicon and gold surfaces. *J. Phys. Chem.* **1988**, *92*, 2597-2601.

(32) Hanke, M.; Arslan, H. K.; Bauer, S.; Zybaylo, O.; Christophis, C.; Gliemann, H.; Rosenhahn, A.; Wöll, C. The Biocompatibility of Metal–Organic Framework Coatings: An Investigation on the Stability of SURMOFs with Regard to Water and Selected Cell Culture Media. *Langmuir* **2012**, *28*, 6877-6884.

(33) Kohli, P.; Blanchard, G. J. Applying Polymer Chemistry to Interfaces: Layer-by-Layer and Spontaneous Growth of Covalently Bound Multilayers. *Langmuir* **2000**, *16*, 4655-4661.

(34) Zhang, Y.; Yang, S.; Guan, Y.; Cao, W.; Xu, J. Fabrication of Stable Hollow Capsules by Covalent Layer-by-Layer Self-Assembly. *Macromolecules* **2003**, *36*, 4238-4240.

(35) Zhang, Y.; Cao, W. Stable Self-Assembled Multilayer Films of Diazo Resin and Poly(maleic anhydride-*co*-styrene) Based on Charge-Transfer Interaction. *Langmuir* **2001**, *17*, 5021-5024.

(36) Crespo-Biel, O.; Dordi, B.; Reinhoudt, D. N.; Huskens, J. Supramolecular Layer-by-Layer Assembly: Alternating Adsorptions of Guest- and Host-Functionalized Molecules and Particles Using Multivalent Supramolecular Interactions. *J. Am. Chem. Soc.* **2005**, *127*, 7594-7600.

(37) Yao, H.; Hu, N. pH-Switchable Bioelectrocatalysis of Hydrogen Peroxide on Layer-by-Layer Films Assembled by Concanavalin A and Horseradish Peroxidase with Electroactive Mediator in Solution. *J. Phys. Chem. B* **2010**, *114*, 3380-3386.

(38) George, S. M. Atomic Layer Deposition: An Overview. *Chem. Rev*. **2009**, *110*, 111-131.

(39) Ritala, M.; Leskela, M. Atomic Layer Deposition. In Handbook of Thin Film Materials. Nalwa, H. S., Ed.; Academic Press; San Diego **2002**; Vol.1.

(40) Johnson, R. W.; Hultqvist, A.; Bent, S. F. A Brief Review of Atomic layer Deposition: from Fundamental to Applications. *Mater. Today* **2014**, *17 (5)*, 236-246.

(41) Chan, R.; Bent, S. F. Chemistry for Positive Pattern Transfer Using Area-Selective Atomic Layer Deposition. *Adv. Mater.* **2006**, *18*, 1086-1090.

(42) Jiang, X.; Bent, S. F. Area-Selective ALD with Soft Lithographic Methods: Using Self-Assembled Monolayers to Direct Film Deposition. *J. Phys. Chem. C* **2009**, *113*, 17613-17625.

(43) Jiang, X.; Huang, H.; Prinz, F. B.; Bent, S. F. Application of Atomic Layer Deposition of Platinum to Solid Oxide Fuel Cells. *Chem. Mater.* **2008**, *20*, 3897-3905.

(44) Kubono, A.; Yuasa, N; Shao, H.-L.; Umemoto, S.; Okui, N. In-situ Study on Alternating Vapor Deposition Polymerization of Alkyl Polyamide with Normal Molecular Orientation. *Thin Solid Films* **1996**, *289*, 107-111.

(45) Du, Y.; George, S. M. Molecular Layer Deposition of Nylon 66 Films Examined Using in situ FTIR Spectroscopy. *J. Phys. Chem. C* **2007**, *111*, 8509-8517.

(46) Kim, A.; Filler, M. A.; Kim, S.; Bent, S. F. Layer-by-Layer Growth on Ge (100) via Spontaneous Urea Coupling Reactions. *J. Am. Chem. Soc.* **2005**, *127*, 6123-6132.

(47) Loscutoff, P. W.; Zhou, H.; Clendenning, S. B.; Bent, S. F. Formation of Organic Nanoscale Laminates and Blends by Molecular Layer Deposition. *ACS Nano* **2010**, *4*, 331-341.

(48) Yoshida, S.; Ono, T.; Esashi, M. Deposition of Conductivity-Switching Polyimide Film by Molecular Layer Deposition and Electrical Modification using Scanning Probe Microscope. *Micro. Nano Lett.* **2010**, *5*, 321-323.

(49) Loscutoff, P. W.; Lee, H. B. R.; Bent S. F. Deposition of Ultrathin Polythiourea Films by Molecular Layer Deposition. *Chem. Mater*. **2010**, *22*, 5563-5569.

(50) Tan, L. K.; Liu, B.; Teng, J. H.; Guo, S.; Low' H. Y; Loh, K. P. Atomic layer deposition of a MoS_2 film. ***Nanoscale* 2014, *6***, 10584-10588.

(51) Zhou, H.; Bent, S. F. Febrication of Organic Interfacial Layers by Molecular Layer Deposition: Present Status and Future Opportunities. *J. Vac. Sci. Technol. A* **2013**, *31(4)*, 040801-(1)-(18).

(52) Adamczyk, N. M.; Dameron, A. A.; George, S. M. Molecular Layer Deposition of Poly(p-phenyleneterephthalamide) Films Using Terephthaloyl Chloride and p-Phenylenediamine. *Langmuir* **2008**, *24*, 2081–2089.

(53) Peng, Q.; Efimenko, K.; Genzer, J.; Pardsons, G. N. Oligomer Orientation in Vapor-Molecular-Layer-Deposited Alkyl-Aromatic Polyamide films. *Langmuir* **2012**, *28*, 10464–10470.

(54) Yoshida, S.; Ono, T.; Esashi, M. Local Electrical Modification of a Conductivity-Switching Polyimide Film Formed by Molecular Layer Deposition. *Nanotechnology* **2011**, *22*, 335302.

(55) Lee, J. S.; Lee, Y. J.; Tae, E. L.; Park, Y. S.; Yoon, K. B. Synthesis of Zeolite as ordered Multicrystal Arrays. *Science* **2003**, *301*, 818–821.

(56) Prasittichai, C.; Zhou, H.; Bent, S. F. Area Selective Molecular Layer Deposition of

Polyurea Films. *ACS Appl. Mater. Interfaces* **2013**, *5*, 13391–13396.

(57) Zhou, H.; Bent. S. F. Molecular Layer Deposition of Functional Thin Films for Advanced Lithographic Patterning. *ACS Appl. Mater. Interfaces* **2011**, *3*, 505–511.

(58) Rashed, M. A.; Laokroekkiat, S.; Hara, M.; Nagano, S.; Nagao, Y. Fabrication and Characterization of Cross-Linked Organic Thin Films with Nonlinear Mass Densities. *Langmuir* **2016**, *32*, 5917−5924.

(59) Qian, H.; Li, S.; Zheng, J.; Zhang, S. Ultrathin Films of Organic Networks as Nanofiltration Membranes via Solution-Based Molecular Layer Deposition. *Langmuir* **2012**, *28*, 17803–17810.

(60) Kim, M.; Byeon, M.; Bae, J-S.; Moon, S. Y.; Yu, G.; Shin. K.; Basarir, F.; Yoon, T. H.; Park, J-W. Preparation of Ultrathin Films of Molecular Networks through Layer-by-Layer Cross-Linking Polymerization of Tetrafunctional Monomers. *Macromolecules* **2011**, *44*, 7092-7095.

(61) Palomaki, P. K. B.; Dinolfo, P. H. A Versatile Molecular Layer-by-Layer Thin Film Fabrication Technique utilizing Copper(I)-Catalyzed Azide–Alkyne Cycloaddition. *Langmuir* **2010**, *26* (12), 9677–9685.

(62) Palomaki, P. K. B.; Dinolfo, P. H. Structural Analysis of Porphyrin Multilayer Films on ITO Assembled Using Copper (I)-Catalyzed Azide-Alkyne Cycloaddition by ATR IR. *ACS Appl. Mater. Interfaces* **2011**, *3*, 4703–4713.

(63) Lee, B. H.; Ryu, M. K.; Choi, S. Y.; Lee, K. H.; Im, S.; Sung, M. M. Rapid vapor-phase fabrication of organic–inorganic hybrid super lattices with monolayer precision. *J. Am. Chem. Soc.* **2007**, *129*, 16034−16041.

(64) Laokroekkiat, S.; Hara, M.; Nagano, S.; Nagao, Y. Metal−Organic Coordination Network Thin Film by Surface-Induced Assembly. *Langmuir* **2016**, *32*, 6648−6655.

(65) Such, G. K.; Johnston, A. P. R.; Caruso, F. Engineered hydrogen bonded polymer multilayers: from assembly to biomedical applications. *Chem. Soc. Rev.* **2011**, *40*, 19−29.

(66) Quinn, J. F.; Johnston, A. P. R.; Such, G. K.; Zelikin, A. N.; Caruso, F. Next generation, sequentially assembled ultrathin films: beyond electrostatics. *Chem. Soc. Rev.* **2007**, *36*, 707−718.

(67) Buck, M. E.; Schwartz, S. C.; Lynn, D. M. Super hydrophobic thin films fabricated by reactive layer-by-layer assembly of azlactone-functionalized polymers. *Chem. Mater.* **2010**, *22*, 6319−6327.

(68) Krishnan, K.; Iwatsuki, H.; Hara, M.; Nagano, S.; Nagao, Y.; Proton Conductivity Enhancement in Oriented, Sulfonated Polyimide Thin Films. *J. Mater. Chem. A* **2014**, *2*, 6895-6903.

(69) Ichiki, I.; Maeda, R.; Morikawa, Y.; Mabune, Y.; Nakada, T.; Momaka, K. Photovoltaic Effect of Lead Lanthanum Zirconate Titanate in a Layered Film Structure Design. *Appl. Phys. Lett.* **2004**, *84*, 395-397.

(70) Eckermann,A. L.; Feld, D. J.; Shaw, J. A.; Meade, T. J. Electrochemistry of redox-active self-assembled monolayers. Coord. Chem. Rev. **2010**, *254*, 1769–1802.

(71) Tao, Y.; McCulloch, B.; Kim, S.; Segalman, R. A. The relationship between morphology and performance of donor–acceptor rod–coil block copolymer solar cells. *Soft Matter* **2009**, *5*, 4219–4230.

(72) Falcaro, P.; Ricco, R.; Doherty, C. M.; Liang, K.; Hill, A. J.; Styles, M. J. MOF Positioning Technology and Device Fabrication. *Chem. Soc. Rev.* **2014**, *43*, 5513–5560.

(73) Ariga, K.; Sakakibara, K.; Richards, G. J.; Hill, J. P. Dynamic Supramolecular Systems at Interfaces. *Supramol. Chem.* **2011**, *23*, 183-194.

(74) Nagao, Y.; Matsui, J.; Abe, T.; Hiramatsu, H.; Yamamoto, H.; Miyashita, T.; Sata, N.; Yugami, H. Enhancement of Proton Transport in an Oriented Polypeptide Thin Film. *Langmuir*, **2013**, *29*, 6798-6804.

Chapter-02

Investigation of Self-assembled Monolayers (SAMs)

Aminosilanes are common coupling agents used to functionalize Si/SiO_2 surfaces. The major problem of aminosilane-modified surfaces is their chemical stabilities. To examine the issue of losing surface functionality, I prepared the self-assembled monolayer of one and three alkoxy group containing 3-aminopropyldimethyl ethoxysilane (APDMES) and 3-aminopropyl trimethoxysilane (APTMS) on SiO_2 substrates respectively. Silanization of APDMES was carried out in four different solvents under various reaction conditions. APDMES layer prepared in ethanol at 70 ºC for 3 hr shows the higher N-at. % along with high free amine %. In contrast, APTMS-modified SiO_2 surface was preapered in ethanol at RT for different time scale (1, 2, 3hr). The same surface response was observed for APTMS-modified surface at 1, 2 and 3 hr of silanization. The chemical stability of APDMES and APTMS-modified SiO_2 substrates were also investigated after 7 hr immersion into H_2O and 0.1 M $HClO_4$ solution at 40 ºC and RT respectively. XPS analysis showed that 22.4 % APDMES and 6.7 % APTMS were removed from the surface when the modified substrates were immersed into H_2O at 40 ºC for 7 hr. On the other hand, 38.7 % APDMES and 14.9 % APTMS were removed from the surface when the modified substrates were immersed into 0.1 M $HClO_4$ (aq) solution at RT for 7 hr.

2.1 Introduction

2.1.1 Self-assembled Monolayers (SAMs)

Modern surface chemistry is an important research field about molecular-level understanding and the control over the surface chemical reactions. Self-assembled monolayer (SAM) is a robust and versatile approach to fine-tune a surface of interest. The molecular self-organization from the solution phase to a surface was first reported by W. C. Bigelow in 1946,[1] but later on J. Sagiv introduced the definition of self-assembled monolayers.[2] Studies on self-assembled monolayers (SAMs) have been reported for several decades[3], the various kinds of device fabrication has been endorsed by this technique.[4-6] SAMs is powerful surface modification technique to tailor the surface properties by the combination of molecules and surface. For SAM formation, at first the molecules should be chemisorbed on the surface and then spontaneously organized into 2D long-range molecular ordered domains.[5,7] SAMs are typically composed of three parts as shown in **Figure 2.1**:

(i) the head group, it is the end of the molecule which binds to the surface. For example: trichloro-, trimethoxy-, triethoxysilane, etc.

(ii) a backbone, made of an aliphatic chain and/or an aromatic oligomer, mostly responsible for the molecular ordering.

(iii) the terminal group, which determines topography,[2] surface energy,[8] and chemistry[2] of the outer interface. For example: halide, methyl, carboxyl, hydroxyl, amino, etc.

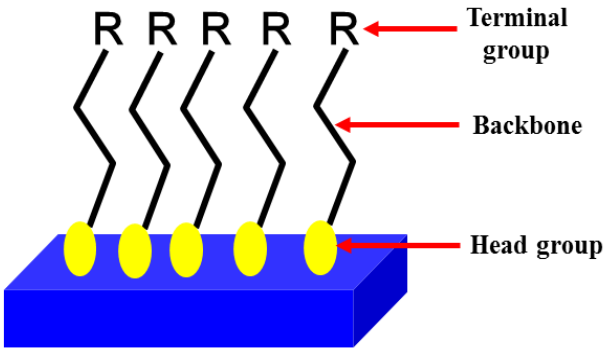

Figure 2.1 Schematic representation of SAMs structure.

Thiols and organosilicon derivatives (silane coupling agent) are commonly used for SAMs preparation. In 1990s, alkanethiol has taken a great attention for gold surface modification.[9] But serval limitations were indentified for the alkanothiol/gold system; such as lack of driving force for monolayer formation leads to labile structure, the thiol head groups are sensitive towords oxidation degradation.[10-11] Later on, organosilane precursors have been widely chosen for the –OH terminated silicon or quartz surfaces. This is because of their strong covalent bond formation possibility between the alkoxy group (−OR) of organosilane molecules and surface substrate surface −OH group to form Si−O−Si bond.[12-17]

2.1.2 Aminosilane

The amine-terminated silane, commonly known as aminosilanes (**Figure 2.2**) are widely used silane coupling agents for silica-based materials because of their bifunctional nature. They have the ability to form a durable chemical bond with organic and inorganic materials. Aminosilanes are widely used to functionalize the hydroxyl-terminated surface for the wide range of applications such as chromatography,[18] biosensor (immobilization of DNA, proteins, etc.),[19-22] inmedicine,[23] for attaching metal nanoparticles,[24] for the detection of specific gases[25] and explosives.[26-27]

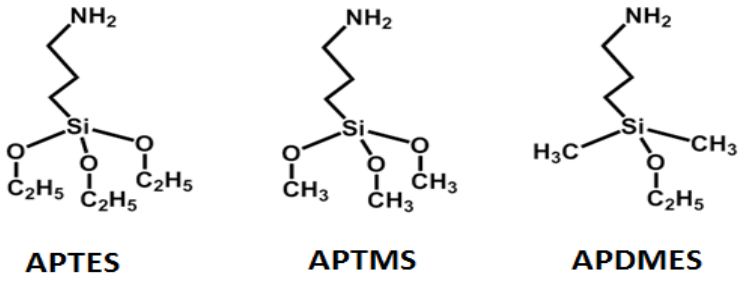

Figure 2.2 Chemical structure and abbreviation of some aminosinale molecules.

Aminosilanes are unique in surface reaction chemistry because of the presence of amine group which act as a built-in catalyst. The amine is capable of catalyzing the formation and hydrolysis of siloxane bonds at ambient temperature. In that case, amine group can bind to the Si atom of the same or neighbor aminosilane molecules by intra or inter molecular interaction and forms a cyclic intermediate that is very reactive to nucleophiles i.e., the surface −OH group or water molecules (**Scheme 2.1**).[28]

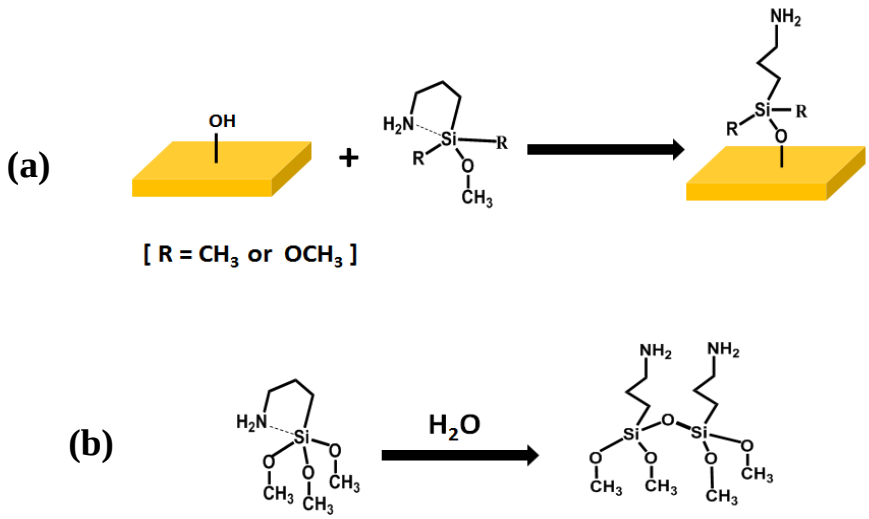

Scheme 2.1 (a) schematic representation of aminosilane modification (b) polymerization of aminosilane in presence of H_2O.

In all aminosilane cases, a lack of reproducibility in SAMs formation arises from different reaction conditions such as reaction temperature, nature of the aminosilane (mono-, di- or trialkoxy), reaction time, solvent system and silane concentration.[28-30] So, it is very important to investigate systematically the reaction conditions before further studies. A more realistic bond orientation of aminosilane-modified surface is shown in **Figure2.3.**

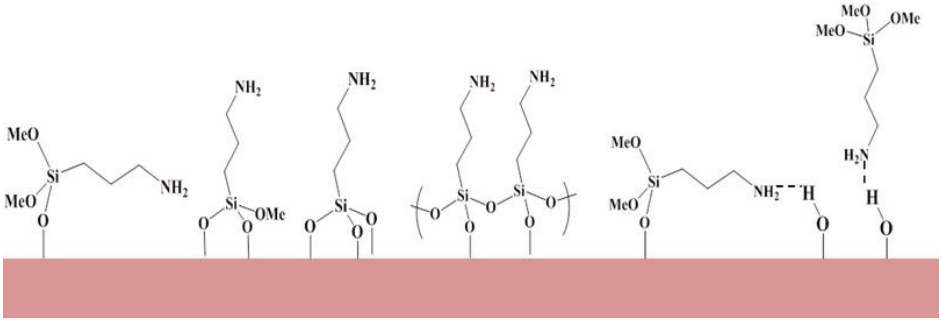

Figure 2.3 The possible realistic bond orientation of APTMS-modified substrate.

2.2 Experimental

2.2.1 Materials

3-aminopropyltrimethoxysilane (APTMS, >96%) was purchased from Tokyo Chemical Industry Co. Ltd., Japan. 3-aminopropyldimethylethoxysilane (APDMES, >96%) was purchased from Gelest, Inc. and stored under Ar atmosphere. For substrate cleaning, HPLC grade ethanol and 2-propanol were purchased from Wako Pure Chemical Industries Ltd., Japan, and were used as-received without further purification. AR grade toluene, ethanol, acetone and N, N-dimethylformamide (DMF) were also obtained from Wako Pure Chemical Industries Ltd., Japan.

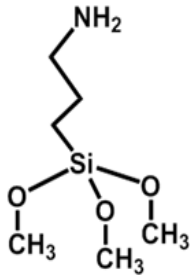

3-aminopropyltrimethoxysilane (APTMS)

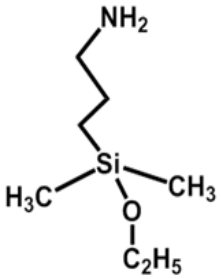

3-aminopropyldimethylethoxysilane (APDMES)

Figure 2.4 Chemical structures of (a) 3-aminopropyltrimethoxysilane, APTMS and (b) 3-aminopropyldimethylethoxysilane , APDMES.

2.2.2 Surface Cleaning

Quartz substrate (SiO_2; 25 × 15 mm^2, t = 0.5 mm) and boron doped p-type silicon wafer (p-Si (100); 5-20 Ω-cm, 30 × 20 mm^2, t = 0.5 mm) were chosen for multilayer thin film fabrication. Before use, these substrates were cleaned by sonication for 3 × 15 min using 2-propanol (HPLC grade) to remove organic contaminants. Finally, rinsed with 2-propanol and streamed with Ar and dried and kept in a clean bench.

2.2.3 Modification of Solid Substrate

2.2.3.1 Self-assembled Monolayer of APDMES

The modification of freshly cleaned SiO_2 and Si substrates were carried out in 10 mM solution (AR grade) of APDMES in toluene, ethanol, acetone and DMF solvents separately. The silanization reaction was carried out in a closed system for a specific time (1, 2, 3 and 6 hr) at room temperature (22 ± 2 ºC) and at high temperature: (a) 70 ºC (toluene, ethanol and DMF) and (b) 50 ºC (acetone). The flask was purged with Ar prior to the silanization. After taking out from the APTMS solution, the substrates were washed with HPLC grade ethanol (twice) and 2-propanol (twice) solvents consecutively with sonication for 5 min each and were finally rinsed with 2-propanol and streamed with Ar and dried in a clean bench.

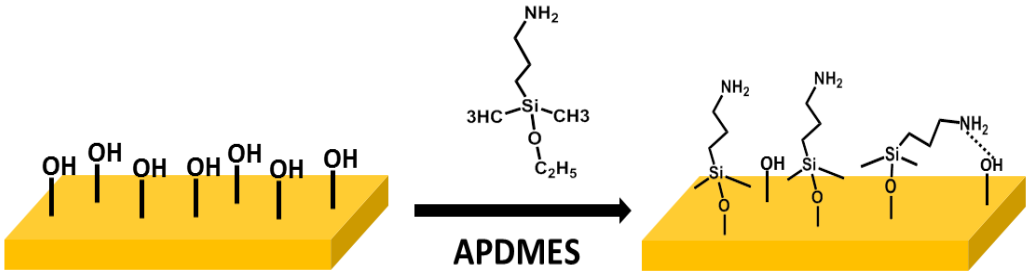

Scheme 2.2 Silanization reaction between APDMES and the hydroxylated solid surface.

2.2.3.2 Self-assembled Monolayer of APTMS

To obtain the self-assembled monolayers of APTMS, clean SiO_2 and Si substrates were immersed into 10 mM ethanol solution (AR grade) of APTMS for 1, 2 and 3 hr with constant stirring at room temperature (22 ± 2 ºC) under an Ar atmosphere. After taking out from the APDMES solution, the substrates were washed and stored as the same process mentioned above.

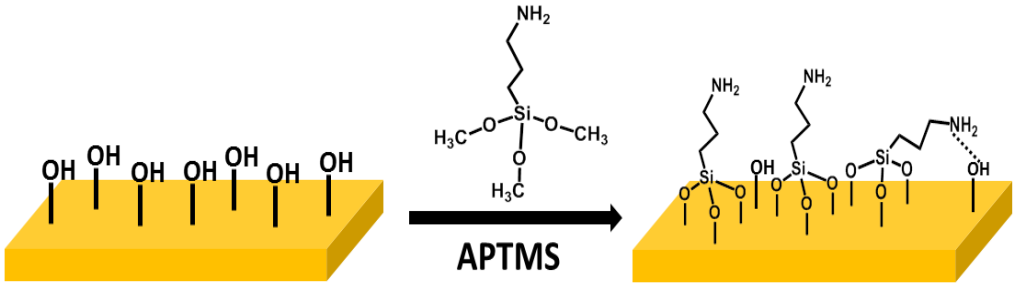

Scheme 2.3 Silanization reaction between APTMS and the hydroxylated solid surface.

2.2.4 Chemical Stability of APDMES and APTMS-modified Surface

The chemical stability of APDMES and APTMS-modified SiO_2 substrate was investigated under H_2O and $HClO_4$ solution. Hydrolytic stability of APDMES and APTMS-modified substrate was investigated by immersing into H_2O for 7 hr at 40 ºC. Acidic stability of APDMES and APTMS-modified substrate was investigated by immersing into 0.1 M $HClO_4$ (aq) solution for 7 hr at room temperature. Finally, the substrates were washed with enough amount of water and dried in a clean bench.

2.2.5 Characterization

Several characterization techniques have been used to investigate multilayer thin film growth on solid surfaces, the physical and chemical properties of the covalent organic thin film and the surface morphology.

2.2.5.1 X-ray Photoelectron Spectroscopy (XPS)

To confirm the elemental characteristics of the thin films, X-ray photoelectron spectroscopy (XPS) study was performed using a DLD spectrometer (Kratos Axis-Ultra; Kratos Analytical Ltd.) with an Al Kα radiation source (1486.6 eV). Energy and component separations were conducted using bundled vision processing software with pure Gaussian profiles with a Shirley background.

2.2.5.2 Atomic Force Microscopy (AFM)

Tapping mode atomic force microscopy (AFM) was used to analyze the film surface morphology and roughness. AFM images were collected using a digital AFM system (NanoScope IIIa; Veeco Instruments). Silicon probes were used as a cantilever (SI-DF3FM; Nanosensors Corp.) with a resonance frequency of 60-66 kHz and a spring constant of 2.8–4.4 Nm^{-1}. The measurements were taken under an air atmosphere with a scan rate of 0.4 Hz and scan sizes of 5 μm × 5 μm and 1 μm × 1 μm.

2.3 Results and Discussion

2.3.1 Investigation of APDMES Self-assembled Monolayer

2.3.1.1 Time Dependent APDMES Modification

Amine functionalized self-assembled monolayers (SAMs) of APDMES on SiO_2 substrate was investigated by XPS analysis. The bare SiO_2 surface showed peaks of carbon, oxygen and silicon. Usually, carbon signal comes from the contamination layer.[30] The XPS spectra of APDMES modified surface contained the signals of carbon, oxygen and silicon and an addition of nitrogen signal. Nitrogen is the most significant response of APDMES molecules on the solid substrate, representing the amine group of the APDMES molecules. **Table 2.1** showed the compositional analysis of SiO_2 surface after different silanization time in ethanol at both room temperature (RT) and high temperatures (70 ºC). At RT condition, a little N-signal appears after 2, 3 and 6 hr of silanization but no signal was observed after 1 hr of silanization. But in the case of high temperature condition, N-signal fairly increased from 1 to 6 hr of silanization. These results indicated that high temperature is more suitable for getting APDMES-modified surface. **Figure 2.5a** presents the XPS survey spectrum of bare SiO_2 and APDMES-modified SiO_2 substrate. It clearly shows that the N and C-signals increases from bare to APDMES-modified substrate, confirming the presence of APDMES on SiO_2 substrate.

Table 2.1 Surface composition (at. %) of the SiO_2 substrate after 1, 2, 3 and 6 hr APDMES-modification at RT and higher temperature (70 ± 2 ºC).

Temperature	At. %	1 hr	2 hr	3 hr	6 hr
Room Temperature (22 ± 2 ºC)	C	5.56	8.57	9.07	8.97
	Si	59.31	56.58	56.42	56.32
	O	35.13	34.48	33.90	34.05
	N	-	0.37	0.61	0.69
Higher Temperature (70 ± 2 ºC)	C	9.89	14.04	14.74	14.90
	Si	55.32	51.69	50.34	50.14
	O	34.30	33.25	33.19	33.22
	N	0.48	1.03	0.71	0.72

(Solvent system = Ethanol)

The N 1s XPS spectra for APDMES-modified solid surface also showed the continuous increase of N-signal from 1 to 3 hr of silanization (**Figure 2.5b**), indicating the increase of APDMES molecules on SiO_2 substrate. Further increase of silanization time didn't show any considerable change in N-at. %.

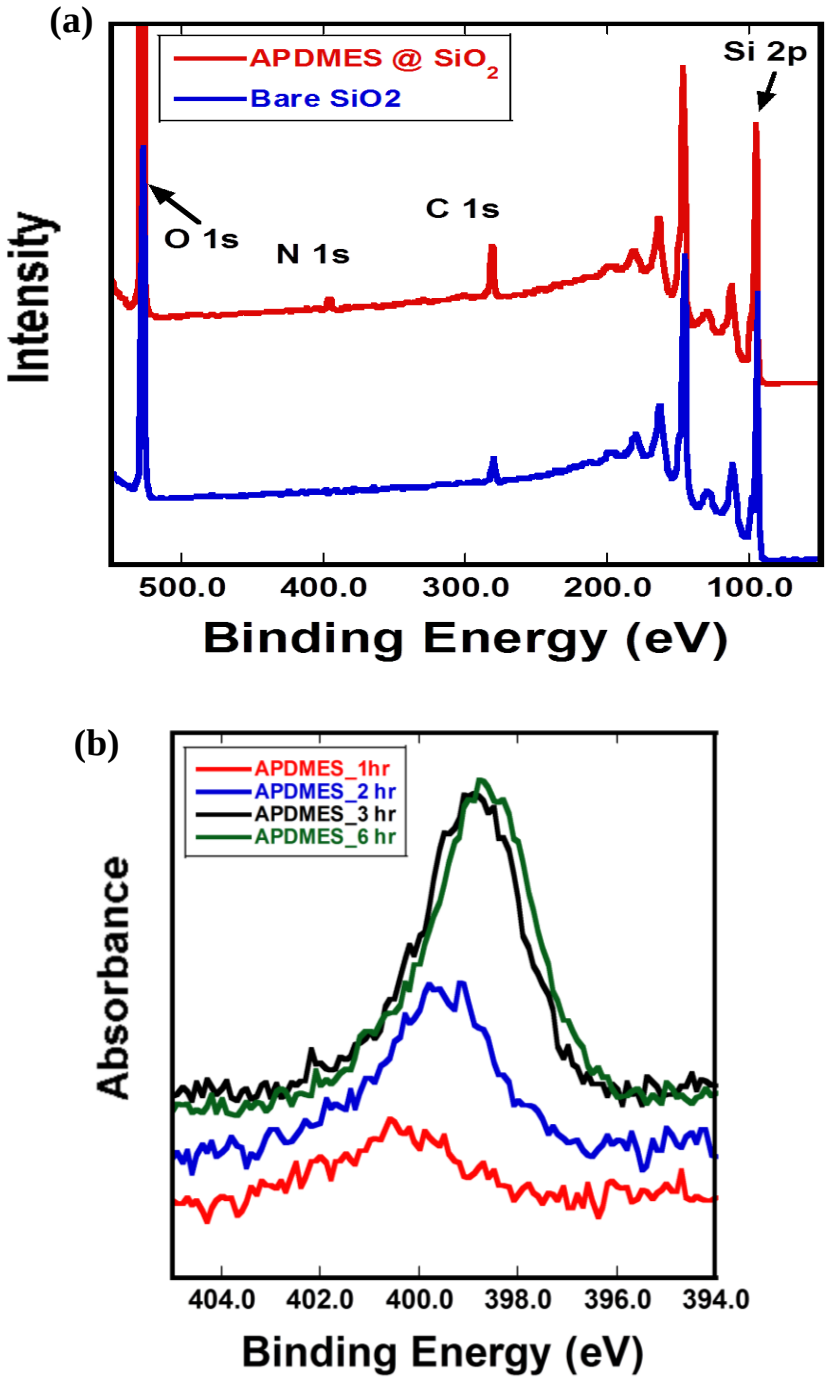

Figure 2.5 (a) XPS survey spectrum of bare and APDMES-modified SiO_2 substrate and (b) N 1s XPS spectra for APDMES-modified solid surface after 1, 2, 3 and 6 hr of silanization at (70 ± 2 ºC).

2.3.1.2 Chemical Bonds of APDMES-modified Solid Surface

Figure 2.6a depicts the Si 2p XPS fine scale spectra for bare SiO_2 substrate. Peaks at the binding energy of 99.0 eV, 99.6 eV corresponds to the bulk Si $2p_{3/2}$ and Si $2p_{1/2.}$ Higher binding energy peak at 103.3 eV corresponds to the native silicon oxide layer of SiO_2 substrate.[29-30] After modification with APDMES, these peaks were shifted towards ca. 0.3 eV lower binding energy (**Figure 2.6b**). This shifting might be occurred because of the chemisorption of APDMES on substrate. In addition, a new peak at the binding energy of 101.6 eV attributed that corresponds to the aminosilane on the silicon oxide layer. The N 1s XPS fine scale spectra showed two different components at the binding energy of 399.2 eV corresponds to free NH_2 and 401.6 eV corresponds to H-bonded NH_2,[29,31] indicating the APDMES growth on the SiO_2 surface as shown in **Figure 2.6c**.

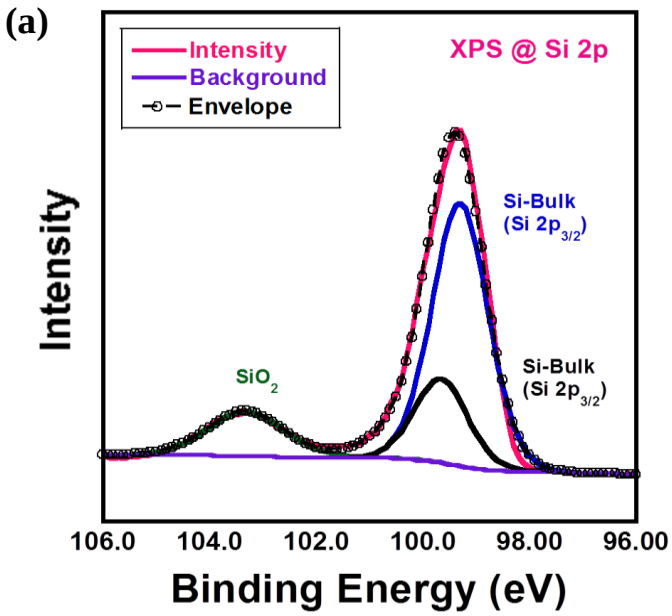

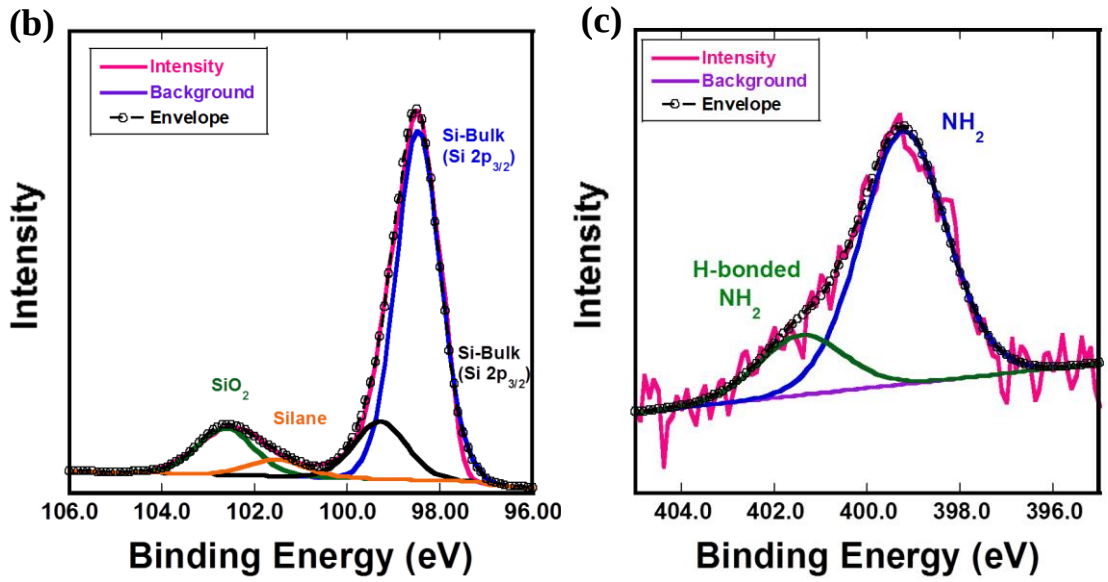

Figure 2.6 (a) Si 2p XPS fine scale spectra for bare SiO_2 substrate. (b) Si 2p and (b) N 1s XPS fine scale spectra for APDMES-modified solid surface after 3 hr of silanization at 70 °C. (Solvent system = Ethanol)

2.3.1.3 Influence of Different Solvent Systems

It is very important to find out the proper solvent system for surface modification as the solvents are different in polar natures. Because of the polar nature of APDMES, I expected its better solubility in polar solvents. The silanization process was carried out at different solvent systems: (a) polar protic solvent (ethanol), (b) polar aprotic solvent (acetone, DMF) and (c) non-polar solvent (toluene). The surface modification at various solvent systems was investigated by XPS analysis. **Table 2.2** represents the summary of the N-composition (at. %) and their chemical environments. Toluene solvent system

showed high N-at. % at both RT and high temperature condition along with the highest free amine %. The maximum number of free amine is desired for further film growth on APDMES-modified surface. So, the suitable condition for APDMES-modification is expected to be the toluene solvent system for 3 hr at high temperature (70 ºC).

Table 2.2 N-at. % of APDMES-modified SiO_2 substrate in different solvent at both room temperature and high temperature and their chemical environments.

Solvent	N-at. %		Room temperature		High temperature	
	Room temperature	High temperature	Free NH_2 %	H-bonded NH_2 %	Free NH_2 %	H-bonded NH_2 %
Toluene	1.27	1.45	76.5	23.53	75.8	24.27
DMF	0.92	1.33	70.9	29.15	75.4	24.59
Acetone	0.82	1.07	79.3	20.68	78.2	21.79
Ethanol	0.61	0.71	70.0	30.05	74.4	15.6

N.B.: High temperature: Ethanol, toluene and DMF (70 ± 2 ºC); acetone (50 ± 2 ºC)
Room temperature: 22 ± 2 ºC

2.3.2 Investigation of APTMS Self-assembled Monolayer

2.3.2.1 Time Dependent APTMS Modification

Due to the high possibilities of APTMS polymerization and different types of interaction between APTMS and silicon oxide layer, the APTMS growth was also investigated by XPS at various silanization times. The N 1s and Si 2p XPS fine scale spectra showed almost similar peak area for various silanization times (1, 2 and 3 hr) at three different points for each (checked for three times), indicating that the polymerization of APTMS molecules is lower in ethanol solvent system as shown in **Figure 2.7**.[30] These results indicated that 1 hr might be enough silanization time for preparing APTMS-modified SiO_2 substrate.

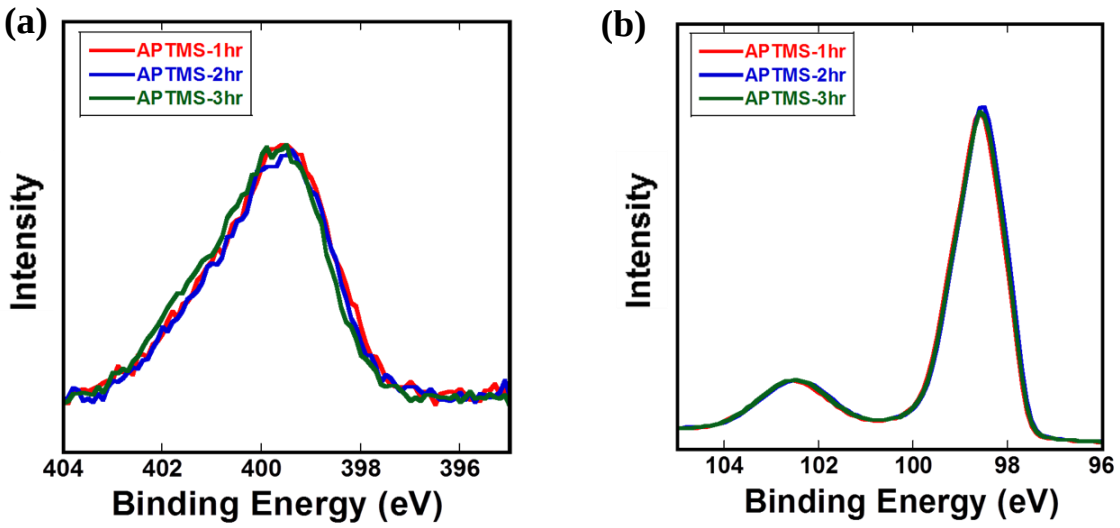

Figure 2.7 XPS survey spectra of (a) N 1s and (b) Si 2p XPS for APTMS-modified solid surface after 1, 2 and 3 hr of silanization at 25 °C.

Contact angle which represents the hydrophilic and hydrophobic behaviors of the bare substrate and APTMS-modified substrates were also investigated. Contact angle increased from bare substrate to APTMS-modified substrates from 37 ± 2° to 62 ± 2° and 35 ± 2° to 60 ± 2° for SiO_2 and Si substrates respectively (**Figure 2.8**), indicating the increase of hydrophobic behavior of the surface due to the presence of hydrophobic APTMS molecules. These also match with the evidences of APTMS growth on solid surface. In addition, 1, 2 and 3 hr APTMS-modified surfaces showed almost the same contact angle, indicating an additional evidence for lower polymerization possibilities of APTMS molecules in ethanol solvent system.

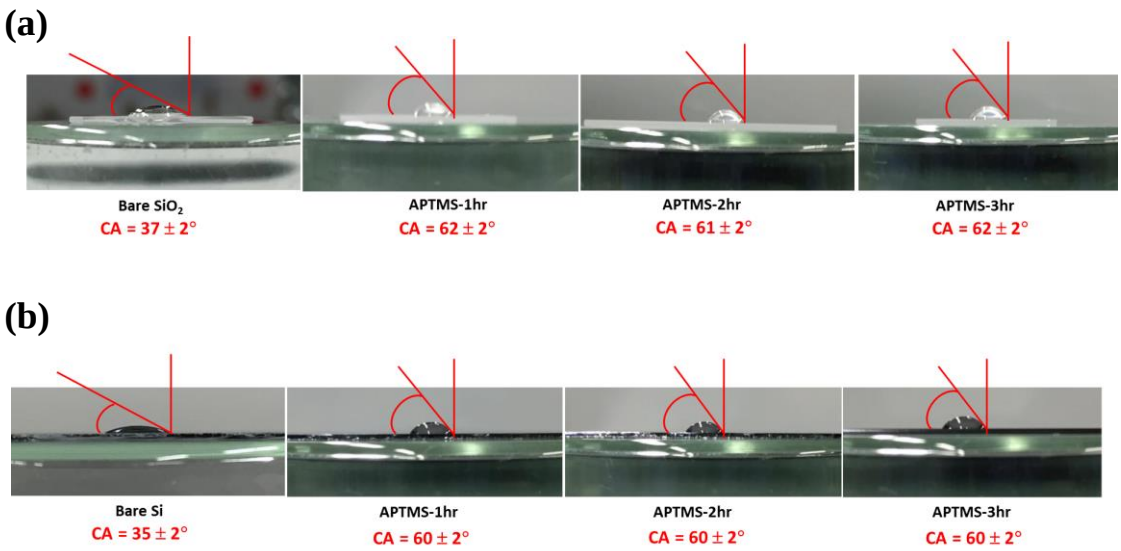

Figure 2.8 Contact angle (CA) of the bare and APTMS-modified (1, 2 and 3 hr) (a) SiO_2 and (b) Si substrate surface. [CA = Contact angle]

This phenomenon can be explained by the solvents polarity and nature. Like hydrolysis in the case of water, the –OH group containing polar protic ethanol solvent can solvolyze the Si-O-Si bonds much faster than the competitive condensation reaction between two –Si–OH groups to form Si–O–Si bonds, which leads to lower polymerization.[30,32]

2.3.2.2 Chemical Bonds of APTMS-modified Solid Surface

Amine functionalized self-assembled monolayer (SAM) of APTMS on Si/SiO_2 substrate was investigated by XPS analysis. Nitrogen signal is the most significant response for the presence of APTMS molecules on the solid substrate, representing the amine group of the APTMS molecules. The N 1s XPS fine scale spectra showed two different components at the binding energy of 399.2 eV corresponds to free NH_2 and 401.2 eV corresponds to H-bonded NH_2,[29,31] indicating the APTMS growth on the surface as shown in **Figure 2.9a**. The Si 2p XPS fine scale spectra also showed a signal at the binding energy of 102.3 eV corresponds to the aminosilane on the silicon oxide layer, which provided an additional evidence of APTMS growth. Other components at the binding energy of 98.5 eV, 99.0 eV and 103.0 eV corresponds to the bulk Si $2p_{3/2}$, Si $2p_{1/2}$ and silicon oxide respectively as shown in **Figure 2.9b**.[29-30]

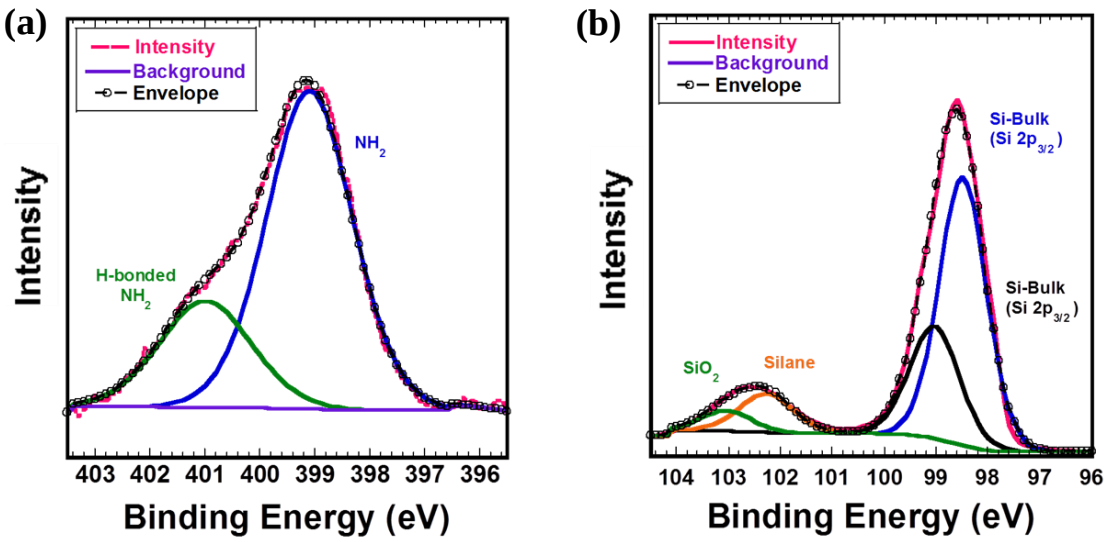

Figure 2.9 (a) The N 1s (b) and Si 2p XPS fine scale spectra for APTMS-modified solid surface after 1 hr of silanization at 25 °C.

2.3.2.3 Atomic force microscopy of APTMS-modified solid substrate

The surface morphology of bare Si and APTMS-modified Si substrates and multilayer thin films were also investigated using tapping mode AFM, as shown in **Figure 2.10**. The surface morphology of thin film showed the distinct properties from the bare and APTMS-modified SiO_2 substrates. It also represents the evidence of thin film formation. The 2D and 3D height images show consistent APTMS-modified surface within 5.0 μm × 5.0 μm areas, which indicates the well deposition process. The root mean square (RMS) roughness was also investigated, where the roughness was slightly increased from 0.17 to 0.25 nm for bare Si and APTMS-modified surfaces

respectively. APTMS-modified surfaces are relatively uniform with the low density of island.

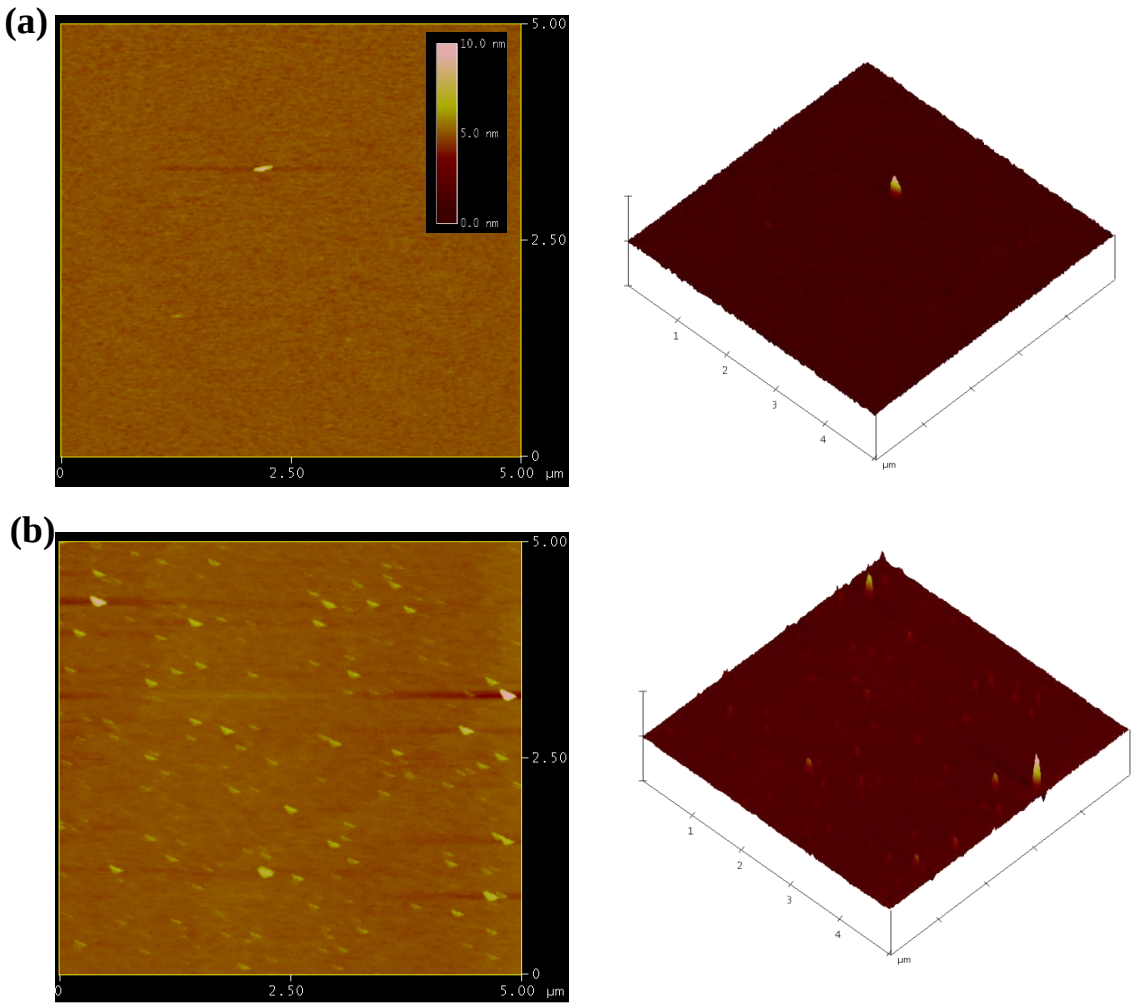

Figure 2.10 AFM 2D and 3D height images of (a) bare SiO_2, (b) 1 hr APTMS-modified SiO_2 substrate. Scan size: 5.0 µm × 5.0 µm. Data scale 10 nm.

2.3.3 Chemical Stability of APDMES and APTMS-modified Surface

APDMES and APTMS have a primary amine group in the propyl (γ) position. This amine group can act as a catalyst for the formation and hydrolysis of siloxane bonds by both intra- and inter-molecularly.[28,32-33] In this case intra-molecular catalysis might be achieved bia the formation of stable five-membered cyclic intermediates.[28] So, the chemical stability of APDMES and APTMS-modified SiO_2 substrate was investigated under H_2O (at 40 ºC) and 0.1 M $HClO_4$ solution. **Figure 2.11** shows the contact angle of APDMES and APTMS-modified SiO_2 surfaces at as prepared and after 7 hr immersing into H_2O and 0.1 M HClO4 (aq) solution separately at 40 ºC and RT respectively. APDMES-modified surface showed much lower contact angle than APTMS-modified surface after immersing into H_2O and 0.1 M $HClO_4$ solutions separately for 7 hr. The result indicated that APDMES is less stable than APTMS in both H_2O and 0.1 M $HClO_4$ solutions. As contact angle represents the hydrophilic and hydrophobic behaviors of the solid surface. Therefore, contact angle decrease means the removal of hydrophobic APDMES or APTMS molecules from the solid surface. This might be happened due to the presence of three alkoxy group in APTMS molecules where APDMES molecules have only one alkoxy group for making siloxane bonds with the surface hydroxyl groups. Where, amine is capable of catalyzing the hydrolysis of siloxane bonds at ambient temperature. In that case, amine group can bind to the Si

atom of the same or neighbor aminosilane molecules by intra or inter molecular interaction and forms a cyclic intermediate that is very reactive to nucleophiles i.e., the water molecules.[28] **Figure 2.12** represents the XPS analysis revealed that 22.4 % APDMES and 6.7 % APTMS were removed from the surface when the modified

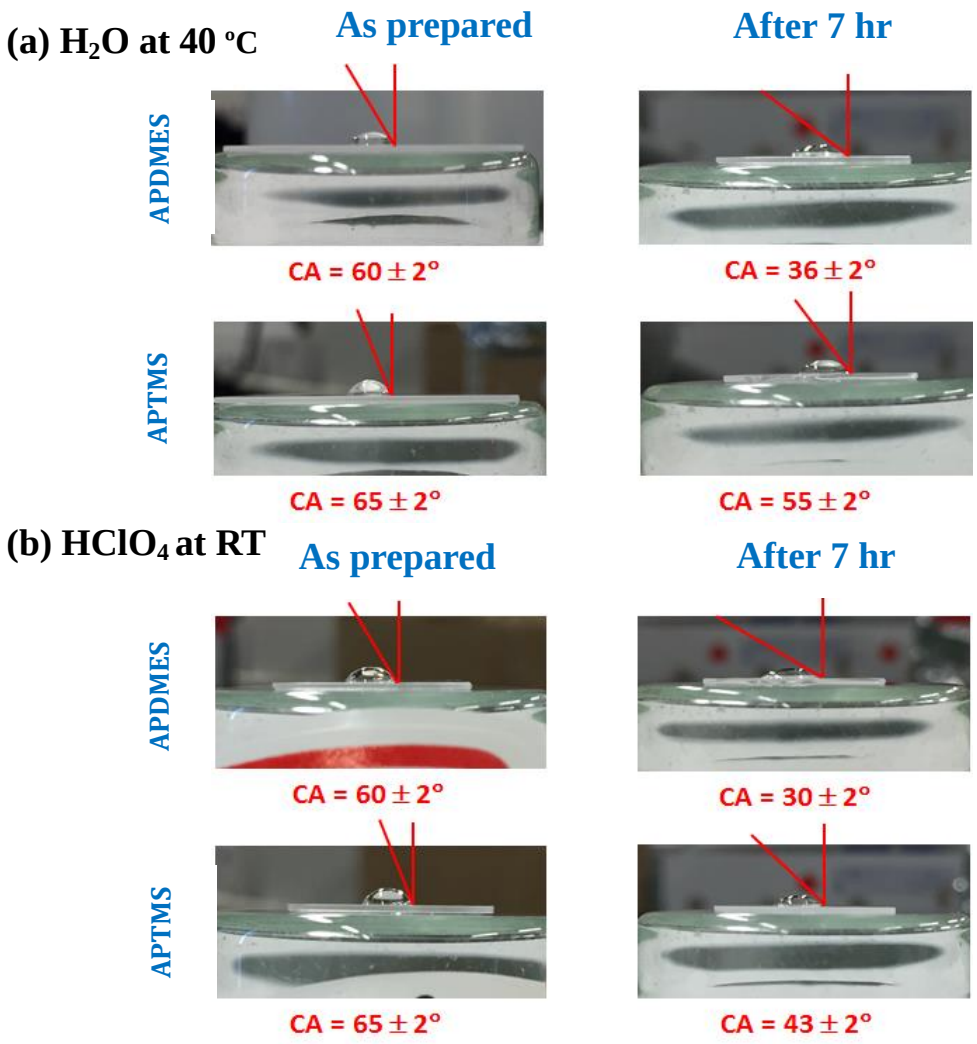

Figure 2.11 Contact angle (CA) of the APDMES and APTMS-modified SiO_2 substrate at as prepared and after 7 hr immersing into (a) H_2O and (b) 0.1 M $HClO_4$ (aq) solution at 40 °C and RT respectively. [CA = Contact angle]

substrates were immersed into H_2O at 40 ºC for 7 hr. On the other hand, 38.7 % APDMES and 14.9 % APTMS were removed from the surface when the modified substrates were immersed into 0.1 M $HClO_4$ (aq) solution at RT for 7 hr.

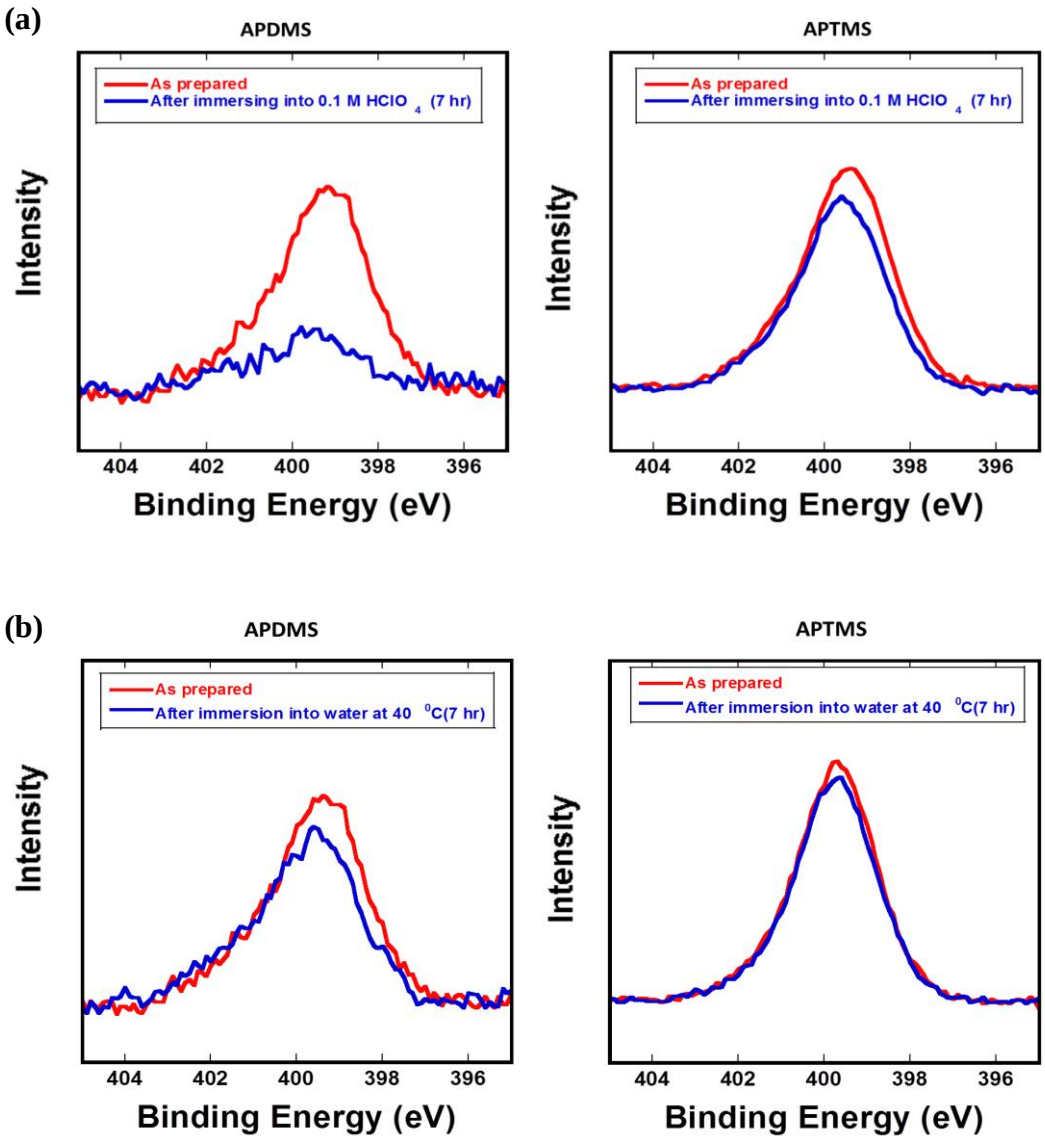

Figure 2.12 XPS survey spectra of N 1s for the APDMES and APTMS-modified SiO_2 substrate at as prepared and after 7 hr immersing into (a) H_2O and (b) 0.1 M $HClO_4$ (aq) solution at 40 ºC and RT respectively.

2.4 Conclusions

In this work, I prepared the self-assembled monolayer of APDMES and APTMS on SiO_2 substrates. APDMES modification was carried out in four different solvents under various reaction conditions. Using the XPS technique, I investigated the surface compositions and chemical bonding of the modified surfaces. Results show the best APDMES-modification in toluene solvent system at both RT and high temperature (70 ºC, 3 hr) along with the higher free amine %. I conclude that the modification of APDMES on SiO_2 surface strongly depends on solvent system. During silanization process, polymerization possibility of APTMS molecules in ethanol solvent system was also investigated at different time scale using XPS, contact angle. Interestingly, no evidence was found for polymerization in ethanol solvent system. The chemical stability of the APDMES and APTMS-modified SiO_2 substrates were also investigated after 7 hr in H_2O and 0.1 M $HClO_4$ solution at 40 ºC and RT respectively. Three methoxy group containing APTMS molecules showed much higher stability on SiO_2 substrate than the one ethoxy group containing APDMES molecules in both aqueous and acidic conditions.

References

(1) Bigelow, W. C.; Pickett, D. L.; Zisman, W. A. Oleophobic monolayers: I. Films adsorbed from solution in non-polar liquids. *J. Colloid Sci.* **1946**, *1*, 513–538.

(2) Sagiv, J. Organized Monolayers by Adsorption, I. Formation and Structure of Oleophobic Mixed Monolayers on Solid Surfaces. *J. Am. Chem. Soc.* **1980**, *399*, 92–98.

(3) Ulman, A. Formation and Structure of Self-Assembled Monolayer. *Chem. Rev.* **1996**, *96*, 1533-1554.

(4) Kobayashi, S.; Nishikawa, T.; Takenobu, T.; Mori, S.; Shimoda, T.; Mitani, T.; Shimotani, H.; Yoshimoto, N.; Ogawa, S.; Iwasa, Y. Control of Carrier Density by Self-Assembled monolayers in Organic Field-Effect Transistors. *Nat. Mater.* **2004**, *3*, 317-322.

(5) Love, J. C.; Estroff, L. A.; Kriebel, J. K.; Nuzzo, R. G.; Whitesides, G. M. Self-Assembled Monolayers of Thiolates on Metals as a Form of Nanotechnology. *Chem. Rev.* **2005**, *105*, 1103-1170.

(6) Ashkenasy, G.; Cahen, D.; Cohen, R.; Shanzer, A.; Vilan, A. Molecular Engineering of Semiconductor Surface and Devices. *ACC. Chem. Res.* **2002**, *35*, 121-128.

(7) Schreiber, F. Structure and growth of self-assembling monolayers. *Prog. Surf. Sci.* **2000**, *65*, 151–257.

(8) Bain, C. D.; Whitesides, G. M. Formation of Monolayers by the Coadsorption of

Thiols on Gold: Variation in the Length of the Alkyl Chain. *J. Am. Chem. Soc*. **1989**, *111*, 7164-7175.

(9) Kohli, P.; Blanchard, G. J. Applying Polymer Chemistry to Interfaces: Layer-by-Layer and Spontaneous Growth of Covalently Bound Multilayers. *Langmuir* **2000**, *16*, 4655-4661.

(10) Karpovich, D. S.; Blanchard, G. C. Direct Measurement of the Adsorption Kinetics of Alkanethiolate Self-Assembled Monolayers on a Microcrystalline Gold Surface. *Langmuir* **1994**, *10*, 3315-3322.

(11) Kohli , P.; **Taylor, K. K.**; **Harris, J. J.; Blanchard, G. J.** Assembly of Covalently-Coupled Disulfide Multilayers on Gold. *J. Am. Chem. Soc.* **1998**, *120 (46)*, 11962–11968.

(12) Prasittichai, C.; Zhou, H.; Bent, S. F. Area Selective Molecular Layer Deposition of Polyurea Films. *ACS Appl. Mater. Interfaces* **2013**, *5*, 13391-13396.

(13) Budd, P. M.; Ghanem, B. S.; Makhseed, S.; McKeown, N. B.; Msayib, K. J.; Tattershall, C. E. Polymers of Intrinsic Microporosity (PIMs): Robust, Solution-processable, Organic Nanoporous Materials. *Chem. Commun.* **2004**, 203-231.

(14) Kim, M.; Byeon, M.; Bae, J-S.; Moon, S. Y.; Yu, G.; Shin. K.; Basarir, F.; Yoon, T. H.; Park, J-W. Preparation of Ultrathin Films of Molecular Networks through Layer-

by-Layer Cross-Linking Polymerization of Tetrafunctional Monomers. *Macromolecules* **2011**, *44*, 7092-7095.

(15) Zhou, H.; Blackwell, J. M.; Lee, H.-B.-R., Bent, S. F. Highly Sensetive, Patternable Organic Films at the Nanoscale made by Bottom-Up Assembly. *ACS Appl. Mater. Interfaces* **2013**, *5*, 3691-3696.

(16) Zhou, H.; Bent. S. F. Molecular Layer Deposition of Functional Thin Films for Advanced Lithographic Patterning. *ACS Appl. Mater. Interfaces* **2011**, *3*, 505-511.

(17) Zhou, H.; Toney, M. F.; Bent, S. F. Cross-Linked Ultrathin Polyurea Films via Molecular Layer Deposition. *Macromolecules* **2013**, *46*, 5638-5643.

(18) Vansant, E. F.; Voort, P. V. D.; Vrancken, K. C. Characterization and chemicalmodification of the silica surface. Elsevier, Amsterdam, **1995**.

(19) Shircliff, R. A.; Stradins, P.; Moutinho, H.; Fennell, J.; Ghirardi, M. L.; Cowley, S. W.; Branz, H. M.; Martin, I. T. Angle-resolved XPS analysis and characterization ofmonolayer and multilayer silane films for DNA coupling to silica. *Langmuir* **2013**, *29*, 4057–4067.

(20) Chrisely, L. A.; Lee, G. U.; Ferrall, C. E. O. Covalent attachment of synthetic DNA to self-assembled monolayer films. *Nucleic Acids Res.* **1996**, *24*, 3031–3039.

(21) Kneuer, C.; Sameti, M.; Haltner, E. G.; Schiestel, T.; Schirra, H.; Schmidt, H.; Lehr, C. M. Silica nanoparticles modified with aminosilanes as carriers for plasmid DNA. *Int. J. Pharm.* **2000**, *196*, 257–261.

(22) Keegan, N.; Suarez, G.; Spoors, J. A.; Ortiz, P., McNeil, H. J. C. J. A microfabrication compatible approach to 3D imensonal patterning of bio-molecules at bio-MEMS and biosensor surfaces. *IEEE Bio CAS* **2009**, 17–20.

(23) Low, S. P.; Voelcker, N. H.; Canham, L. T.; Williams, K. A. The biocompatibility of porous silicon in tissues of the eye. *Biomaterials* **2009**, *30*, 2873–2880.

(24) Chen, C. F.; Tzeng, S. D.; Lin, M. H.; Gwo, S. Electrostatic assembly of gold colloidal nanoparticles on organosilane monolayers patterned by microcontact electrochemical conversion. *Langmuir* **2006**, *22*, 7819–7824.

(25) Tran, T. H.; Lee, J. W.; Lee, K.; Lee, Y. D.; Ju, B. K. The gas sensing properties ofsingle-walled carbon nanotubes deposited on an aminosilane monolayer. *Sens.Actuators B: Chem.* **2008**, *129*, 67–71.

(26) Senesac, L.; Thundat, T. G.; Nanosensors for trace explosive detection. *Mater.Today* **2008**, *11*, 28–36.

(27) Engel, Y.; Elnathan, R.; Pevzner, A.; Davidi, G.; Flaxer, E.; Patolsky, F. Super sensitive detection of explosives by silicon nanowire arrays. *Angew. Chem.* **2010**, *49*, 6830–6835.

(28) Kanan, S. M.; Tze, W. T. Y.; Tripp, C. P. Method to Double the Surface Concentration and Control the Orientation of Adsorbed (3-Aminopropyl) dimethylethoxysilane on Silica Powders and Glass Slides. *Langmuir* **2002**, *18*, 6623−6627.

(29) Jaksa, G.; Stefane, B.; Kovac, J. XPS and AFM characterization of aminosilanes with different numbers of bonding sites on a silicon wafer. *Surf. Interface Anal.* **2013**, *45*, 1709–1713.

(30) Jaksa, G.; Stefane, B.; Kovac, J. Influence of different solvents on the morphology of APTMS-modifiedsilicon surfaces. *Appl. Surf. Sci.* **2014**, *315*, 516–522.

(31) Graf, N.; Yegen, E.; Gross, T.; Lippitz, A.; Weigel, W.; Krakert, S.; Terfort, A.; Unger, W. E. S. XPS and NEXAFS studies of aliphatic and aromatic amine species on functionalized surfaces. *Surf. Sci.* **2009**, *603*, 2849–2860.

(32) Zhu, M.; Lerum, M. Z.; Chen, W. How to prepare reproducible, homogeneous, andhydrolytically stable aminosilane-derived layers on silica. *Langmuir* **2011**, *28*, 416–423.

(33) Smith, E. A.; Chen, W. How To Prevent the Loss of Surface Functionality Derived from Aminosilanes. *Langmuir* **2008**, *24*, 12405-12409.

Chapter-03

Synthesis and Characterization of Porphyrin-based Polyurea Thin Film Using Solution-Based MLD Technique

Synthesis of organic thin film materials on solid surfaces is important for prospective applications in many research fields today. In this article, we demonstrated a solution-based molecular layer deposition (MLD) approach to prepare porphyrin-based covalent molecular networks on a 3-aminopropyl trimethoxysilane (APTMS) modified substrate surface using the urea coupling reaction between 1,4-phenylene diisocyanate (1,4-PDI) and 5,10,15,20-tetrakis-(4-aminophenyl)porphyrin (H_2TAPP) at room temperature (22 ± 2 ^{o}C). Multilayer growth was investigated under different relative humidity (RH) conditions. Sequential molecular growth at low relative humidity (≤14% RH) was observed using UV-vis absorption spectroscopy and atomic force microscopy (AFM). The high-RH condition shows limited film growth. Infrared spectroscopy (IR) and X-ray photoelectron spectroscopy (XPS) revealed the polyurea bond formation in sequential multilayer thin films, demonstrating that stepwise multilayer film growth was achieved using the urea coupling reaction.

3.1 Introduction

Thin film growth is a crucially important consideration in today's research world because many devices related to modern technology require it. Control of thin film growth at the molecular level is necessary for device miniaturization because morphology plays a crucially important role in the performance of many devices.[1-3] Thin film materials with nanoscale level have some considerable implications such as molecular electronics,[4] photovoltaics,[5] sensor,[6] nonlinear optics,[7] and bio-resistant coatings.[8,9] Scientists from different backgrounds have introduced versatile new methods for thin film synthesis. Langmuir–Blodgett (LB)[10-11] and spin coating[12] are well-known techniques used for thin film fabrication. Molecular level layer-by-layer (LbL) thin film fabrication, known as molecular layer deposition (MLD) has attracted considerable attention because of its simplicity and its attractive control over film thickness, composition, and conformality through sequential self-limiting surface reaction at the single-molecule level.[13-16] To date, most MLD processes have been conducted through polymerization of volatile bifunctional monomers under vacuum conditions to prepare polyamide,[17-19] polyimide,[20-21] polyurethane,[22] and polyurea[13,23-24] based nanostructures. However, this vapor-based MLD technique is not applicable for macromolecules because of their high boiling points.[25] Solution-based MLD process offers an alternative route to overcome some limitations of vapor-based MLD techniques. Compared to conventional MLD film fabrication based on

non-covalent interactions such as coulombic interactions[26-27]and hydrogen bonding,[28] covalently bonded films possess much higher chemical and thermal stability because of their chemical characteristics.[25,29-30] Bent et al.[31-33] and Park et al.[34] reported polyurea-based multilayer thin films using chemical vapor deposition (CVD) and solution-based MLD processes respectively. Blanchard and co-workers also reported the solution-based polyurea multilayer thin film growth using bifunctional amine and isocyanate group-containing monomers and separately using only isocyanate group-containing monomers. For the isocyanate group-containing monomers, they demonstrated that the reactive amine group was accomplished by the deliberate hydrolysis of the isocyanate groups, providing uncontrolled molecular growth.[35]

Porphyrin, the most well-known and widely studied macromolecule, has attracted considerable attention because of its various possibilities for application to molecular electronics,[36-37] artificial photosynthesis,[38] semiconductor sensitization,[39-41] and biological fields.[42] A few works have been reported by Dinolfo and co-workers to fabricate porphyrin-based covalent organic thin films, but they have introduced a solution-based MLD thin film fabrication technique utilizing copper (I)-catalyzed azide-alkyne cycloaddition (CuAAC) or click chemistry to build porphyrin-based multilayer thin films.[43-44] Still, introducing new materials of porphyrin-based covalent organic thin films presents a demanding issue that must be addressed to support prospective applications in

many research fields.

This report is the first of the relevant literature to describe a study in which the solution-based MLD technique was chosen to establish a well-controlled porphyrin-based covalent organic thin film through the urea coupling reaction. Specifically, 1,4-phenylene diisocyanate (1,4-PDI) was used as the bifunctional monomer, whereas 5,10,15,20-tetrakis-(4-aminophynyl) porphyrin (H_2TAPP) was used as the tetrafunctional counter molecule for multilayer film growth (**Scheme 1**). The choice of these monomers was based on their chromophore properties in the multilayer thin film and commercial availability. Two different wavelength regions of phenylurea and porphyrin in UV-vis absorption spectroscopy assisted to investigate the multilayer film growth at different RH conditions of the reaction chamber. The main focus of this paper is on demonstrating the use of conventional isocyanate-amine chemistry to fabricate porphyrin-based polyurea multilayer assemblies. Moisture sensitive 1,4-PDI (containing isocyanate group) was used as one precursor,[34-35] which might have different degrees of self-polymerization with respect to relative humidity (RH) conditions. I conducted this investigation of how sequential molecular growth might be improved by appropriate choice of RH conditions of the reaction chamber. According to my knowledge, no report of the relevant literature describes RH effects on polyurea-based sequential molecular growth by solution-based MLD process. Systematic characterization of the sequential molecular growth at low RH

(≤10% RH) was accomplished using UV-vis absorption spectroscopy and atomic force microscopy (AFM). Moreover, chemical characteristics of the multilayer organic thin film were characterized using infrared spectroscopy (IR) and X-ray photoelectron spectroscopy (XPS).

3.2 Experimental

3.2.1 Materials

Silicon wafer (Si (100), p-type) and quartz (SiO_2) substrates were purchased from Electronics and Materials Corp. Ltd. and Sendai Sekiei Glass Seisakusho respectively. 5,10,15,20-tetrakis-(4-aminophynyl) porphyrin (H_2TAPP, >95%), 1,4-phenylene diisocyanate (1,4-PDI, >98%) and 3-aminopropyltrimethoxysilane (APTMS, >96%) were purchased from Tokyo Chemical Industry Co. Ltd., Japan. Before use, 1,4-PDI was further purified by sublimation. HPLC (99.7%) grade of ethanol and 2-propanol was used for substrate modification with APTMS. Super dehydrated (H_2O, ≤0.001%) chloroform ($CHCl_3$), tetrahydrofuran (THF), toluene and N, N-dimethylformamide (DMF) were used for the formation of multilayer thin films. All solvents were purchased from Wako Pure Chemical Industries Ltd., Japan, and were used as-received without further purification.

3.2.2 Surface Cleaning

Quartz substrate (SiO_2; 25 × 15 mm^2, t = 0.5 mm) and boron doped p-type silicon wafer (p-Si (100); 5-20 Ω-cm, 30 × 20 mm^2, t = 0.5 mm) were chosen for multilayer thin film fabrication. Before use, these substrates were cleaned by sonication for 3 × 15 min using 2-propanol (HPLC grade, 99.7%)) to remove organic contaminants. Finally, rinsed with 2-propanol and streamed with Ar and dried and kept in a clean bench.

3.2.3 Modification of Solid Substrate

To obtain the amine-functionalized self-assembled monolayers (SAMs), clean SiO_2 and Si substrates were immersed into 10 mM ethanol solution (AR grade, 99.5%)) of APTMS for 1 hr with mild shaking at room temperature (22 ± 2 ºC) under an Ar atmosphere. After taking out from the APTMS solution, the substrates were washed with HPLC grade ethanol (twice) and 2-propanol (twice) solvents consecutively with sonication for 5 min each and were finally rinsed with 2-propanol and dried with an Ar stream in a clean bench.

3.2.4 Fabrication of Multilayer Thin Film on Solid Substrate

Amine-functionalized substrates were used for the fabrication of multilayer thin films in a closed chamber at different relative humidity (RH) conditions. The RH of the reaction chamber was controlled by using Ar gas flow, which was monitored by RH sensor. Fabrication of multilayer thin film was carried out in super dehydrate solvents at room temperature with the following steps:

1) The amine-functionalized substrate was immersed into 6.2 mM 1,4-PDI in the mixture solvent of $CHCl_3$ and THF (8:2, v/v) for 25 min. Then the substrate was rinsed successively with two beakers of super-dehydrated toluene and two beakers of super-dehydrated THF separately for each 1 min washing.

2) The resulting isocyanate functionalized substrate was immersed into 1.5×10^{-1}

mM H_2TAPP in the mixture solvent of $CHCl_3$ and THF (8:2, v/v) for 25 min, with subsequent washing successively using two beakers of super-dehydrated DMF and two beakers of super-dehydrated THF separately for each 1 min washing to remove the unreacted precursors onto the deposited film and dried under Ar atmosphere.

This bilayer deposition obtained from step (1) and (2) was regarded as the 1 MLD cycle. The steps described above were repeated 5, 8, and 10 times to fabricate the multilayer films used for characterization.

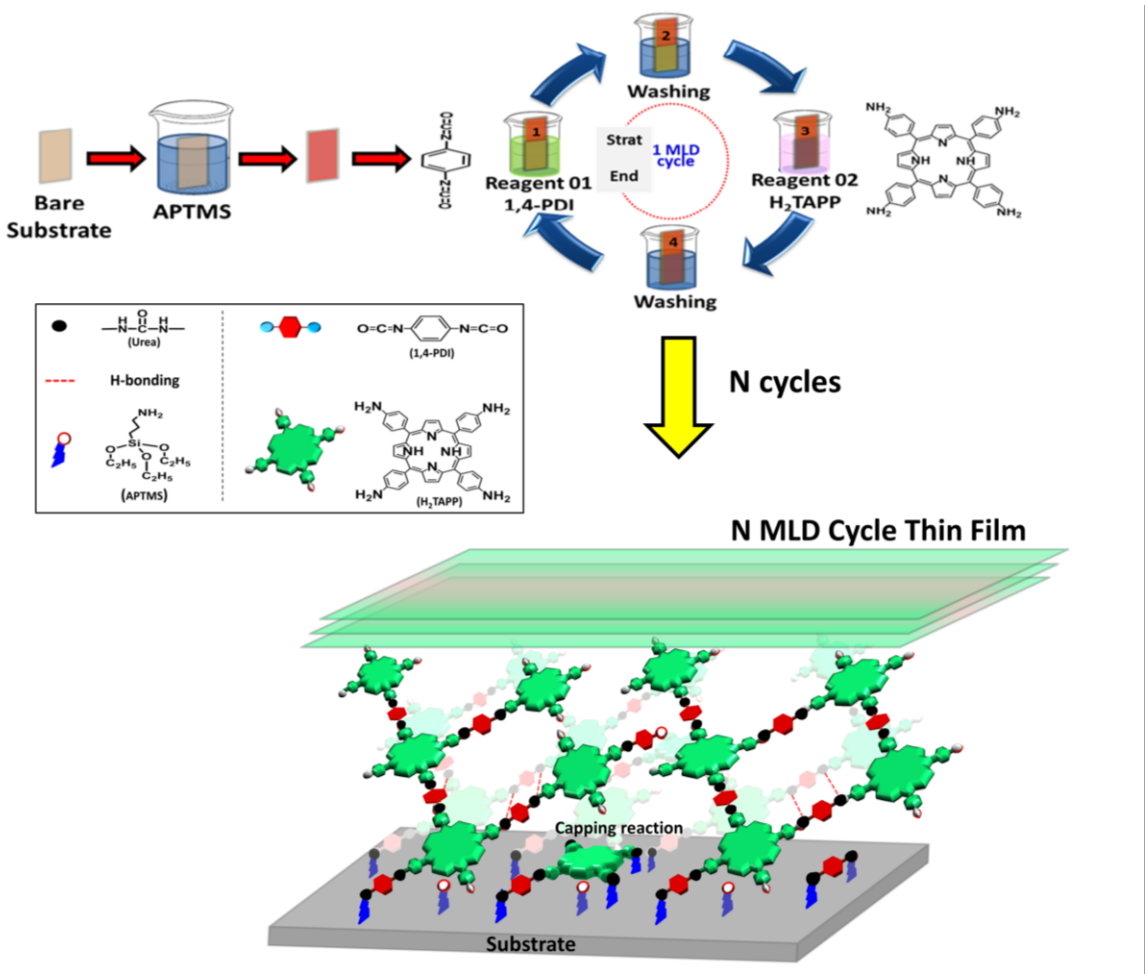

Scheme 3.1 Schematic representation for the fabrication of porphyrin-based polyurea thin film.

3.2.5 Characterization

Several characterization techniques have been used to investigate multilayer thin film growth on solid surfaces, the physical and chemical properties of the covalent organic thin film and the surface morphology.

3.2.5.1 UV-vis Absorption Spectroscopy

UV-vis absorption spectra of the multilayer thin film deposited on the SiO_2 substrates were measured using a UV-vis spectrometer (Jasco V-630BIO-IM; Jasco Corp., Japan). The APTMS-modified SiO_2 substrate was used as a reference sample.

3.2.4.2 Transmission Fourier Transform Infrared (FTIR) Spectroscopy

Transmission Fourier transform infrared (FTIR) was used to characterize the MLD film formation. IR spectra were collected with a Fourier transform infrared (FTIR) spectrometer (Nicolet 6700, Thermo Fisher Scientific Inc.) equipped with a mercury cadmium telluride (MCT) detector. An APTMS-modified Si substrate was used as a reference sample. The signal noise has been subtracted by smoothing process.

3.2.4.3 Atomic Force Microscopy (AFM)

Multilayer film thickness was measured using AFM (VN-8000; Keyence Co.) equipped with a DFM/SS mode cantilever (OP-75041; Keyence Co.). Before APTMS and further multilayer film growth, a portion of clean bare substrate was covered by thin Au coating with sputter machine. During thickness measurements, thin Au coated portion was

carefully removed from the substrate surface by using cotton bar. Measurements were taken at four positions, at least, to estimate the average film thickness. The thickness of APTMS-modified substrate was used as a baseline thickness, which was subtracted from the subsequent total film thickness to get the thickness of multilayer thin film.

Tapping mode atomic force microscopy (AFM) was used to analyze the film surface morphology and roughness. AFM images were collected using a digital AFM system (NanoScope IIIa; Veeco Instruments). Silicon probes were used as a cantilever (SI-DF3FM; Nanosensors Corp.) with a resonance frequency of 60-66 kHz and a spring constant of 2.8–4.4 Nm^{-1}. The measurements were taken under an air atmosphere with a scan rate of 0.4 Hz and scan sizes of 500 nm × 500 nm and 1 μm × 1 μm.

3.2.4.4 White interference microscope

Multilayer film thickness was measured using white interference microscope (BW-S506, Nikon Co.) along with AFM.

3.2.4.5 X-ray Photoelectron Spectroscopy (XPS)

To confirm the elemental characteristics of the thin films, X-ray photoelectron spectroscopy (XPS) study was performed using a DLD spectrometer (Kratos Axis-Ultra; Kratos Analytical Ltd.) with an Al Kα radiation source (1486.6 eV). Energy and component separations were conducted using bundled vision processing software with pure Gaussian profiles with a Shirley background.

3.3 Results and Discussion

3.3.1 Investigation of Self-assembled Monolayer Growth on Solid Substrate

Prior to multilayer film growth, amine functionalized self-assembled monolayer (SAM) of APTMS was prepared on Si/SiO_2 substrate. As mentioned in chapter 02, APTMS-modified solid surfaces were investigated using X-ray photoelectron spectroscopy (XPS). **Figure 3.1 (a)** depicts the XPS survey spectrum of bare SiO_2 and APTMS-modified SiO_2. Here, nitrogen (N) is the significant element that represents the amine group of the APTMS molecule on the solid substrate. So, the presence of N 1s peak for APTMS-modified SiO_2 substrate referred to the availability of APTMS on SiO_2 substrate. Whether, N 1s peak was not observed for bare SiO_2 substrate. In addition, N 1s XPS fine scale spectra of APTMS-modified SiO_2 substrate showed two different types of components at the binding energy of 399.2 eV and 401.2 eV correspond to the free NH_2 and H-bonded NH_2 respectively **Figure 3.1 (b)**.[45-46] Si 2p XPS fine scale spectra also showed a signal at the binding energy of 102.3 eV corresponds to the aminosilane on the silicon oxide layer, which provided an additional evidence of APTMS growth. Other components at the binding energy of 98.5 eV, 99.0 eV and 103.0 eV corresponds to the bulk Si $2p_{3/2}$, Si $2p_{1/2}$ and silicon oxide respectively as shown in **Figure 3.1 (c)**.[45,47]

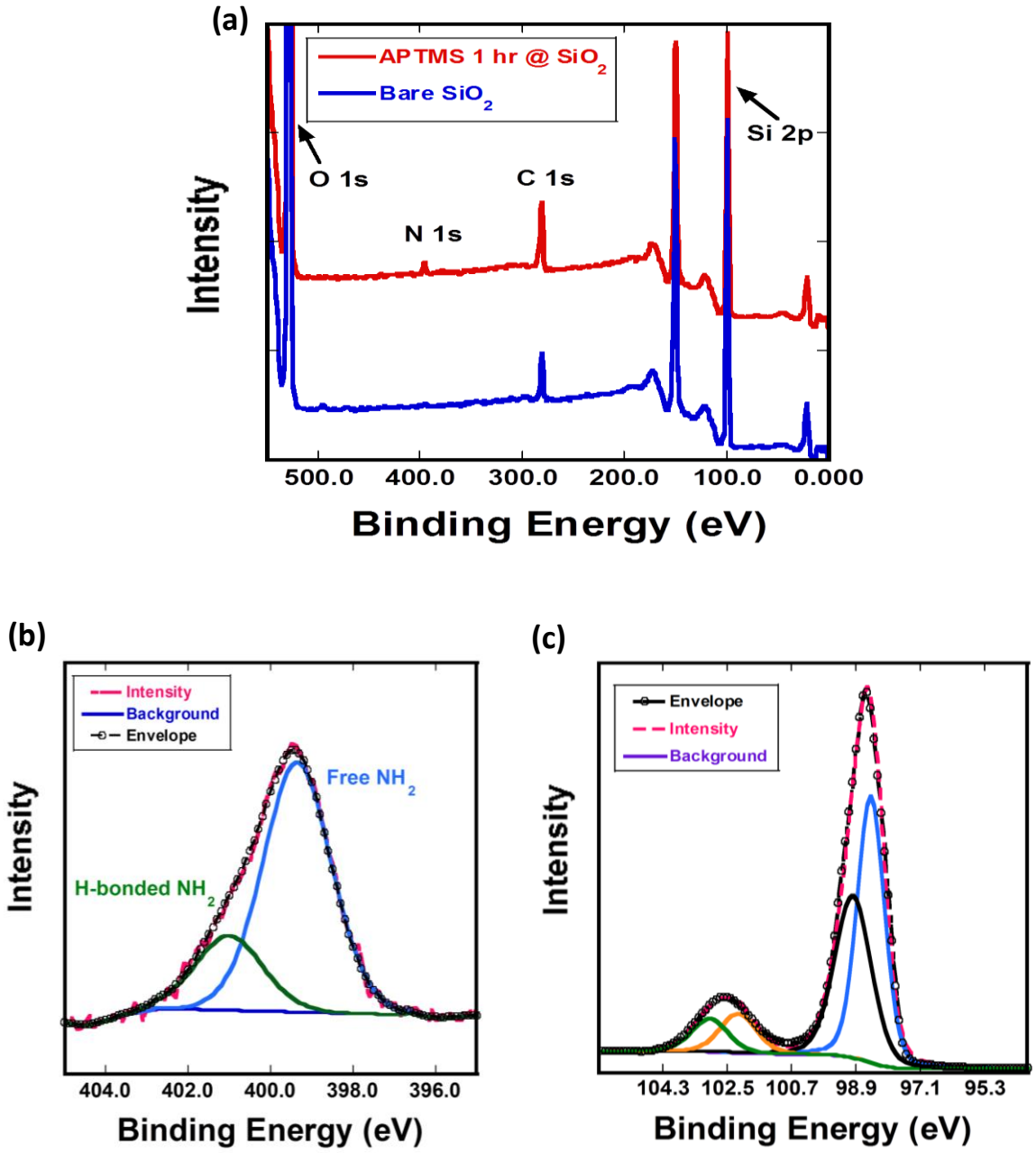

Figure 3.1 (a) XPS survey spectrum of bare SiO_2 and APTMS-modified SiO_2 substrates. (b) N 1s and (c) Si 2p XPS fine scale spectra of APTMS-modified SiO_2 substrate.

3.3.2 Investigation of Optimal Reaction Condition for Multilayer Film Growth

3.3.2.1 UV-vis Absorption Property of Thin Film

UV-vis absorption spectroscopy is an effective and easy technique to preliminary investigates the film growth of UV-active materials. Prior to the study of optimized reaction condition, a point relating to the identity of UV-active materials and their absorption wavelength was investigated first. **Figure 3.2a** depicts the UV-vis absorption spectra of 0.5 MLD and 1 MLD cycle films on quartz substrates. In the case of 0.5 MLD cycle film, the UV-vis absorption maxima centered at ~260 nm represented the aromatic polyurea.[13,35,48] Whether 1 MLD cycle film showed an additional set of bands for typical

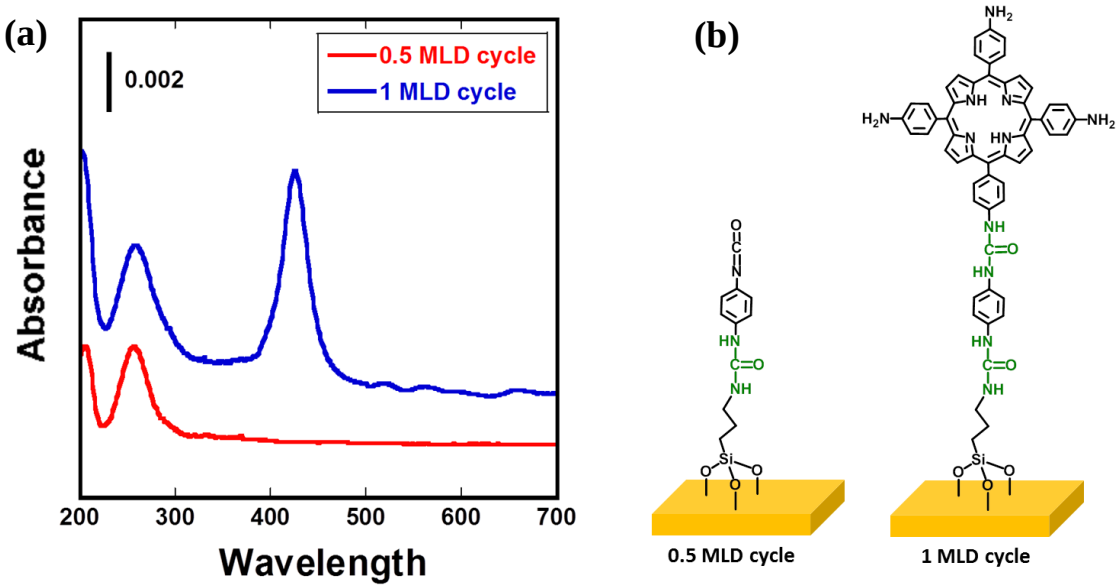

Figure 3.2 (a) UV-vis absorption spectra and (b) schematic representation of 0.5 and 1 MLD cycle films on APTMS-modified SiO_2 substrate.

porphyrin soret band at ~430 nm along with four Q-bands in the range of 500-700 nm, representing the presence of pyrrole group containing porphyrin into the multilayer thin film.[49-50] **Figure 3.2b** depicts the expected schematic representation of 0.5 and 1 MLD cycle film on APTMS-modified SiO_2 substrates.

3.3.2.2 Optimization of Reactant Concentration for Thin Film Growth

Chemical reaction requires specific amount of reagents which may not work without the proper concentrations. In most of the cases, the rate of the reaction increases along with the increase of the reactant concentration. But in a few cases, increasing the concentration of one of the reactants may have little noticeable effect of the reaction rate. The optimal reactant concentration was investigated using transparent UV-vis absorption spectroscopy. **Figure 3.3** depicts the UV-vis absorption spectra of 0.5 and 1 MLD cycle films as a function of 1,4-PDI and H_2TAPP concentrations respectively. The UV-vis absorption maxima centered at ~260 nm for 0.5 MLD cycle films showed that minimum 6.2 mM 1,4-PDI solution was needed to confirm the maximum surface coverage by the 1st MLD (0.5 MLD cycle) of 1,4-PDI on APTMS-modified SiO_2 substrate (**Figure 3.3a**). From the absorbance of 1 MLD cycle films at ~430 nm, 1.5×10^{-1} mM H_2TAPP solution was determined as the maximum useable concentration for the preparation of 2nd MLD (1 MLD cycle) of H_2TAPP on 0.5 MLD cycle film.

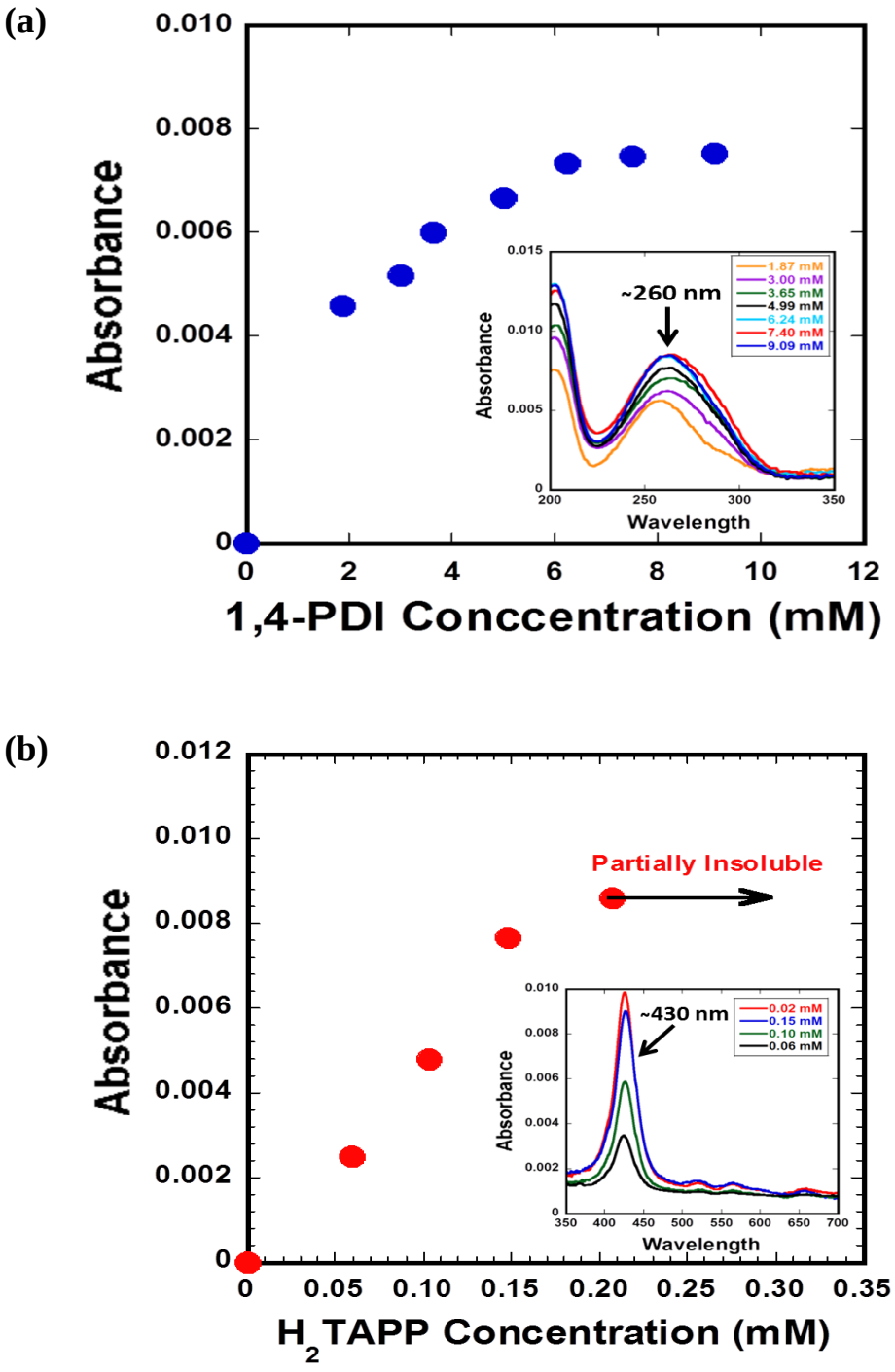

Figure 3.3 Optimization of (a) 1,4-PDI and (b) H_2TAPP concentration for solution-based MLD process at 0.5 and 1 MLD cycle respectively.

3.3.2.3 Investigation of Optimal Reaction Time

To achieve the well-controlled film growth throughout the deposition process, it is essential to confirm the maximum surface coverage in each half cycle of molecular deposition. To get the best reaction condition as possible, the optimized reaction time was investigated during the step of 2nd MLD (1 MLD cycle) film formation of H_2TAPP molecules on 0.5 MLD cycle film. **Figure 3.4** portrays the absorbance at ~260 (0.5 MLD cycle) and ~430 nm (1 MLD cycle) as a function of immersion time in 1,4-PDI and H_2TAPP solution respectively. The reaction between isocyanate group of 1,4-PDI and amine group of APTMS-modified surface showed almost constant absorbance with the

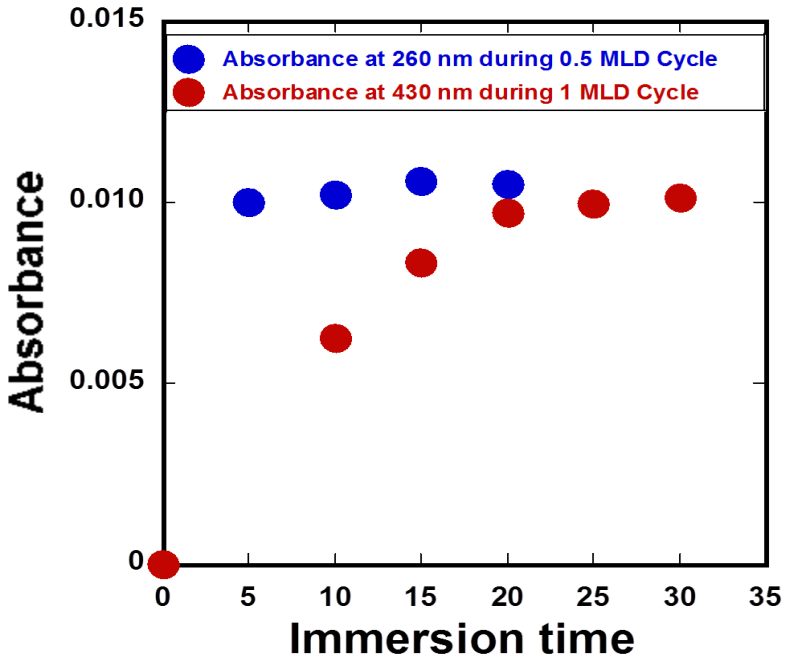

Figure 3.4 Absorbance at ~260 (blue) and ~430 nm (red) as a function of immersion time in 1,4-PDI (0.5 MLD cycle) and H_2TAPP solution (1 MLD cycle) respectively.

immersion time of 1,4-PDI from 5 to 20 min. But in the case of reaction between isocyanate group of 1,4-PDI and amine group of H_2TAPP, absorbance increases continuously with the immersion time of H_2TAPP and stopped after 25 min, indicating that 25 min is the optimized reaction time to get the maximum surface coverage.

As it is hypothesized that the amine group of H_2TAPP may effectively react with the free isocyanate group of 0.5 MLD cycle film to promote the film growth. To verify this assumption, 1 MLD cycle film was immersed into the H_2TAPP solution for additional 30 min and the results showed no increase of the absorbance. But the absorbance at ~260 nm and ~430 nm increases when 1 MLD cycle film was immersed into the 1,4-PDI solution and followed by H_2TAPP solution to prepare 2 MLD cycle film as shown in **Figure 3.5**.

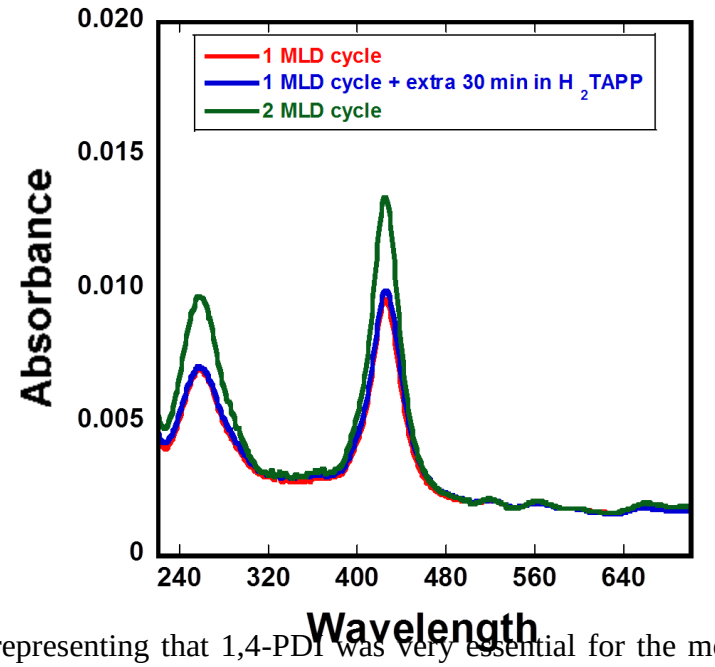

Figure 3.5 Physisorption check: UV-vis absorption spectra of (red) 4 MLD cycle thin film and (black) 4 MLD cycle + extra 30 min H_2TAPP dipped film.

These results representing that 1,4-PDI was very essential for the molecular growth and

the physisorption of porphyrin didn't occurred in this system.

3.3.3 Humidity Effect on Molecular Growth

3.3.3.1 Study of UV-vis Absorption Spectroscopy

In this work, moisture-sensitive 1,4-PDI (containing isocyanate group) was used as one precursor,[34-35] which may have different degrees of self-polymerization with respect to relative humidity (RH) conditions of the reaction chamber. Considering this issue, the effect of RH on film growth was investigated using UV-vis absorption spectroscopy. **Figure 3.6** depicts the UV-vis absorption spectra of 1 MLD cycle films as a function of RH conditions of the reaction chamber. The absorbance increased significantly at ~260 nm

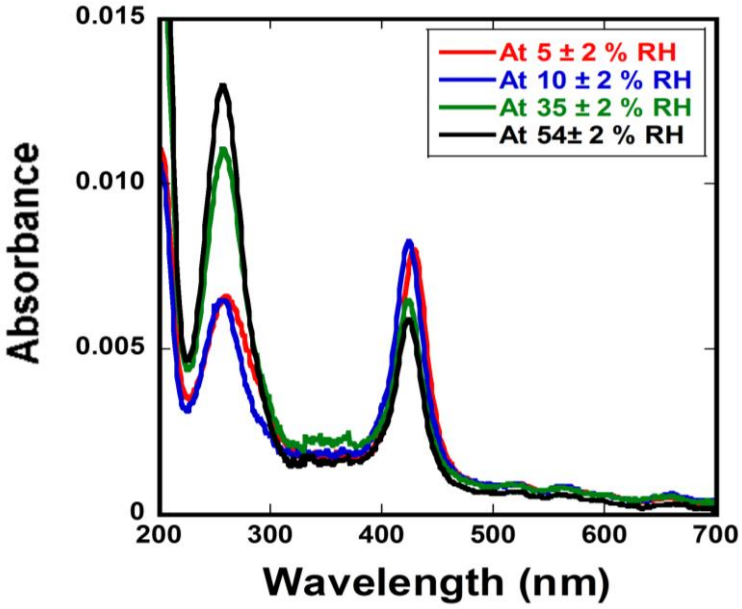

Figure 3.6 UV-vis absorption spectra of 1 MLD cycle films on the SiO_2 substrate as a function of RH of the reaction chamber (immersion time = 25 min/0.5 MLD cycle).

and decreased at ~430 nm from 54 ± 2% to 10 ± 2% RH of the reaction chamber. But the

absorbance remains almost same in the cases of 5 ± 2% and 10 ± 2% RH, representing a tentative RH condition for the fabrication of porphyrin-based polyurea thin film. It represents the higher number of diphenylurea formation (at ~260 nm)[13,35,48] at high–RH that reduced the reaction possibilities of porphyrin precursors. That might have occurred because of the self-polymerization of 1,4-PDI,[35] which can block the reactive surface area that interrupts the entry of incident porphyrin precursors for reaction. At high RH condition of the reaction chamber, hydrolysis of isocyanate group is expected to form the corresponding carbamic acid at the presence of water vapor (at high RH) that might be converted to amine with the evolution of carbon dioxide.[35] Thus, another isocyanate group containing 1,4-PDI molecule can react with the carbamic acid intermediate or amine to form corresponding urea as the final product of self-polymerization (**Scheme 3.2**).[35] As a consequence the top surface of the film could be blocked by the self-polymerization of 1,4-PDI molecules. These might reduce the availability of isocyanate groups that is required for the molecular growth of H_2TAPP through the urea coupling reaction (**Scheme 3.3**).

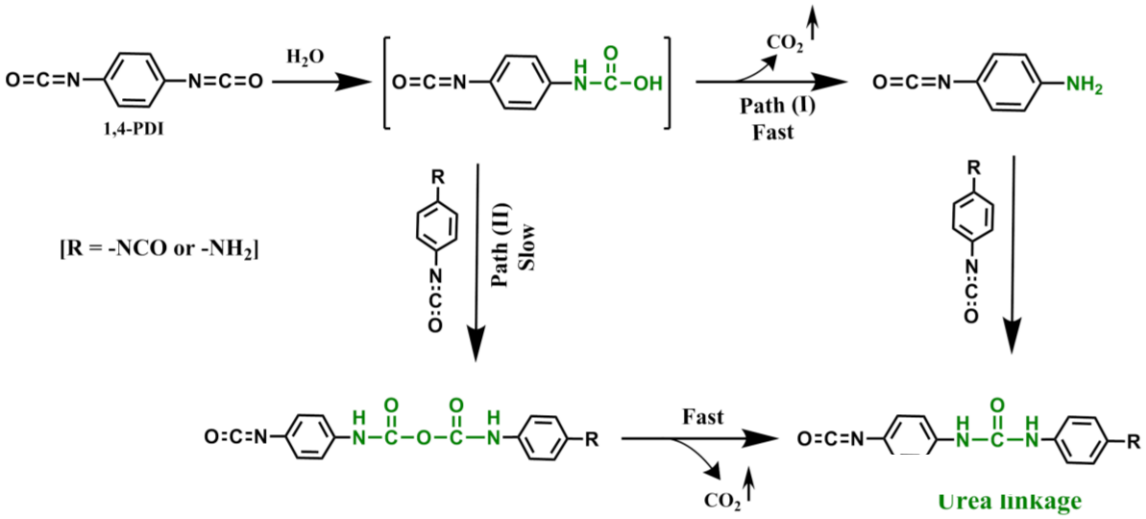

Scheme 3.2 Hydrolysis of isocyanate group to form a carbamic acid (intermediate) and the subsequent decomposition to produce amine, leading self-polymerization of 1,4-PDI molecules period.

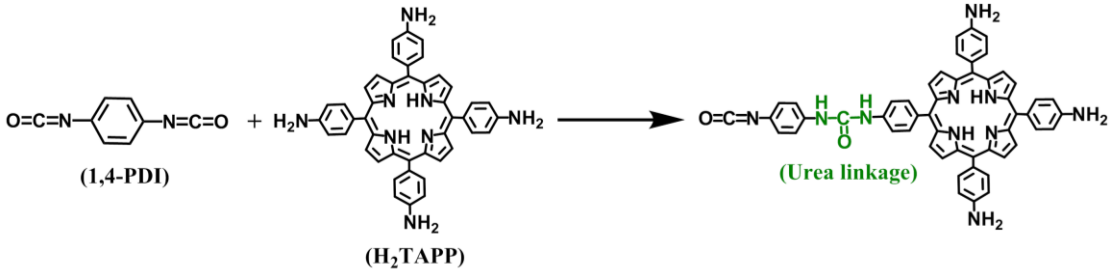

Scheme 3.3 Reaction between isocyanate and amine group to form urea linkage period

3.3.3.2 Study of X-ray photoelectron spectroscopy (XPS)

For clarification, XPS spectra of 1 MLD cycle films were taken at both low (10 ± 2%) and high (34 ± 2%) RH conditions. **Figure 3.7** presents the N 1s XPS fine scan spectra of H_2TAPP powder and 1 MLD cycle films prepared at both low and high RH conditions. The lowest binding energy peak at 398.0 eV and higher binding energy peak at 400.4 eV correspond to the iminic (=N-) and pyrrolic (N–H) groups respectively.[52] The intermediate binding energy peak at 399.4 eV resulted from the non-hydrogen bonded free amine (NH_2).[13,46,52] A minor peak at the higher binding energy around 401.9 eV represents the hydrogen bonded amine and nitrogen shakeup satellite of porphyrin.[46,52] The binding energies of N 1s XPS fine scan spectra for 1 MLD cycle film showed good matching with the N 1s XPS fine scan spectra for H_2TAPP powder with an additional peak at 399.7 eV representing the urea (O=C–N–H) groups as shown in **Table 3.1**. The N 1s XPS fine scan spectra showed that the peak area of urea response prepared at the high–RH condition is 70% higher than the film prepared at the low–RH condition. The iminic (=N-) and pyrrolic (N–H) peak areas of porphyrin showed 10% lower response from low to high RH conditions. That can only occur when 1,4-PDI becomes self-polymeraized at high-RH self-polymerized at the high–RH condition. The high free amine response might be observed because of the presence of free amine groups from each porphyrin molecules.[46]

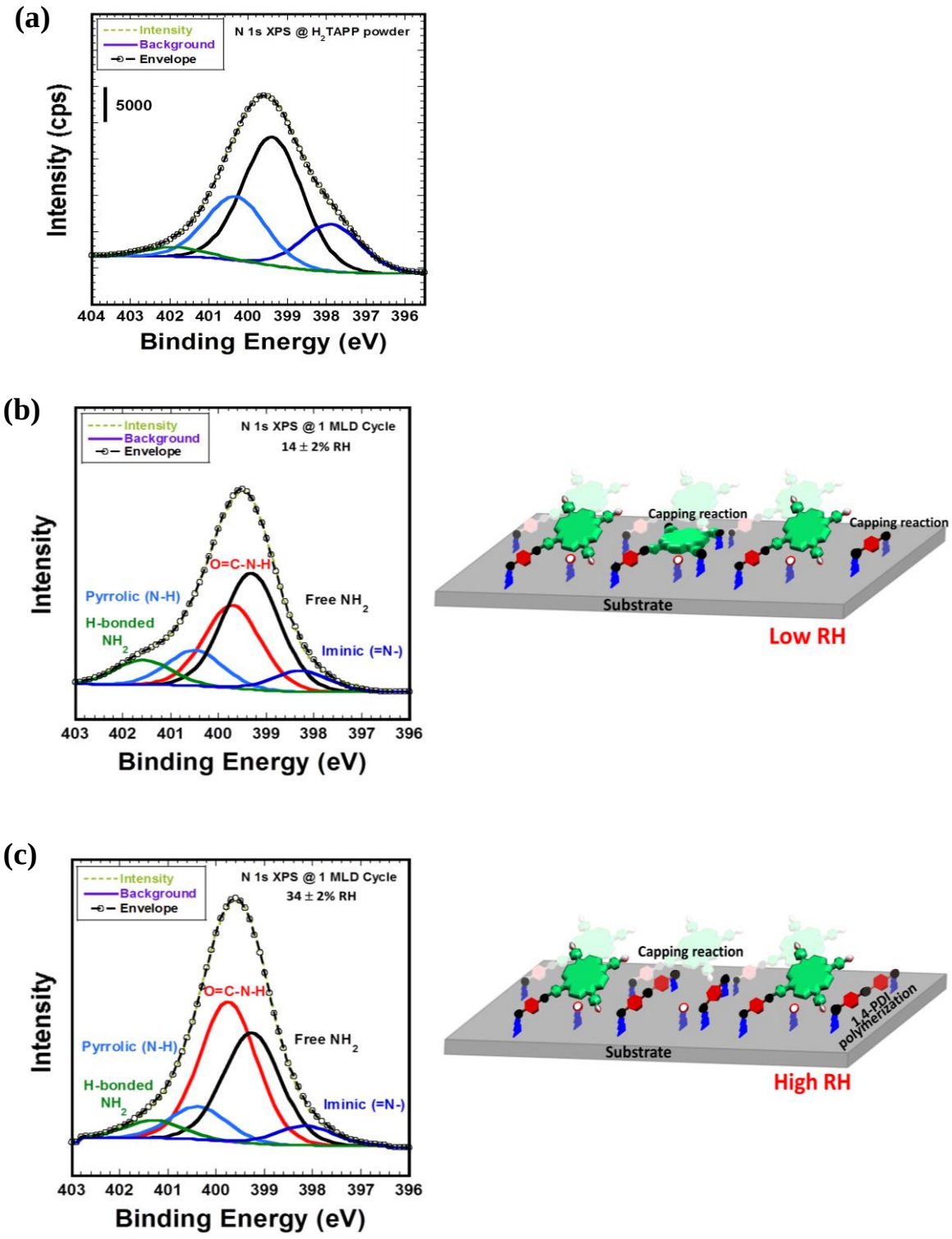

Figure 3.7 The N 1s XPS fine scan spectra of (a) H_2TAPP powder and 1 MLD cycle film prepared at (b) 10 ± 2 % and (c) 34 ± 2 % RH conditions and there schematic representation.

Table 3.1 Peak assignments of the N 1s XPS fine scan spectra for H_2TAPP powder and 1 MLD cycle films at both low and high RH conditions

Sample	=N- (Iminic)	Free NH_2	N–H (Pyrrolic)	H-bonded NH_2 / N-shakeup satellite	O=C–N–H
H_2TAPP powder	397.9 eV	399.4 eV	400.4 eV	401.9 eV	
1 MLD cycle (Low RH)	398.0 eV	399.4 eV	400.4 eV	401.9 eV	399.7 eV
1 MLD cycle (High RH)	398.0 eV	399.4 eV	400.4 eV	401.9 eV	399.7 eV

3.3.4 Porphyrin-based Multilayer Thin Film Formation

3.3.4.1 Investigation of Multilayer Film Growth by UV-vis absorption Specctroscopy

To investigate the porhyrin-based multilayer film growth on APTMS-modified SiO_2 substrate, transparent UV-vis absorption spectroscopy has been used as a function of MLD

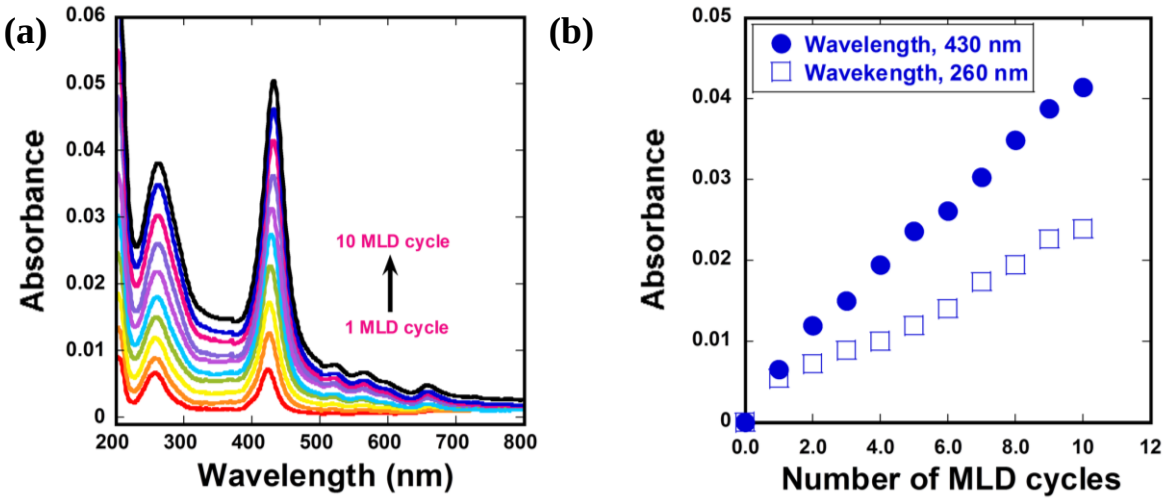

Figure 3.8 (a) UV-vis spectra of multilayer thin film as a function of MLD cycles on APTMS-modified quartz slides and (b) linear plot of absorption intensity vs. the number of MLD cycles at 10 ± 2 % RH of the reaction chamber.

cycles. According to the above study, it is expected that RH has a significant effect on multilayer film growth. So, multilayer film growth was investigated at both low and high RH conditions. **Figure 3.8** portrays the continuous increase of absorbance as a function of MLD cycles at 10 ± 2% RH of the reaction chamber, indicating stepwise film growth on APTMS-modified SiO_2 substrate.[13,34,43]

The surface density (Γ) of porphyrin-based urea thin films were calculated by using

equation 1.

$$\Gamma = \left[\left(\frac{A_\lambda}{2} \right) \varepsilon_\lambda^{-1} N_A \right] \times 10^{-3} \qquad \text{(eq. 1)}$$

Here, A_λ is the absorbance of polyurea or porphyrin in the film at wavelength λ, ε_λ is the extinction co-efficient ($\varepsilon_{phenyl\ urea}$ = 37200 M^{-1} cm^{-1} and $\varepsilon_{porphyrin}$ = 391590 M^{-1} cm^{-1}) in solution at λ, and N_A is Avogadro's number (6.023×10^{23}).

The surface density of phenyl urea and porphyrin were estimated to be 4.3×10^{13} and 5.0×10^{12} molecules / cm^2 respectively for 1 MLD cycle film. Whether, next MLD cycle showed the surface density of 1.29×10^{13} and 4.3×10^{12} molecules / cm^2 for phenyl urea and porphyrin respectively. It represents that only 45 % of the 1,4-PDI molecules take part is the reaction for the formation of 2 MLD film growth. This might be happened due to the surface blocking (capping reaction) caused by the double reaction of 1,4-PDI molecules at 0.5 MLD cycle. Stepwise film growth at 10 ± 2% RH shows almost similar tends with 5 ± 2% RH condition (Figure 9a). However, limiting film growth was observed in a high–RH condition as shown in **Figure 3.9b**. These results signify that, at high RH, an considerable amount of 1,4-PDI self-polymerization blocks the reactive surface sites that leads to a lower accessibility of the porphyrin molecules for molecular growth.[17,31] **Figure 3.9c-3.9d** depicts the expected schematic representation of multilayer film growth at both low and high RH conditions. During multilayer film growth, 1 MLD cycle film showed higher

absorbance at 260 nm compared to the growth sequence of following MLD cycles. It might have occurred as a result of capped region caused by the double reaction of 1,4-PDI or H_2TAPP precursors because the molecular population is largest at the initial steps of film growth.[16,38]

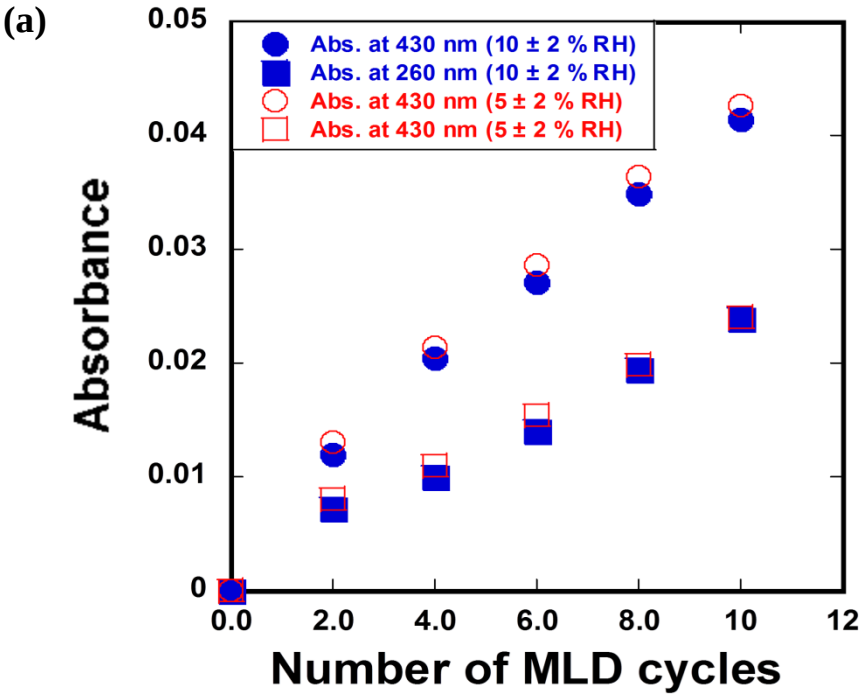

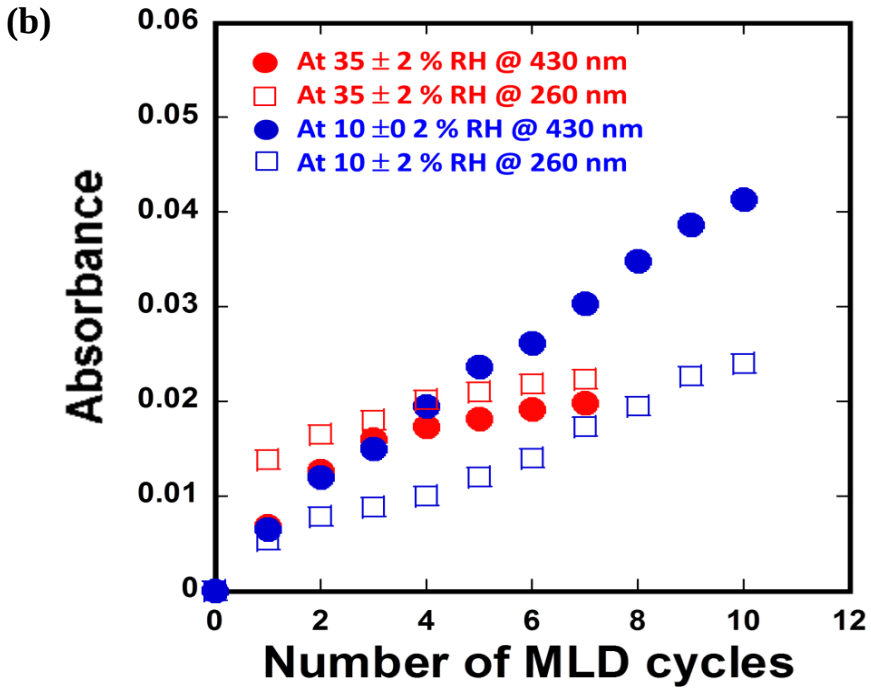

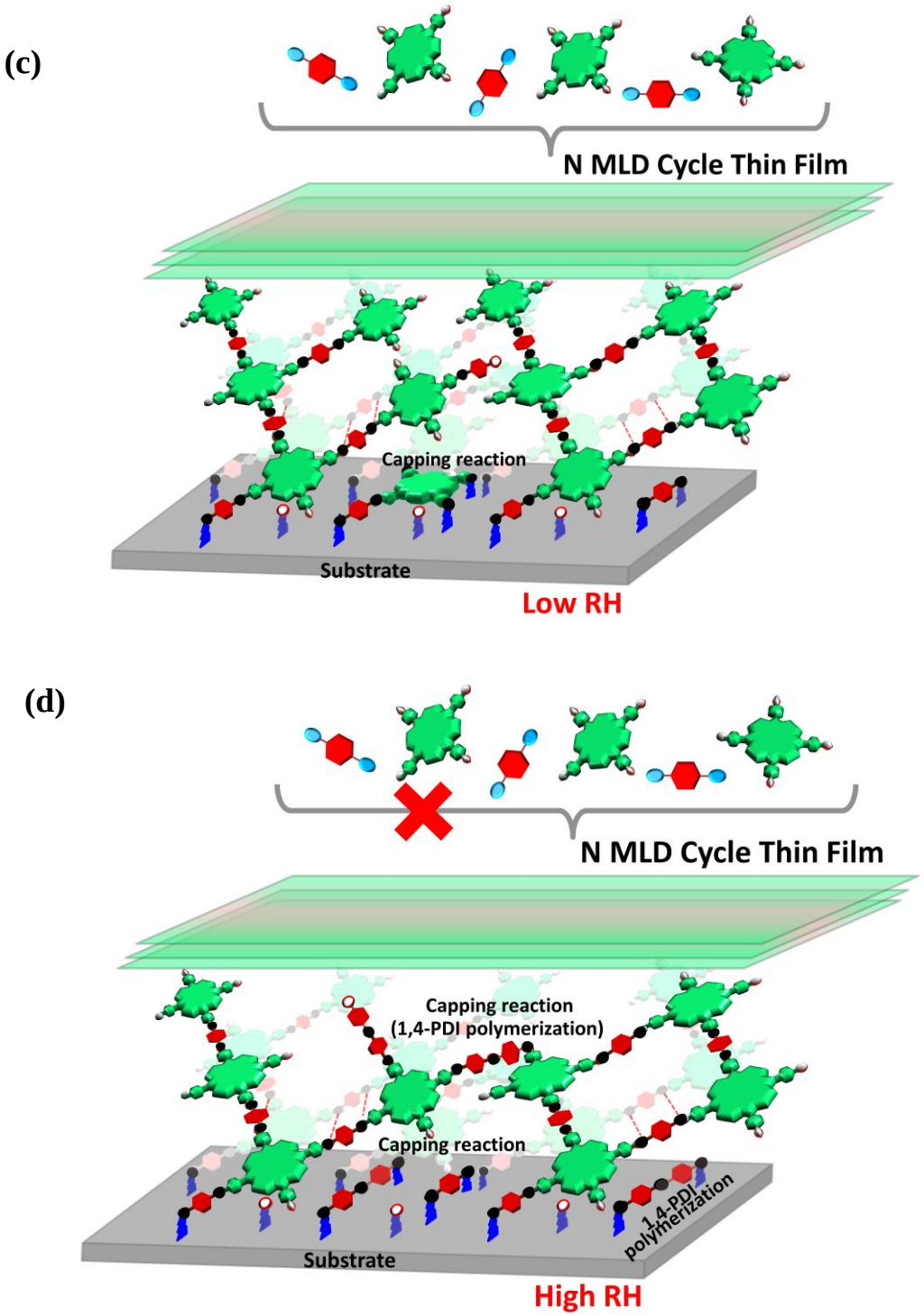

Figure 3.9 Linear plot of absorption intensity as a function of MLD cycles at (a) 5 ± 2% and 10 ± 2%, and (b) 10 ± 2% and 34 ± 2% RH of the reaction chamber. [1] (c) Schematic representation of multilayer film growth at low and high RH.

3.3.4.2 Film Thickness Measurement by AFM

To demonstrate the growth behavior, thickness of 2, 5, 8, and 10 MLD cycle thin films were investigated using AFM and white interference microscope (**Figure 3.10**).

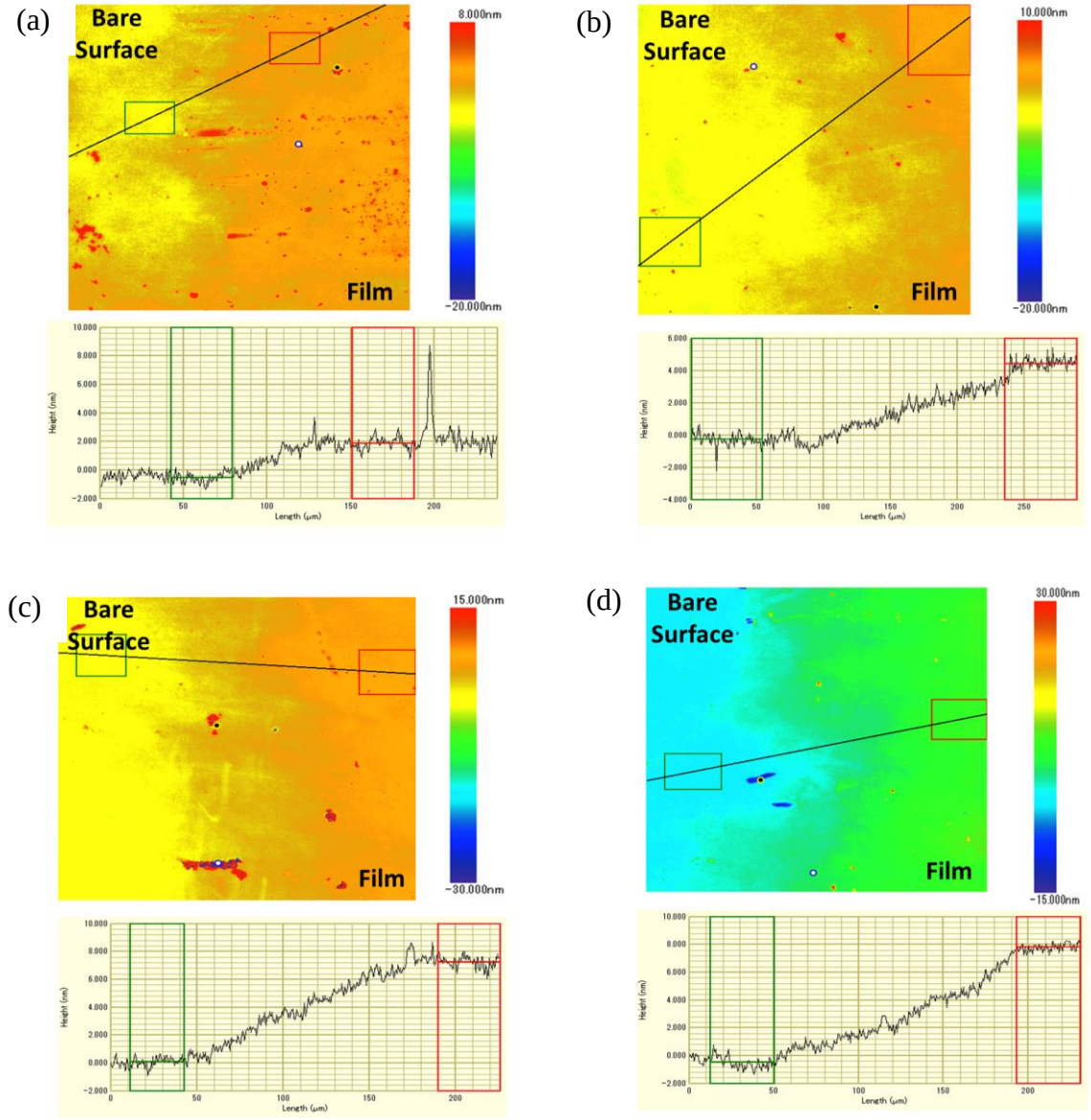

Figure 3.10. Thickness measurements of (a) 2, (b) 5, (c) 8 and (10) 10 MLD cycle thin films by white interference microscope.

Figure 3.11 depicts the sequential growth behavior with the number of MLD cycles, confirming stepwise film formation at 10 ± 2 % RH of the reaction chamber.[16,27] The film growth rate for 1,4-PDI/H_2TAPP film was found be approximately 0.80 ± 0.03 nm/MLD cycle. The thickness of AFM results are well matched to the white interference microscope results. This growth rate is lower than the combined molecular length of 1,4-PDI and H_2TAPP molecules, which is estimated as approximately 2.08 nm, based on the constituent bond length of 1,4-PDI and H_2TAPP molecules. Deviation of the growth rate can be attributed to several factors. First, the film growth direction is not perpendicular to the substrate surface. In fact, the tilted configuration of MLD film with respect to the surface

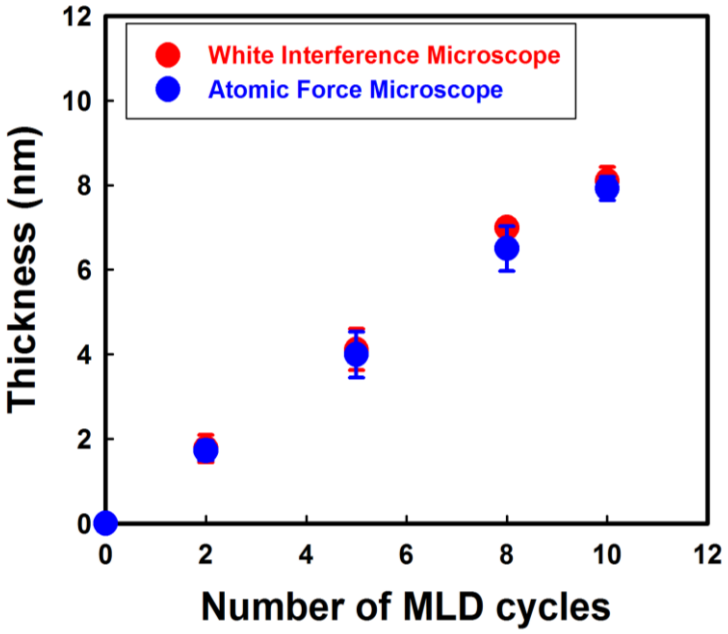

Figure 3.11 Film thickness as a function of number of MLD cycles prepared at 10 ± 2 % RH of the reaction chamber.

might dominate the structure.[32] It is expected that the multilayer films are growing at an average angle of 64° from the substrate. Second, all functional groups in a fraction of incident precursors may react with the reactive film surface to form a capped region.[16,31]

3.3.4.3 Determination of Chemical Bond Using FTIR

From the discussion presented above, it was not confirmed that the multilayer film growth occurred by a urea coupling reaction between isocyanate and amine groups. Therefore, IR spectroscopic measurements were taken to investigate chemical bonding into the molecular films. **Figure 3.12** presents the IR spectra for 5 and 10 MLD cycle thin films at lower wavenumber region (1100-1700 cm^{-1}). Several characteristic peaks were observed

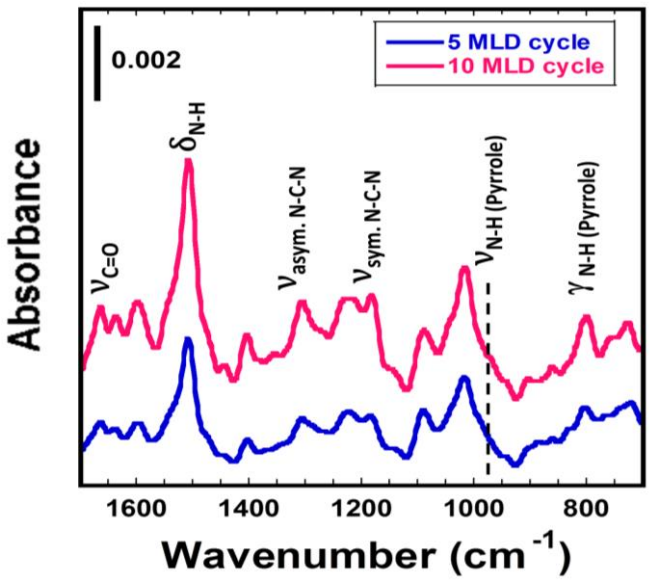

Figure 3.12 IR spectra of 5 and 10 MLD cycle thin films on the APTMS-modified Si substrate at lower wavenumber region (1100-1700 cm^{-1}).

in the IR fingerprint region. The band around 1635 and 1665 cm^{-1} can be assigned as amide I band resulting from the H-bonded and free υ(C=O) stretching vibration mode of urea group respectively. The amide II band as δ(N–H) bending vibration was observed around 1510 cm^{-1}. Peaks around 1311 and 1180 cm^{-1} can be assigned for the asymmetric υ_{as}(N–C–N) and symmetric υ_{s}(N–C–N) stretching modes respectively. All characteristic peaks confirmed the formation of urea linkage.[13,32-33,35,51] In addition, the out-of-plane γ(N–H) vibration of pyrrole in free-base porphyrin was observed at around 730 and 800 cm^{-1}. A shoulder type υ(N–H) band was also observed at around 965 cm^{-1} for in-plane N–H vibration of pyrrole.[53-54]

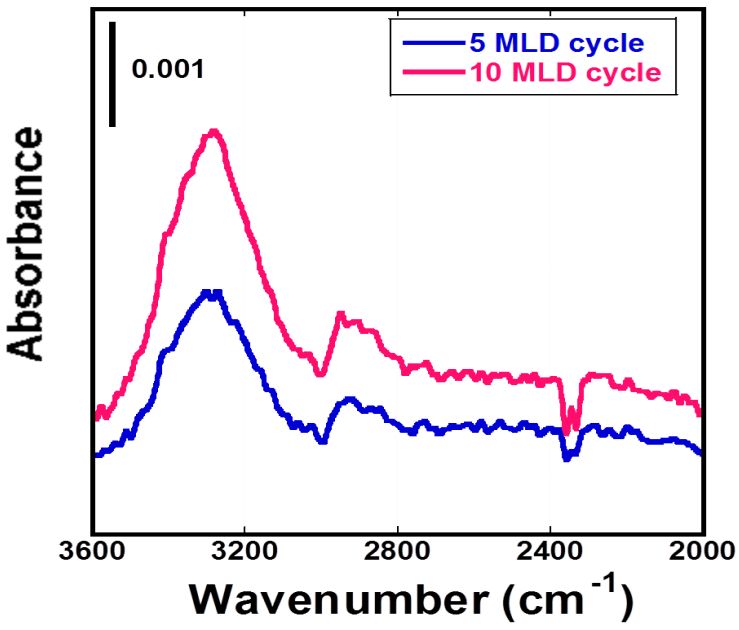

Figure 3.13 IR spectra of 5 and 10 MLD cycle thin films on the APTMS-modified Si substrate at higher wavenumber region (2000-3600 cm^{-1}).

Figure 3.13 shows the infrared (IR) spectra of 5 and 10 MLD cycle thin films at higher wavenumber region. A broad peak was observed with the center wavenumber at around 3270 cm^{-1}, representing the presence of ν(N–H) stretching band of polyurea and amine groups.[13] Furthermore, the absorbance increased with the number of MLD cycles, reflecting that the polyurea-based growth behavior occurred along with the multilayer film formation. No peak was observed at around 2270 cm^{-1} for υ_{as}(N=C=O) stretching, indicating the absence of unreacted isocyanate groups in the multilayer films.[33]

3.3.4.4 Investigation of Chemical Environments and Bond by XPS

For further characterization, XPS was used to explore the chemical nature of the molecular networks. Elemental fine scan spectra revealed the atomic environment and chemical bonding in the multilayer thin films. The N 1s XPS fine scan spectra of 5 and 10

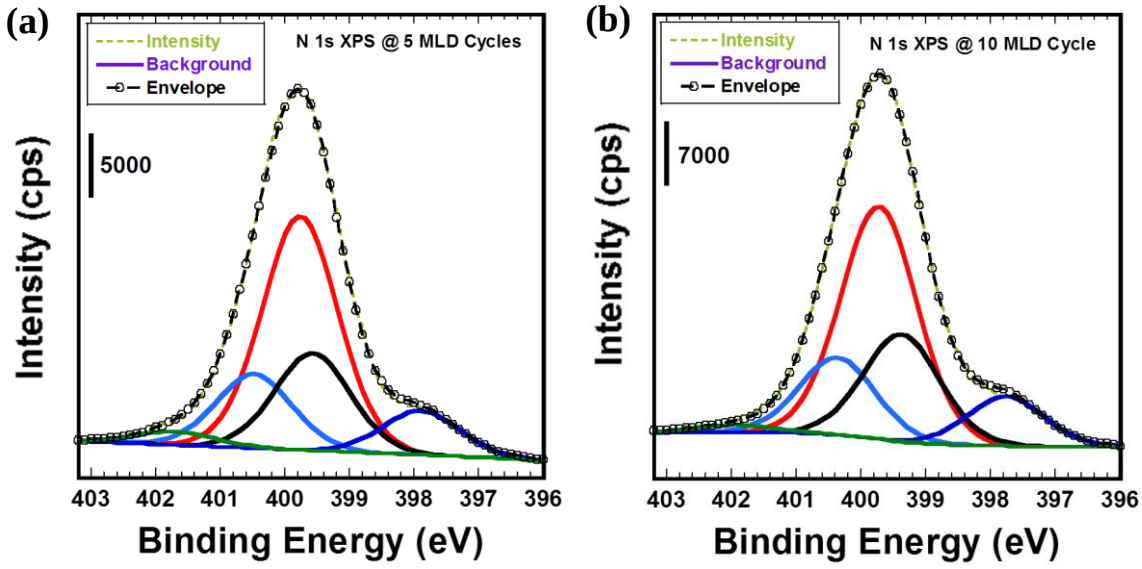

Figure 3.14 N 1s XPS fine scan spectra of (a) 5 and (b) 10 MLD cycle film films on APTMS-modified SiO_2 substrate.

MLD cycle films showed five different types of components **(Figure 3.14**). The main peak at 399.8 eV represents the urea (O=C–N–H) groups.[13,32,34] The lowest binding energy peak at 397.9 eV and higher binding energy peak at 400.4 eV correspond to the iminic (=N-) and pyrrolic (N–H) groups respectively.[50] The intermediate binding energy peak at 399.4 eV resulted from the non-hydrogen bonded free amine (NH_2).[13,46,50] Finally, the minor peak at the higher binding energy around 401.9 eV represents the hydrogen bonded amine and nitrogen shakeup satellite of porphyrin.[46,50] The binding energies of N 1s XPS fine scan spectra of 5 and 10 MLD cycle films showed good matching with the N 1s XPS fine scan spectra of H_2TAPP powder **(Figure 3.7a)**, as shown in **Table 3.2**.

Table 3.2 Peak assignments of the N 1s XPS fine scan spectra for H_2TAPP powder and 5 and 10 MLD cycle films

Sample	=N- (Iminic)	Free NH_2	N–H (Pyrrolic)	H-bonded NH_2 / N-shakeup satellite	O=C–N–H
H_2TAPP powder	397.9 eV	399.4 eV	400.4 eV	401.9 eV	
5 MLD cycle film	397.9 eV	399.4 eV	400.4 eV	401.9 eV	399.8 eV
10 MLD cycle film	397.9 eV	399.4 eV	400.4 eV	401.9 eV	399.8 eV

The deconvoluted N-components revealed that the peak area ratio of pyrrolic N-H and iminic N=C is 1.3:1.0 for both porphyrin powder and multilayer thin film, indicating that multilayer film growth occurred through the reaction between isocyanate group of 1,4-PDI and amine group of H_2TAPP (Free porphyrin) rather than pyrrole group of porphyrin center. It was also revealed that the peak area of urea (O=C–N–H) and free amine (NH_2) responses are 3.2 and 1.3 times higher than the pyrrolic (N–H) group respectively.

Suggesting that, on average, only 2–3 amine groups of each porphyrin molecule took part in the reaction during stepwise film growth. Some additional urea and free amines might be observed because of the capping reaction of incident precursors[31] and unreacted amine and isocyanate groups which were easily converted to amine by humid air.

In addition, C 1s XPS spectra for 10 MLD cycle film showed four components **(Figure 3.15)**. The lowest binding energy peak at 284.5 eV is attributed to the aromatic carbon (C=C) and C–H bonds.[13] The highest binding energy peak at 288.5 eV corresponds to the carbonyl (C=O) group of urea linkage.[13,46] And the intermediate binding energy peaks at 285.7 eV and 286.5 eV denote the sp^2 C–N and C=N bond respectively.[46] No isocyanate peak was observed from N 1s and C 1s XPS fine scan spectra.[55] These assignments of N 1s and C 1s XPS fine scan spectra are consistent with IR results and were previously reported polyurea-based works.[13,31-35,46,51-52] All results confirmed the urea bond formation consistently into the multilayer thin film.

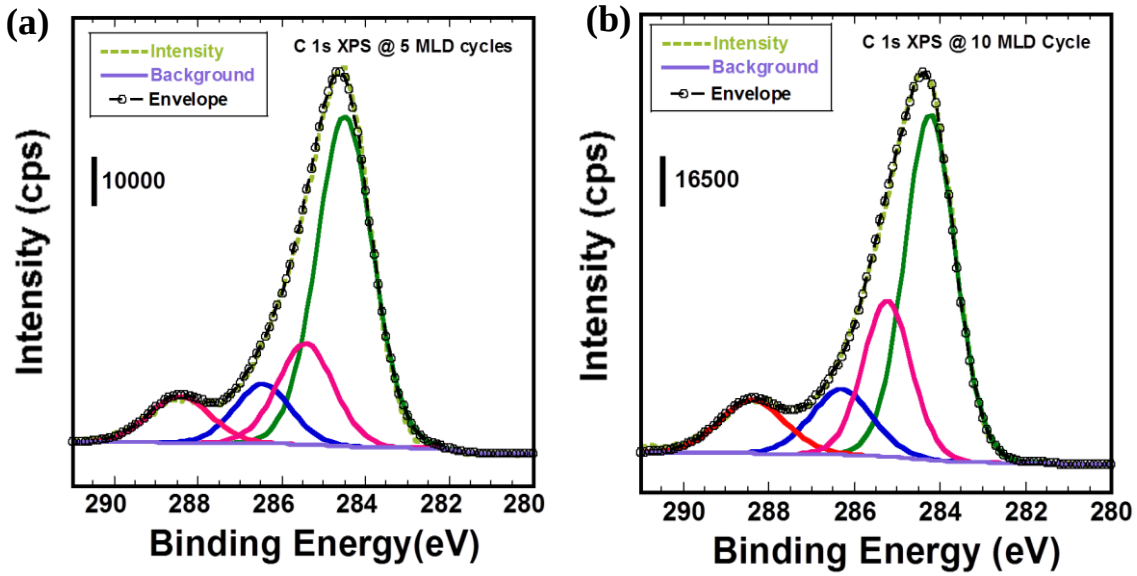

Figure 3.15 C 1s XPS fine scan spectra for (a) 5 and (b) 10 MLD cycle films on APTMS-modified SiO_2 substrate.

Figure 3.16 presents survey spectra of APTMS-modified SiO_2 substrate and 1, 5 and 10 MLD cycle thin films on APTMS-modified SiO_2 substrate. Results show that N 1s and C 1s peak intensities in5crease concomitantly with decreasing Si 2p peak intensity from APTMS to 10 MLD cycle thin films, indicating that the multilayer film covers the SiO_2 surface. Additionally, it is noteworthy that N 1s peak intensity for 1 MLD cycle film is higher than the calculated one MLD cycle of 5 and 10 MLD cycle thin films. That result might have occurred due to the presence of unreacted amine-functionalized APTMS (H-bonded amine)[46] and the capped region caused by the double reaction of 1,4-PDI or H_2TAPP precursors because the molecular population is larger at the initial steps of film

growth.[16,31] These results are relevant with the results obtained from UV-vis absorption for multilayer thin film growth (**Figure 3.8**).

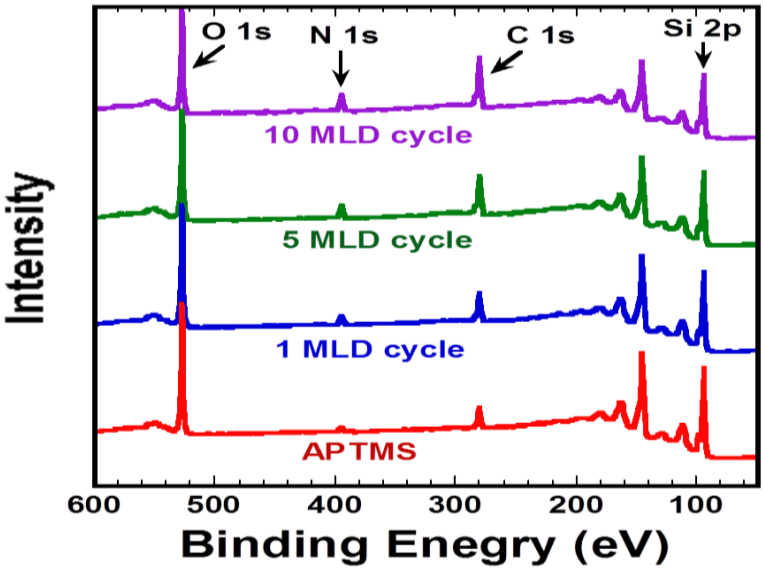

Figure 3.16 XPS survey spectrum for APTMS-modified SiO_2 substrate and 1, 5 and 10 MLD cycle thin films on APTMS-modified SiO_2 substrate.

3.3.4. 5 Study of Surface Morphology by AFM

The surface morphology of bare Si and APTMS-modified Si substrates and multilayer thin films were also investigated using tapping mode AFM, as shown in **Figure 3.17** and **3.18**. The surface morphology of thin film showed the distinct properties from the bare and APTMS-modified Si substrates. It also represents the evidence of thin film formation. The 2D and 3D height images of 5 and 10 MLD cycle thin films show

consistent surface within 500 nm × 500 nm areas, which indicates the well deposition process (**Figure 3.18**). It was made up of numerous small grain-like domains along the horizontal axis with the diameter of *ca.* 10–20 nm, which increases slightly from 5 to 10 MLD cycle thin films. The root mean square (RMS) roughness was also investigated; where roughness increased from 0.36 to 0.48 nm for 5 and 10 MLD cycle thin films respectively. In comparison to the bare Si substrate and APTMS-modified Si substrate, 5 and 10 MLD cycle films show greater domain size and RMS roughness **(Table 3.3)**, which signifies the molecular layer growth on the APTMS-modified Si substrate.[13,27]

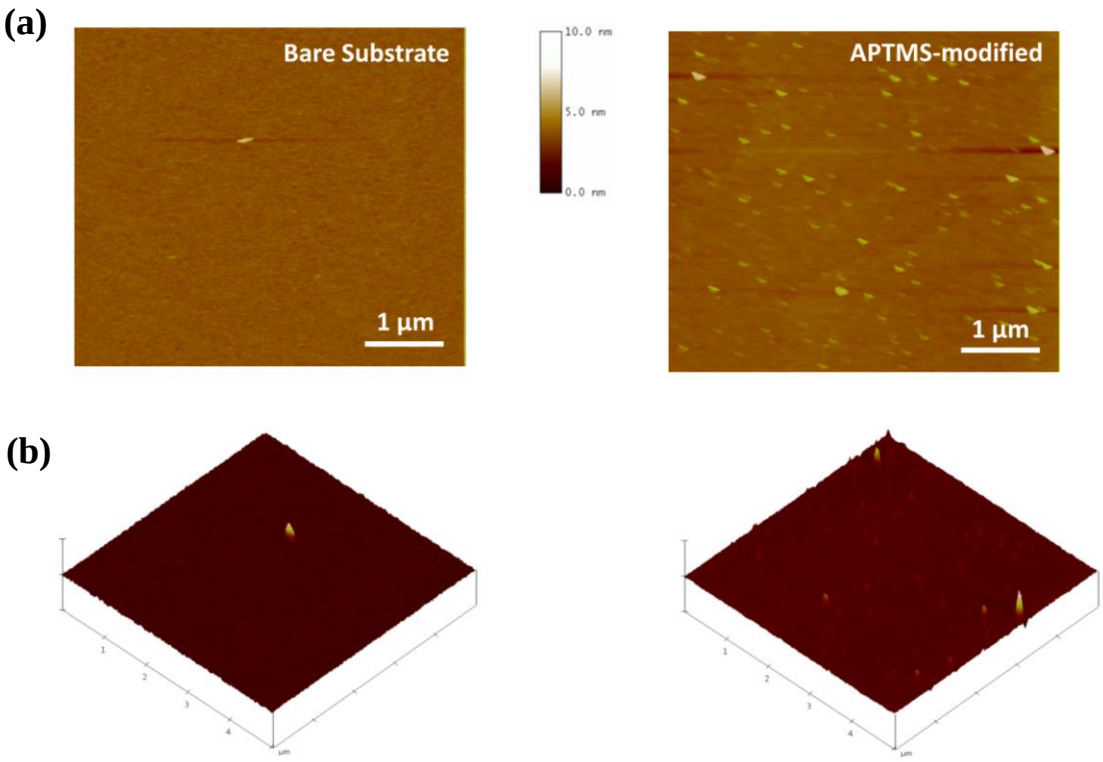

Figure 3.17 AFM height images (a) 2D and (b) 3D of bare Si and APTMS-modified Si substrate respectively. Scan size: 5.0 µm × 5.0 µm. Data scale 10 nm.

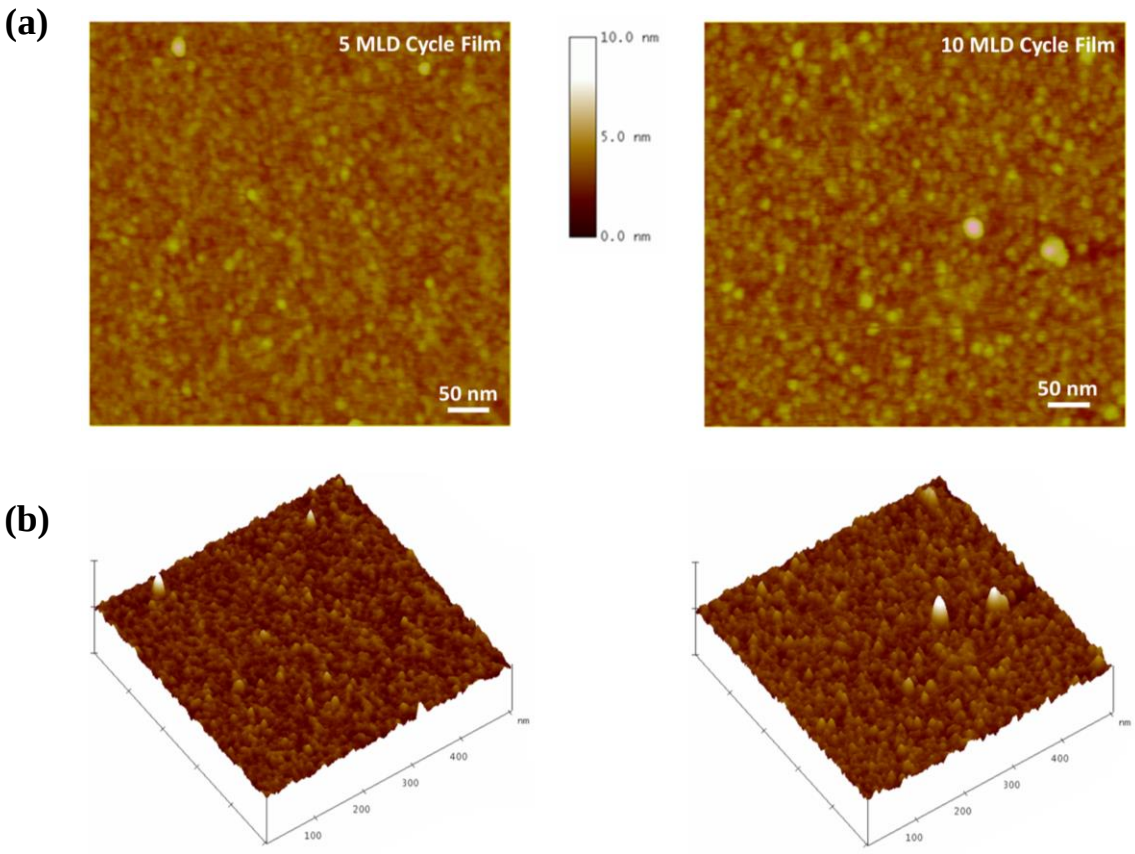

Figure 3.18 AFM (a) 2D and (b) 3D height images of 5 MLD and 10 MLD cycle thin films on Si-substrate. Scan size: 500 nm × 500 nm. Data scale 10 nm.

Table 3.3 Surface roughness and the estimated domain size of bare Si substrate, APTMS-modified Si substrate, 5 and 10 MLD cycle films on APTMS-modified Si substrate.

Sample	Scan size	Roughness Analysis: RMS, R_q (nm)	Estimated domain size (nm)
Bare Si substrate	5 μm × 5 μm	0.17	N.A.
APTMS-modified Si substrate	5 μm × 5 μm	0.25	N.A.

5 MLD cycle film	500 nm × 500 nm	0.36	10-20
10 MLD cycle film	500 nm × 500 nm	0.48	10-20

N.A. = Not Applicable

3.4 Conclusions

I have demonstrated the solution-based MLD thin film growth of porphyrin-based covalent molecular networks on a APTMS-modified substrate surface using the urea coupling reaction between 1,4-PDI and H_2TAPP at room temperature. UV-vis absorption spectra showed stepwise multilayer film growth at ≤10% RH condition of the reaction chamber, whereas the high RH condition showed film growth-limiting behavior. Presumably, numerous 1,4-PDI self-polymerization took place at high RH conditions. This might block the reactive surface area that leads to a lower accessibility of porphyrin molecules for multilayer film growth. From surface density calculation, it was observed that only 45 % of the 1,4-PDI molecules take part is the reaction for the formation of 2 MLD film growth at low RH condition. And the multilayer film showed a low molecular density. White interference microscope confirms the film thickness measured by AFM and indicates that the multilayer films prepared at 10 ± 2% RH of the reaction chamber are growing at an average angle of 64° relative to the substrate surface normal. FTIR spectra of multilayer thin films showed four characteristic IR vibrational bands for urea linkage along with the in-plane and out-of-plane vibrational modes of pyrrole from metal free porphyrin. The IR responses at around 1635 and 1670 cm^{-1} confirmed the presences of hydrogen bonded and free urea respectively into the multilayer thin film. The IR signal also increased significantly with the number of MLD cycles, representing the sequential

multilayer film growth caused by consecutive urea coupling reaction. Furthermore, deconvoluted high resolution N 1s and C 1s XPS fine scale spectra represent an additional evidence of urea bond formation into the multilayer thin films. Peak area ratio of the deconvoluted N-component revealed that, on average, only 2-3 amine groups of each porphyrin molecule took part in the urea coupling reaction for multilayer film formation.

References

(1) Huang, W.; Gann, E.; Cheng, Y-B.; McNeill, C. R. In-Depth Understanding of the Morphology−Performance Relationship in Polymer Solar Cells. *ACS Appl. Mater. Interfaces* **2015**, *7*, 14026−14034.

(2) Roberson, L. B.; Poggi, M. A.; Kowalik, J.; Smestad, G. P.; Bottomley, L. A.; Tolbert, L. M. Correlation of morphology and device performance in inorganic–organicTiO_2–polythiophene hybrid solid-state solar cells. *Coord. Chem. Rev.* **2004**, *248*, 1491–1499.

(3) Tao, Y.; McCulloch, B.; Kim, S.; Segalman, R. A. The relationship between morphology and performance of donor–acceptor rod–coil block copolymer solar cells. *Soft Matter* **2009**, *5*, 4219–4230.

(4) DiBenedetto, S. A.; Facchetti, A.; Ratner, M. A.; Marks, T. J. Molecular Self-Assembled Monolayers and Multilayers for Organic and Unconventional Inorganic Thin-Film Transistor Applications. *Adv. Mater*. **2009**, *21*, 1407.

(5) Campbell, W. M.; Jolley, K. W.; Wagner, P.; Wagner, K.; Walsh, P. J.; Gordon, K. C.; Schmidt-Mende, L.; Nazeeruddin, M. K.; Wang, Q.; Gra1tzel, M.; Officer, D.L. Highly Efficient Porphyrin Sensitizers for Dye-Sensitized Solar Cells. *J. Phys. Chem. C* **2007**, *111*(32), 11760–11762.

(6) Roberts, M. E.; Sokolov, A. N.; Bao, Z. Material and device considerations for

organic thin-film transistor sensors. *J. Mater. Chem.* **2009**, *19*, 3351–3363.

(7) Lvov, Y.; Yamada, S.; Kunitake, T. Non-linear optical effects in layer-by-layer alternate films of polycations and an azobenzene-containing polyanion. *Thin Solid Films* **1997**, *300*, 107–112.

(8) Nakazawa, M.; Kosugi, T.; Nagatsuka, H.; Maezawa, A.; Nakamura, K.; Ueha, S. Polyurea Thin Film Ultrasonic Transducers for Nondestructive Testing and Medical Imaging. *IEEE Trans.* **2007**, *54*, 2165–2174.

(9) Evans-Nguyen, K. M.; Tolles, L. R.; Gorkun, O. V.; Lord, S. T.; Schoenfisch, M. H. Interactions of Thrombin with Fibrinogen Adsorbed on Methyl-, Hydroxyl-, Amine-, and Carboxyl-Terminated Self-Assembled Monolayers. *Biochemistry* **2005**, *44*, 15561–15568.

(10) Gole, A.; Jana, N. R.; Selvan, S. T.; Ying, J. Y. Langmuir-Blodgett Thin Films of Quantum Dots: Synthesis, Surface Modification, and Fluorescence Resonance Energy Transfer (FRET) Studies. *Langmuir* **2008,** *24*, 8181–8186.

(11) Choudhury, S.; Betty, C. A.; Bhattacharyya, K.; Saxena, V.; Bhattacharya, D. Nano-structured PdO Thin Film from Langmuir−Blodgett Precursor for Room-Temperature H_2 Gas Sensing. *ACS Appl. Mater. Interfaces* **2016**, *8*, 16997−17003.

(12) Seon, J-B.; Lee, S.; Kim, J. M. Spin-Coated CdS Thin Films for n-Channel Thin Film Transistors. *Chem. Mater.* **2009**, *21*, 604–611.

(13) Rashed, M. A.; Laokroekkiat, S.; Hara, M.; Nagano, S.; Nagao, Y. Fabrication and Characterization of Cross-Linked Organic Thin Films with Nonlinear Mass Densities. *Langmuir* **2016**, *32*, 5917−5924.

(14) Sundberg, P.; Karppine, M. Inorganic–Organic Thin Film Structures by Molecular Layer Deposition: A review. *Beilstein J. Nanotechnol.* **2014**, *5*, 1104–1136.

(15) Zhou, H.; Bent, S. F. Fabrication of Organic Interfacial Layers by Molecular Layer Deposition: Present Status and Future Opportunities. *J. Vac. Sci. Technol., A* **2013**, *31*, 040801–040818.

(16) George, S. M.; Yoon, B.; Dameron, A. A. Surface Chemistry for Molecular Layer Deposition of Organic and Hybrid Organic-Inorganic polymers. *Acc. Chem. Res.* **2009**, *42*, 498–508.

(17) Adamczyk, N. M.; Dameron, A. A.; George, S. M. Molecular Layer Deposition of Poly(p-phenyleneterephthalamide) Films Using Terephthaloyl Chloride and p-Phenylenediamine. *Langmuir* **2008**, *24*, 2081–2089.

(18) Du, Y.; George, S. M. Molecular Layer Deposition of Nylon 66 Films Examined Using in situ FTIR Spectroscopy. *J. Phys. Chem. C* **2007**, *111*, 8509–8517.

(19) Peng, Q.; Efimenko, K.; Genzer, J.; Pardsons, G. N. Oligomer Orientation in Vapor-Molecular-Layer-Deposited Alkyl-Aromatic Polyamide films. *Langmuir* **2012**, *28*, 10464–10470.

(20) Yoshida, S.; Ono, T.; Esashi, M. Deposition of Conductivity-Switching Polyimide Film by Molecular Layer Deposition and Electrical Modification using Scanning Probe Microscope. *Micro. Nano Lett.* **2010**, *5*, 321–323.

(21) Yoshida, S.; Ono, T.; Esashi, M. Local Electrical Modification of a Conductivity-Switching Polyimide Film Formed by Molecular Layer Deposition. *Nanotechnology* **2011**, *22*, 335302.

(22) Lee, J. S.; Lee, Y. J.; Tae, E. L.; Park, Y. S.; Yoon, K. B. Synthesis of Zeolite as ordered Multicrystal Arrays. *Science* **2003**, *301*, 818–821.

(23) Prasittichai, C.; Zhou, H.; Bent, S. F. Area Selective Molecular Layer Deposition of Polyurea Films. *ACS Appl. Mater. Interfaces* **2013**, *5*, 13391–13396.

(24) Zhou, H.; Bent. S. F. Molecular Layer Deposition of Functional Thin Films for Advanced Lithographic Patterning. *ACS Appl. Mater. Interfaces* **2011**, *3*, 505–511.

(25) Qian, H.; Li, S.; Zheng, J.; Zhang, S. Ultrathin Films of Organic Networks as Nanofiltration Membranes via Solution-Based Molecular Layer Deposition. *Langmuir* **2012**, *28*, 17803–17810.

(26) Lee, B. H.; Ryu, M. K.; Choi, S. Y.; Lee, K. H.; Im, S.; Sung, M. M. Rapid vapor-phase fabrication of organic–inorganic hybrid super lattices with monolayer precision. *J. Am. Chem. Soc.* **2007**, *129*, 16034−16041.

(27) Laokroekkiat, S.; Hara, M.; Nagano, S.; Nagao, Y. Metal−Organic Coordination

Network Thin Film by Surface-Induced Assembly. *Langmuir* **2016**, *32*, 6648−6655.

(28) Such, G. K.; Johnston, A. P. R.; Caruso, F. Engineered hydrogen bonded polymer multilayers: from assembly to biomedical applications. *Chem. Soc. Rev.* **2011**, *40*, 19−29.

(29) Quinn, J. F.; Johnston, A. P. R.; Such, G. K.; Zelikin, A. N.; Caruso, F. Next generation, sequentially assembled ultrathin films: beyond electrostatics. *Chem. Soc. Rev.* **2007**, *36*, 707−718.

(30) Buck, M. E.; Schwartz, S. C.; Lynn, D. M. Super hydrophobic thin films fabricated by reactive layer-by-layer assembly of azlactone-functionalized polymers. *Chem. Mater*. **2010**, *22*, 6319−6327.

(31) Zhou, H.; Toney, M. F.; Bent, S. F. Cross-Linked Ultrathin Polyurea Films via Molecular Layer Deposition. *Macromolecules* **2013**, *46*, 5638−5643.

(32) Loscutoff, P. W.; Zhou, H.; Clendenning, S. B.; Bent, S. F. Formation of Organic Nanoscale Laminates and Blends by Molecular Layer Deposition. *ACS Nano* **2010**, *4* (1), 331–341.

(33) Kim, A.; Filler, M. A.; Kim, S.; Bent, S. F. Layer-by-Layer Growth on Ge (100) via Spontaneous Urea Coupling Reactions. *J. Am. Chem. Soc.* **2005**, *127*, 6123–6132.

(34) Kim, M.; Byeon, M. Bae, J-S.; Moon, S-Y.; Yu, G.; Shin, K.; Basarir, F.; Yoon, T-H.; Park, J-W. Preparation of Ultrathin Films of Molecular Networks through Layer-by-

Layer Cross-Linking Polymerization of Tetrafunctional Monomers. *Macromolecules* **2011**, *44*, 7092–7095.

(35) Kohli, P.; Blanchard, G. J. Applying polymer chemistry to interface: Layer-by-layer and spontaneous growth of covalently bound multilayers. *Langmuir* **2000**, *16*, 4655–4661.

(36) Jurowa, M.; Schuckmanb, A. E.; Batteasb, J. D.; Drain, C. M. Porphyrins as Molecular Electronic Components of Functional Devices. *Coord. Chem. Rev.* **2010**, *254*, 2297–2310.

(37) Thamyongkit, P.; Yu, L.; Padmaja, K.; Jiao, J.; Bocian, D. F.; Lindsey, J. S. Porphyrin Dyads Bearing Carbon Tethers for Studies of High-Density Molecular Charge Storage on Silicon Surfaces. *J. Org. Chem.* **2006**, *71*, 1156–1171.

(38) Wasielewski, M. R. Photoinduced Electron Transfer in Supramolecular Systems for Artificial Photosynthesis. *Chem. Rev.* **1992**, *92*, 435–461.

(39) Cho, Y.-J.; Ahn, T. K.; Song, H.; Kim, K. S.; Lee, C. Y.; Seo, W. S.; Lee, K.; Kim, S. K.; Kim, D.; Park, J. T. Unusually High Performance Photovoltaic Cell Based on a [60] Fullerene Metal Cluster-Porphyrin Dyad SAM on an ITO Electrode. *J. Am. Chem. Soc.* **2005**, *127*, 2380–2381.

(40) Abdelrazzaq, F. B.; Kwong, R. C.; Thompson, M. E. Photocurrent Generation in Multilayer Organic-Inorganic Thin Films with Cascade Energy Architectures. *J. Am.*

Chem. Soc. **2002**, *124*, 4796–4803.

(41) Odobel, F.; Blart, E.; Lagree, M.; Villieras, M.; Boujtita, H.; El Murr, N.; Caramori, S.; Bignozzi, A. C. Porphyrin dyes for TiO2 sensitization. *J. Mater. Chem.* **2003**, *13*, 502–510.

(42) Karimipour, G.; Kowkabi, S.; Naghiha, A. New Aminoporphyrins Bearing Urea Derivative Substituents: Synthesis, Characterization, Antibacterial and Antifungal Activity. *Braz. Arch. Biol. Technol.* **2015**, *58* (3), 431-442.

(43) Palomaki, P. K. B.; Dinolfo, P. H. A Versatile Molecular Layer-by-Layer Thin Film Fabrication Technique utilizing Copper(I)-Catalyzed Azide–Alkyne Cycloaddition. *Langmuir* **2010**, *26* (12), 9677–9685.

(44) Palomaki, P. K. B.; Dinolfo, P. H. Structural Analysis of Porphyrin Multilayer Films on ITO Assembled Using Copper (I)-Catalyzed Azide-Alkyne Cycloaddition by ATR IR. *ACS Appl. Mater. Interfaces* **2011**, *3*, 4703–4713.

(45) Jaksa, G.; Stefane, B.; Kovac, J. XPS and AFM characterization of aminosilanes with different numbers of bonding sites on a silicon wafer. *Surf. Interface Anal.* **2013**, *45*, 1709–1713.

(46) Graf, N.; Yegen, E.; Gross, T.; Lippitz, A.; Weigel, W.; Krakert, S.; Terfort, A.; Unger, W. E. S. XPS and NEXAFS studies of aliphatic and aromatic amine species on functionalized surfaces. *Surf. Sci.* **2009**, *603*, 2849–2860.

(47) Jaksa, G.; Stefane, B.; Kovac, J. Influence of different solvents on the morphology of APTMS-modifiedsilicon surfaces. *Appl. Surf. Sci.* **2014**, *315*, 516–522.

(48) Nalwa, H. S.; Watanabe, T.; Kakuta, A.; Mukoh, A.; Miyata, S. N-Phenylated aromatic polyurea: a new non-linear optical material exhibiting large second harmonic generation and u.v. transparency. *Polymer* **1993**, *34* (3), 657–659.

(49) Wijesekera, T.; Dolphin, D. Synthtic Aspect of Porphyrin and Metalloporphyrin Chemistry. In *Metalloporphyrins in Catalytic Oxidations*; Sheldon, R. A.., Ed.; Marcel Dekker Inc., 1994, Chapter 7, pp 193-239.

(50) Josefsen, L. B.; Boyle, R. W. Photodynamic Therapy and the Development of Metal-Based Photosensetisers. *Met.-Based Drugs*. **2008**.

(51) Coleman, M. M.; Sobkowiak, M.; Pehlert, G. J.; Painter, P. C. Infrared temperature studies of a simple polyurea. *Macromol. Chem. Phys.* **1997**, *198*, 117–134.

(52) Hu, Y.; Goodeal, N.; Chen, Y.; Ganose, A. M.; Palgrave, R. G.; Bronstein, H.; Blunt, M. O. Probing the chemical structure of monolayer covalent-organic frameworks grown via Schiff-base condensation reactions. *Chem. Commun.* **2016**, *52*, 9941-9944.

(53) Adam, F.; Oo, W-T. Selective oxidation of benzyl alcohol to benzaldehyde over Co-metalloporphyrin supported on silica nanoparticles. *Appl. Catal. A: Gen*. **2012**, *445–446*, 252– 260.

(54) Sen, P.; Hirel, C.; Andraud, C.; Aronica, C.; Bretonniere, Y.; Mohammed, A.; Hans

Agren, H.; Minaev, B.; Minaeva, V.; Baryshnikov, G.; Lee, H-H.; Duboisset, J.; Lindgren, M. Fluorescence and FTIR Spectra Analysis of *Trans*-A_2B_2-Substituted Di- and Tetra-Phenyl Porphyrins. *Materials* **2010**, *3*, 4446-4475.

(55) Shimizu, K.; Phanopoulos, C.; Loenders, R.; Abela M. L.; Watts, J. F.; The characterization of the interfacial interaction between polymeric methylene diphenyl diisocyanate and aluminum: A ToF-SIMS andXPS study. *Surf. Interface Anal.* **2010**, *42*, 1432–1444.

Chapter 04

4.1 General Conclusion

Molecular level layer-by-layer (LbL) thin film fabrication known as molecular layer deposition (MLD) has taken a great attention due to its simplicity and attractive control over the film thickness, composition and conformality through the sequential self-limiting surface reaction at single molecular level. Up to date, most of the MLD processes have been conducted by the polymerization of volatile bifunctional monomers under vacuum conditions to prepare polyamides, polyimides, polyurethanes and polyureas based nanostructures. But this vapor-based MLD technique is not appropriate for the high molecular weight and low vapor pressure molecules such as macromolecules. Solution based MLD process offers an alternative way to overcome some of the limitations of vapor-based MLD technique. By considering the above points, the solution based MLD technique was chosen in this research to fabricate the porphyrin-based covalent molecular network through the urea coupling reaction. In that case, I focused on some of the main factors such as appropriate self-assembled monolayer of aminosilane, humidity and other reaction condition for the multilayer film growth that can affect the sequential molecular growth on the solid substrate and the physical and chemical properties.

In the first part of this work, I prepared the self-assembled monolayer of APDMES

and APTMS on SiO_2 substrates. APDMES modification was carried out in four different types of solvent under various reaction conditions. Using the XPS technique, I investigated the surface compositions and chemical bonding of the modified surfaces. Results show the best APDMES-modification in toluene at both RT and high temperature (70 ºC, 3 hr) along with the higher free amine %. I conclude that the modification of APDMES on SiO_2 surface strongly depends on solvent system. During silanization process, polymerization possibility of APTMS molecules in ethanol was also investigated at different time scale using XPS and contact angle. Interestingly, no evidence was found for polymerization in ethanol solvent system. The chemical stability of the APDMES and APTMS-modified SiO_2 substrates were also investigated after 7 hr in H_2O and 0.1 M $HClO_4$ solution at 40 ºC and RT respectively. Three methoxy group containing APTMS molecules showed much higher stability on SiO_2 substrate than the one ethoxy group containing APDMES molecules in both aqueous and acidic conditions.

In the second part of this work, I have demonstrated the solution-based MLD thin film growth of porphyrin-based covalent molecular networks on a APTMS-modified substrate surface using the urea coupling reaction between 1,4-PDI and H_2TAPP at room temperature. Multilayer growth at different RH conditions was investigated using UV-vis absorption spectroscopy. Stepwise multilayer film growth was observed at ≤14% RH, whereas the high RH conditions showed film growth-limiting behavior. Presumably,

numerous 1,4-PDI self-polymerization took place at high RH conditions, which might block the reactive surface area that leads to a lower accessibility of porphyrin molecules for multilayer film growth. The urea linkage was confirmed using IR and XPS studies. The signal increased significantly with the number of MLD cycles, representing stepwise multilayer film growth caused by consecutive urea coupling reaction.

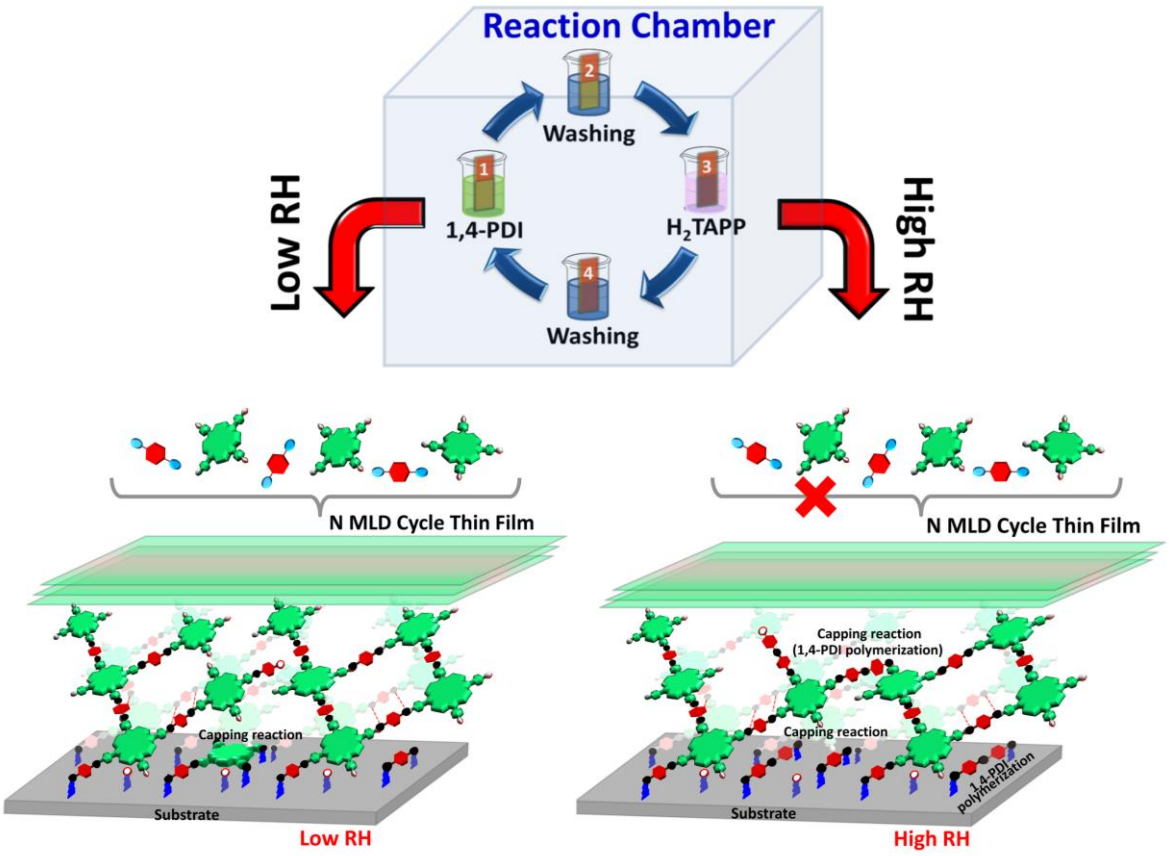

4.2 Future Prospects

The results of my research suggested that it is possible to fabricate porphyrin-based urea thin film with a low molecular density using solution-based MLD techniques. The future prospects of this work can be mentioned as following aspects:

1. Based on my research results, porphyrin-based urea thin film can provide both H-bonded and free urea linkages. This free urea linkage offers an opportunities to use this film for selective anion sensor. According to previous literatures, it is anticipated that free urea bond and free pyrrole group of porphyrin can act as a neutral receptor for anion hydrogen bonding through the N-H fragment of urea and/or pyrrole. The selective anion

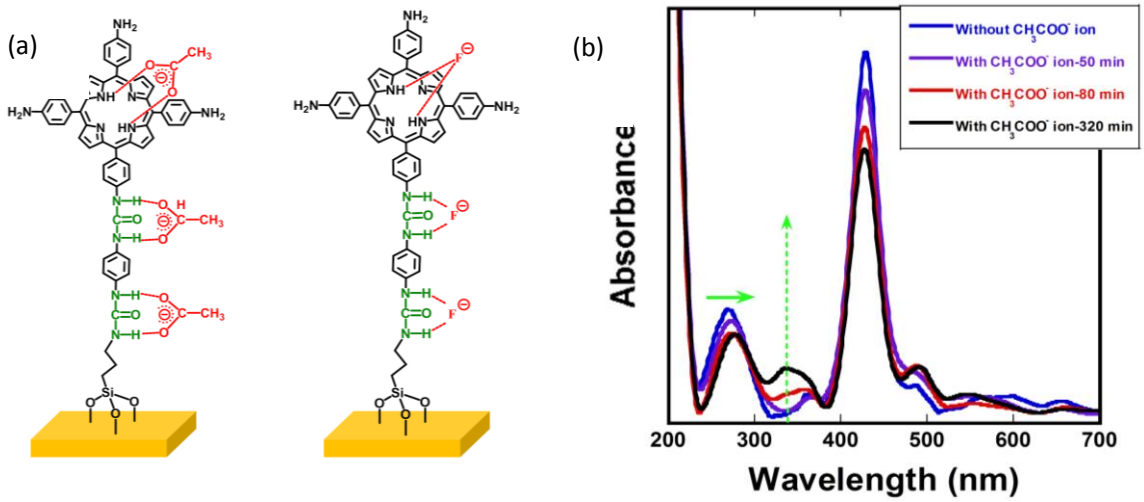

Figure 4.1. (a) The proposed host-guest binding mode of urea based thin film and anion (F^- and CH_3COO^-) and (b) UV-vis absorption spectra thin film towards various dipping time in 24 mM CH_3COO^- solution.

sensing activity of porphyrin-based urea thin film is now on under investigation in our laboratory.

2. The presence of free amine-group and non-metallated porphyrin centers into the multilayer film offers an opportunity for post-metallation with a verity of metal ions (e.g., gold, nickel, iron, cobalt, zinc etc.). I hope, this criteria will make it more interesting for the application in biological field as sensor, anti-bacterial and anti-fungal materials.

Acknowledgement

This study could not able to be completed without the help and contribution of many peoples. I would like to express my deepest gratitude to my supervisor, Associate Professor Yuki Nagao, School of Material Science, Japan Advanced Institute of Science and Technology for his valuable suggestions, kind encouragements, supervision, and great supports throughout my doctoral study. I learned how to pursue a world class research as well as how to face difficulties in scientific research I learned from him, how to pursue a world class research as well as how to face difficulties in scientific research.

I also express my grateful thank to Professor Noriyoshi Matsumi, School of Material Science, Japan Advanced Institute of Science and Technology for being my second supervisor and his kind guidance in this study.

I would like to gratefully thank to Associate Professor Tsutomu Hamada for considering me to complete my minor research under his supervision, which widen my knowledge in another research field. I also express my special thanks to Ms. Shino Mizuno for her kind supports and suggestions in this research.

I express my sincere gratitude to the former and current members in Nagao laboratory for their supports and sharing knowledge.

Finally, I profoundly appreciate the encouragement, understanding and support from my parents and all of friends.

S. M. Nizam Uddin

Achievements

Journals

1. **S. M. Nizam Uddin**, Yuki Nagao, "Multilayer Growth of Porphyrin-Based Polyurea Thin Film Using Solution-Based Molecular Layer Deposition Technique." (*Langmuir* **2017**, *33*, 12777−12784)

Conference

Poster presentation

1. **S. M. Nizam Uddin**, Banjongsak Lamlua, Takahiro Ohyama, Salinthip Laokroekkiat, Mitsuo Hara, Shusaku Nagano, Yuki Nagao, "Effect of Heat Treatment on Co (II) TAPP-Based Surface Nanostructure for Oxygen Reduction Reaction." The 96th CSJ Annual Meeting, 24-26 March 2016, Kyoto, Japan.

2. **S. M. Nizam Uddin**, Banjongsak Lamlua, Takahiro Ohyama, Laokroekkiat Salinthip, Mitsuo Hara, Shusaku Nagano, Yuki Nagao, "Positive effect of heat treatment on the electrocatalytic activity of Porphyrin-based nanostructure" IISc-JAIST Joint Workshop on Functional Inorganic and Organic Materials, 7 March 2016, Ishikawa, JAIST, Japan.

3. **S. M. Nizam Uddin**, Banjongsak Lamlua, Takahiro Ohyama, Salinthip Laokroekkiat, Shusaku Nagano, Yuki Nagao, "Fabrication of Covalent-Based Co(II)TAPP Nanostructure by Using Solution-Based Layer-by-layer Technique for ORR Electrocatalyst." 平成27年度北陸地区講演会と研究発表会, 27 November 2015, Kanazawa, Japan.

4. **S. M. Nizam Uddin**, Yuki Nagao, "Synthesis and Characterization of Porphyrin-Based Polyurea Thin Films by Molecular Layer Deposition Technique." JAIST Japan-India Symposium on Materials Science, 6-7 March 2017, Ishikawa, JAIST, Japan.

5. **S. M. Nizam Uddin**, Yuki Nagao, "Fabrication of Porphyrin-Based Polyurea Networks by Solution-Based Molecular Layer Deposition (MLD) Technique." The 66th SPSJ Annual Meeting, 29-31 May 2017, Mihama-ku, Chiba-city, Japan.

Abstract of Minor Research

Title: Investigation of Ion Transport Phenomena in the Prussian Blue Nanoparticle Embedded Hybrid Liposome

In this study, long alkyl chain modified Prussian blue nanoparticles (PBNP) were used to prepare the hybrid liposome. As the PBNPs is well known for its ion transfer properties at room temperature, it could be a good choice as ion transfer channel for preparing hydride liposome. Ion transport property of PBNPs-liposome was investigated by optical microscope with respect to their fluorescence responses in UV and blue excitation at different pH conditions. The pyranine dye was used as a fluorescein derivative for the measurement of intracellular pH change to monitor the ion transport property of the PBNPs-liposome through the ionic channel of lipid bilayers. Results showed the clear evidence for ion transfer phenomena of PBNPs-liposome through the PBNPs embedded into the liposome bilayers.